CONTROLLED RELEASE OF CARBENDAZIM IN CU-BASED MOF AGAINST RICE BLAST MANAGEMENT UNDER A CONTROLLED ENVIRONMENT

Jyotirmoy Pathak

A Thesis Submitted in Partial Fulfillment of the Requirements for the Degree of Master of Science in Bio-Nano Material Science and Engineering

Examination Committee:	Dr. Raffaele Ricco (Chairperson)
	Dr. Suriyan Cha-um (Co-Chairperson)
	Dr. Tanujjal Bora
	Dr. Pranab Dutta (External expert)

Nationality:	Indian
Previous Degree:	Bachelor of Science (Honors) Agriculture
	Assam Agricultural University, India
Scholarship Donor:	AIT Scholarship

Asian Institute of Technology
School of Engineering and Technology
Thailand
May 2024

AUTHOR'S DECLARATION

I, Jyotirmoy Pathak, declare that the research work carried out for this thesis was in accordance with the regulations of the Asian Institute of Technology. The work presented in it is my own and has been generated by me as the result of my original research, and if external sources were used, such sources have been cited. It is original and has not been submitted to any other institution to obtain another degree or qualification. This is a true copy of the thesis, including final revisions.

Date:

Name (in printed letters) : Jyotirmoy Pathak

Signature: 

ACKNOWLEDGMENTS

I would like to express my sincere gratitude to everyone who provided their steadfast support during my master's program and the completion of my thesis. My thesis adviser, Dr. Raffaele Ricco, stands out among them because of his helpful advice, unwavering support, and unremitting encouragement which have been crucial to my research process. My ideas and the core of my work have greatly benefited from Dr. Ricco's extensive knowledge, sharp observations, and rigorous comments.

Additionally, I am indebted to the distinguished members of my thesis committee, Dr. Suriyan Cha-um, Dr. Tanujjal Bora, and Dr. Pranab Dutta, whose sharp insights, helpful criticism, and astute suggestions greatly improved the caliber and rigor of my research. Specially, I would like to express my sincere gratitude to Dr. Suriyaan Cha-um for granting me the opportunity to work within the esteemed laboratory of “National Center for Genetic Engineering and Biotechnology, National Science and Technology Development Agency”, conveying my utmost appreciation for his support and trust.

Furthermore, I would like to recognize the significant contributions made by Miss Daonapa Chungloo, Research Assistant at the “National Science and Technology Development Agency”, whose invaluable insights and recommendations facilitated the operation of various research instruments and equipment crucial to my work.

In addition to these academic mentors, I would also like to convey my profound appreciation to the almighty, my family and friends, whose support, ongoing motivation, and continual encouragement have been a source of strength and inspiration for me throughout my academic journey. They have been a constant source of strength because of their unending love, tolerance, and understanding.

Finally, I would like to express my sincere thanks to the “Bio-Nano Material Science and Engineering department at the Asian Institute of Technology (AIT)” for providing me with the tools, chances, and facilities I needed to pursue and realize my academic and professional goals.

ABSTRACT

In order to fulfill both the quantity and quality needs for food on a worldwide scale, agrochemicals including fertilizers, insecticides, and growth hormones are essential. However, their persistent, indiscriminate use puts the environment, human health, and the viability of the economy in serious danger. Researchers are investigating novel delivery techniques based on "Metal-Organic Frameworks (MOFs)" to solve these challenges and advance sustainable agriculture. Metal-organic frameworks, specifically copper-based MOFs like HKUST-1, have recently garnered increased attention for their potential applications in agriculture. $CuSO_4$ and other copper salts are already recognized as effective fungicides and vital plant nutrition. Copper is a fascinating option for agricultural advances because of its dual nature. In this study, a straightforward one-step method was developed to create HKUST-1 utilizing basic copper carbonate (BCC), a naturally occurring substance present in rocks including malachite and azurite, and a ligand called trimesic acid (1,3,5-benzentricarboxylic acid). A guest species was added which is known as carbendazim to the MOF structure during the synthesis. The generated carbendazim@HKUST-1 composite was used to treat seeds in order to determine how it affects the vigor index and germination percentage. Toxicology tests were also carried out to guarantee the security of this innovative delivery mechanism. Additionally, the assessments were done to check how well carbendazim@HKUST-1 prevents rice blast, a prevalent disease that affects rice plants. In order to evaluate it, its inhibition rate was contrasted with that of commercially available carbendazim. Additionally, some morphological and physiological parameters were analyzed to determine their statistical differences among each treatment.

In order to improve agricultural sustainability, this study intends to maximize the potential of MOFs like HKUST-1, offering a viable route for safer and more effective pesticide delivery methods.

Keywords: Metal Organic Framework, Encapsulation, Toxicology, Plant Disease Management

CONTENTS

LIST OF TABLES

LIST OF FIGURES

LIST OF ABBREVIATIONS

A	= Surface area
C	= Concentration
CB	= Carbendazim
gm	= Gram
Ha	= Hectare
HKUST-1	= 'Hong Kong University of Science and Technology'
mM	= Milli molar
MOF	= Metal Organic Framework
NSTDA	= 'National Science and Technology Development Agency'
OPA MOF	= Oxalate Phosphate Amine Metal Organic Framework
Yr	= Year
μM	= Micro molar
μg	= Micro gram

CHAPTER 1
INTRODUCTION

1.1 Background of the Study

Chemicals used in agriculture are referred to as agrochemicals, and this group of substances includes fertilizers, insecticides, and chemicals for plant protection. Modern agriculture heavily relies on agrochemicals to boost crop productivity by eliminating dangerous pests, illnesses, and weeds. Currently, there is a danger to the preservation of the ecological balance, soil biodiversity, human and environmental health, and food (Mandal et al., 2020). Agrochemicals are a product of contemporary technology that relies on synthetic fertilizers and pesticides. In addition to hurting pest species, the applied pesticide has the potential to spread from the area where it was sprayed to unintended places far from the crop. There has been a significant increase in the usage of pesticides, and concurrently, there has been a rise or accumulation of contaminated chemicals as a result of the toxic environment, which has affected soil, plants, and animal products including grains, fruits, and vegetables (Bhandari, 2014).

On average, agricultural fields receive “73 kg N ha-1 yr-1 of N2-based fertilizer” worldwide. Their utilization efficiency is “65% in the United States, 33% in Eastern China, and 31% in Western Europe” (L. Liu et al., 2020). However, 5-10% of the total nitrogen fertilizer used is lost through leaching (An et al., 2022) and approximately 50% to 70% is lost by self-evaporation (Derosa et al., 2010).

The use of nanotechnology in agricultural practices has grown in recent years, with the potential to greatly boost crop productivity. Due to the agriculture industry's rapid increase in nano-agrochemical manufacture and use, more chemicals will unavoidably wind up in water bodies (Y. Zhang & Goss, 2022). It can potentially disrupt the current agricultural and food sector landscape thanks to newly developed tools for treating plant diseases, rapid pathogen identification using nano-based assays, boosting plant nutrient uptake, etc. (Rai & Ingle, 2012). Nano-pesticides, which are essentially conventional active ingredients or inorganic nanomaterials formulated at the nano-scale, and nano-

fertilizers, comprising nano-sized nutrients or fertilizers coated with nanoparticles or engineered nanomaterials, offer the potential for precise and controlled release of agricultural chemicals. This targeted delivery system aims to maximize their effectiveness in promoting crop growth and pest control while minimizing the risk of over-application (Iavicoli et al., 2017).

Figure 1 describes that incorporating nanomaterials into fertilizers can enhance their performance in an environmentally friendly manner. These tiny materials function as regulators, causing the fertilizer to be released more gradually. This not only boosts the fertilizer's efficiency but also curbs the risk of groundwater pollution and minimizes the loss of nutrients due to leaching. In essence, the introduction of nanomaterials into fertilizers brings about a dual advantage improving their efficacy while also lessening their negative impact on the surrounding ecosystem.

Figure 1.1

Nanomaterial Incorporation Reduces Fertilizer Release rate, Enhances Efficacy, and Minimizes Groundwater Contamination and Leaching Losses.

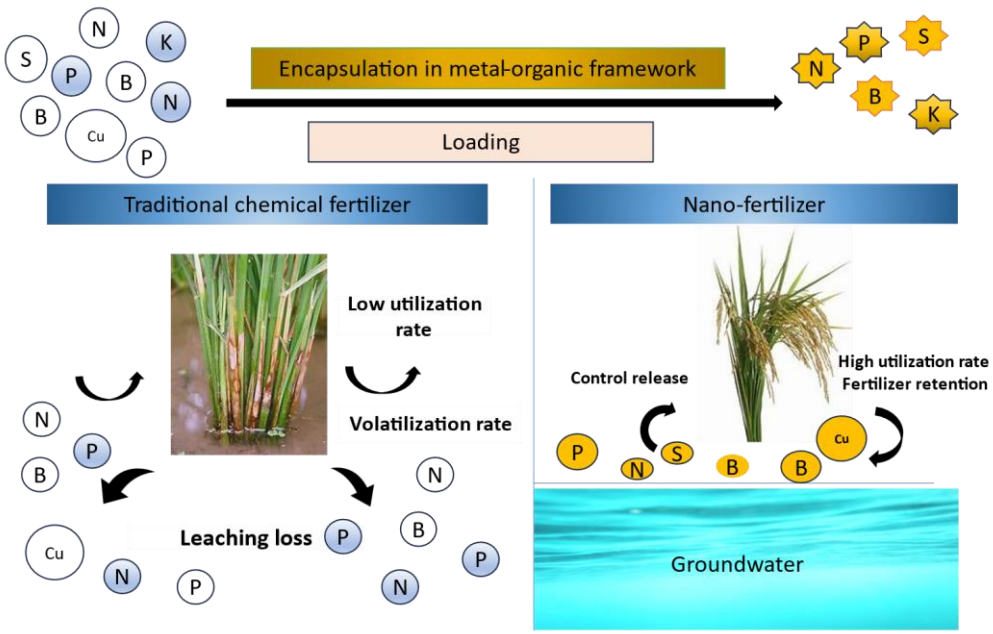

Agrochemicals in the environment are frequently in touch with humans and can have short-term and long-term health effects. Acute and chronic neurotoxicity (induced by fumigants, fungicides, and insecticides), lung damage (produced by paraquat), chemical burns (caused by anhydrous ammonia), neonatal methemoglobinemia, etc. are a few instances. Exposure to pesticides containing organochlorines, organophosphates, and carbamates as well as a variety of fungicides (such as mercurial, diphenyl, hexachlorophene, and hexachlorobenzene) and fumigants (such as methyl bromide, sulfuryl fluoride, and carbon disulfide) has all been connected to long-term neurologic harm (Weisenburger, 1993).

Figure 1.2

Cases of Pesticide Poisoning by Age Group in Thailand in 2019 (Laohaudomchok et al., 2020)

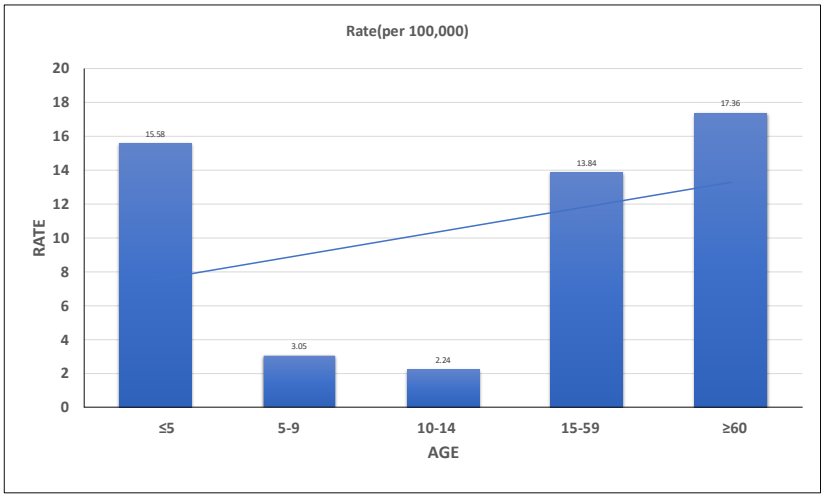

In the broader spectrum of agrochemical utilization across various crops, this chapter narrows its focus to the specific domain of rice cultivation. Here, the many sides of pesticide application are examined, including its use and any consequences, as well as a thorough examination of illnesses particular to rice and creative management techniques.

Rice [Family: Poaceae (Gramineae), Subfamily: Bambusoideae, Tribe: Oryzeae, and Genus: Oryza] is an important crop which is grown in all the six continents of the world (Asia, Africa, Australia, Europe, North America, South America) leaving only the cold continent of Antarctica, where no crops can be grown. One of the world's top rice exporters is Thailand. Thus, it is crucial to the security of the world's food supply (Pame et al., 2023).

The most significant staple food crop in the world, rice, is essential to maintaining food security worldwide. More than two billion people are fed by it, providing a sizeable amount of the calories consumed by the world's population (Ahmad et al., 2008, 2009). Annually, a substantial amount of milled rice is produced, contributing significantly to the world's food supply. Approximately 20% of the world's total food supply, equivalent to 480 million metric tons, is comprised of milled rice (Muthayya et al., 2014; Nganga et al., 2022). This emphasizes the pivotal role that rice production and consumption play in ensuring food security for billions of people worldwide. The quantity and quality of rice require significant attention due to its crucial role in providing 21% of the energy and 15% of the protein needed by the human body (Gnanamanickam, 2009).

By utilizing biotechnology, a range of crops around the world are being improved; rice is one among them. Rice production has now grown both numerically and qualitatively as a result of employing the target characteristic without damaging the non-target loci of the rice genome, moving cost-effective essential features from the genus/species fence into the rice gene pool, and stopping the breeding cycle.(Pathak et al., 2018). Genetic engineering has been applied to rice with an emphasis on traits like resistance to drought, salinity, and cold; resistance to insects, pests, and diseases; and nutritional traits (iron improvement to reduce vitamin A deficiency), prioritizing the two promising areas of nutrition improvement and plant protection for immediate use.(Peng et al., 2020; Rasool et al., 2020).

In addition to the aforementioned factor, Zibaee et al., (2009) mentioned that effective and secure control of rice pests and diseases is being implemented to avoid any loss in production. Although spraying of inorganic pesticides is the primary method employed by farmers to eradicate pests and damage caused by them, they should also employ a number of additional methods besides the biotechnological approaches. Researchers and farmers are looking for safer and more effective strategies due to growing concerns about environmental pollution, resurgence, resistance, and the emergence of secondary pests brought on by synthetic chemicals, such as using in small quantities that should have a positive impact in particular on the affected portion of the plant.

One of the most limiting biotic variables that has an impact on rice production all around the world is disease. A "major" disease is one that reduces rice yield economically, and a "minor" disease is one that has less of an impact on the economy. More than 70 % of diseases have been caused by fungi, viruses, bacteria, and nematodes (H. Zhang et al., 2009). Blast is the world's most devastating disease among the different rice illnesses (Miah et al., 2012).

Plant disease poses a hazard to the safety of the world's food supply (Strange & Scott, 2005). Depending on the illness, crop, and production conditions evaluated, this hazard may lead to great loss (Savary et al., 2006). Plant diseases cause the loss of at least 10% of the world's food supply, and over 800 million people do not have access to enough food. (Christou et al., 2003). “Rice blast (Pyricularia grisea / Magnaporthe grisea / Magnaporthe grisea), bacterial blight (Xanthomonas oryzae pv. oryzae), and sheath blight (Rhizoctonia solani)” are a few of the primary diseases that affect rice. The primary barrier to rice production is thought to be fungal rice infections, which result in losses in both terms of quality and quantity. The most serious disease, specifically, has been documented to be Pyricularia grisea-caused rice blast disease, which can cause yield losses of up to 50% (Devreese et al., 2017; Kongcharoen et al., 2020).

“Rice blast” is a severe threat to rice production because of its widespread dispersion (Greer & Webster, 2001; Miah et al., 2012). Because the disease may rapidly travel to new areas and can live and grow under hard climatic circumstances, it is more difficult to control (Alexandre Meybeck et al., 2012; De Araújo et al., 2000).The disease's tolerance to various treatments has reduced as a result of the introduction of new, more virulent strains, making management and control more challenging. (Laha et al., 2017). Magnaporthe grisea is an ascomycete filamentous fungus that affects over 50 hosts. The first mention of a rice blast is from China (1637), followed by Japan (1704). The disease became more well-known in India when a terrible epidemic struck the “Thanjavur (Tanjore) delta of Tamil Nadu” in 1919. It was first discovered in Andhra Pradesh's Chittoor district, then in Telangana's Nizamabad. The disease has been reported from practically all of India's rice-growing regions. However, the severity of the illness varies from year to year and from location to region (Nagarajan, 1988).

Although regional epidemics can be more damaging resulting in grain yield loss of up to 100% under favorable conditions, average losses in the range of 10 to 30% are normal (R. Dean et al., 2012). This disease is the principal production bottleneck in West Africa, the greatest producing region in Africa. Plants in all stages of growth and development can become infected by the fungus, which can affect both lowland and highland rice production systems. Lowland rice cultivated in temperate and subtropical climates in Asia is more susceptible to the virus, but tropical highland regions are only susceptible when they get irrigation (Nutsugah et al., 2008). In Thailand, rice blast disease is one of the most common rice illnesses. The pathogen's level of infection of the rice crop in this location can change according to changing environmental circumstances. Moderate field infections can reduce grain yields by about 50% (Kirtphaiboon et al., 2021).

Magnaporthe grisea, a hemibiotrophic fungus, infects crops at all stages and shows signs on leaves, stems, panicles and nodes (Ribot et al., 2008; Seebold et al., 2007; Usman Ghazanfar et al., 2009).Purple dots on a young leaf may be seen following an incubation period. These spots develop into “spindle-shaped lesions” with a gray core

and a purple-to-brown border, which are eventually encircled by a yellow zone. Only the older leaves from cultivars with resistance show brown patches. Especially at the seedling and tillering phases, lesions that are present in immature or vulnerable leaves combine and induce the leaves to wither. Lesion development on the n-leaf, where n is the top developing leaf, shortens the n + 1 leaf sheath and the n + 2 leaf blade, which results in the plant as a whole becoming stunted (Kato, 2001). Leaf blast lesions significantly lower each leaf's net photosynthetic rate compared to the visible diseased leaf portion.

According to Zhu et al. (2005), neck blast, which is thought to be the disease's most damaging phase, can develop without being preceded by severe leaf blast (Zhu et al., 2007). The panicle becomes infected by the neck blast, which prevents the seeds from filling or causes the panicle to topple over due to decay.

The economic worth of the crop is significantly decreased by neck infections, which can be quite devastating. The panicle's branches may typically become discolored a greyish brown, and the lesions may eventually cause the branches to split. The neck blast symptom is the most harmful of the three (Singh et al., 2018).

Rice blast is brought on by a filamentous ascomycete fungus and is transmitted by asexual spores (conidia) that attack the above-ground tissues of rice plants (Couch et al., 2005; R. A. Dean et al., 2005; Ebbole, 2008; Ou, 1985; Wilson & Talbot, 2009). An infection cell known as an appressorium is necessary for the infection pathway. It breaks the thick cuticle of the rice plant using a pressure-driven process and adheres securely utilizing an adhesive contained in the spore apex. This mechanism produces turgor pressure of up to 8.0 Mpa (Bourett & Howard, 1990; Dagdas et al., 2012; Vaneault-Fourrey et al., 2006). As soon as the fungus enters the tissue, it produces invasive hyphae that swiftly infiltrate live host cells and release compounds that compromise host defenses and encourage infection.(Giraldo et al., 2013).

Rice blast conidia can disperse within 230 meters of their source; dissemination is encouraged by darkness, high relative humidity, and winds of more than 3.5 m s^{-1}. Infected leftovers and rice seeds are the main sources of inoculum, and in the tropics, airborne conidia are always available, allowing stable epidemics to last all year (Guerber et al., 2006; Ou, 1985; Raveloson et al., 2018). Older lesions are often larger and may cluster to destroy entire leaves. Initial symptoms of rice blast manifest as oval-shaped lesions, typically measuring 0.3 to 0.5 cm in width and 1.0 to 1.5 cm in length. These lesions vary in color from white to gray and are outlined by darker hues (Ghatak et al., 2013).

Air temperatures between 25 and 28°C, relative humidity levels between 92% and 96% , and extended leaf wetness periods are all favorable for sporulation and lesion formation (Kankanala et al., 2007; Padmanabhan, 1965). At night, when the relative humidity is 100% and the air temperature is close to 22 °C, spore formation peaks (Raquel Ghini, 2014; Wilson & Talbot, 2009). Fungal growth in rice cells causes necrotic lesions and the death of the infected tissues in 3 to 5 days (Wilson & Talbot, 2009). The pathogen continues to exist in the tissues of host plants' leftovers, and the cycle repeats. It is possible for there to be one cycle each week under ideal circumstances, with a single lesion releasing hundreds of spores every night for more than 20 days (Kato, 2001; Kingsolver et al., 1984)

Chemicals are a crucial component of successful integrated pest management (IPM) systems for managing plant diseases. Fungicides with various sites of action, protective, and contact qualities against a variety of target sites played a significant role in fungal metabolism in the first half of the 20^{th} century after their introduction in the 1960s. In the middle of the 1800s, lime sulfur and Bordeaux mixture were introduced, marking the beginning of chemical control (Hirooka & Ishii, 2013; Knight et al., 2003).

Rice blast can be successfully managed by a variety of fungicides with different modes of action, such as “organophosphorus” (Katagiri & Uesugi, 1977), “methyl benzimidazole carbamate (MBC)” (Zhang et al., 2004), melanin biosynthesis inhibitors

(MBIs) (Woloshuk et al., 1980), “14α-demethylation inhibitors (DMIs)” (Fang et al., 2009), and “quinone outside inhibitors (Qols)” (Hirooka & Ishii, 2013). Although there are many different disease management strategies available (Miah et al., 2017), modern agriculture practices frequently show a considerable dependence on farmers applying chemical fertilizers and pesticides (Anwar et al., 2022.; Oh, 2008).

The majority of fungicides have very short active periods. Because of this, farmers must use pesticides regularly, which raises questions about misuse. Other issues include the absence of nitrogen fixation, which reduces plant growth and raises the need for chemical fertilizer, and plant hormones (such as 3,4-dichlorophenoxyacetic acid, NAA, and IAA), which impair cell division, differentiation, elongation, flowering, and senescence (Amjad Bashir et al., 2022). Although most fungicides can have chronic effects with repeated exposure, their acute toxicity to humans is often modest. Implementing preventative measures, such as crop rotation, sanitation, and the application of suitable fungicides or pesticides, is crucial for the prevention and management of plant diseases (Schneider & Dickert, 2010).

Carbendazim, a benzimidazole fungicide can be used for the control of rice's two major diseases, “blast (*Magnaporthe grisea*) and sheath blight (*Rhizoctonia solani*)”, as well as five minor diseases, “sheath rot (*Sarocladium oryzae*), stem rot (*Magnoporthe salvinii*), narrow brown leaf spot (*Sphaerulina oryzina*), backanae and foot rot (*Gibberella fujikuroi*), and false smut (*Claviceps oryzae satire*)” (Parida et al., 1990). However, the fungicidal efficacy of carbendazim was systematically evaluated across three concentrations (500 ppm, 1000 ppm, and 1500 ppm) against *P.oryzae* Cav. The findings underscore its profound fungi toxic attributes, as evidenced by the complete growth inhibition of *P. oryzae* Cav. at all tested concentrations (Slater et al., 2006).

(Hajano et al., 2012) reported that the food poisoning method was used to evaluate five fungicides, including “Topsin-M (70% Thiophanate-methyl), Bavistin (50% Carbendazim), Aliette (80% Fosetyl-aluminum), Dithane M-45 (80% Mancozeb), and Copper oxychloride (50% Copper oxychloride)”. Increasing concentrations of all the

fungicides gradually inhibited the colony growth of *Pyricularia grisea*. Mancozeb, one of the fungicides used, entirely prevented the test fungus from growing.

Pyricularia grisea appeared to be extremely resistant to the fungicide mancozeb at doses of 10,000 and 1000 ppm, respectively. Numerous researchers examined a variety of fungicides and discovered that many of them were efficient against the rice blast fungus "*M. oryzae"* (Misra et al., 1990; Prajapati et al., 2004). Similarly, "Tricyclazole, Mancozeb, Carbendazim, Iprobenfos, Propiconazole, and Edifenphos" were shown to be extremely efficient against the test fungus by evaluation of 19 fungicides against *Pyricularia grisea* (Gohel et al., 2008).

According to (Varma & Santhakumari, 2012), blast was reduced by foliar spraying isoprothiolane 40% EC at 1.5 ml/l, followed by carpropamid 27.8% SC (Protiga) and carbendazim 50% WP (Bavistin). Carpropamid came in second place (67.5 and 80.5% illness incidence and intensity, respectively) while carbendazim came in third place (56.9 and 73.1% disease incidence and intensity, respectively) compared to the control. Isoprothiolane 40% EC greatly reduced disease incidence (78.3%) and intensity (89.7%). When compared to other controls, the application of isoprothiolane boosted both grain and straw yield. Chemical management techniques lack both environmental familiarity and practicality. Using Tricyclazole 22% + Hexaconazole 3% SC thrice from the booting stage at weekly intervals, Magar et al. found that the combination had the highest disease control (87.03% and 79.62% in leaf and neck blast respectively) and the highest grain yield (4.23t/ha) (Magar et al., 2015).

Chemicals and fertilizers are vital parts of the agricultural landscape, yet their release into nearby waterways and the atmosphere causes serious environmental problems. Porous solid-phase materials show promise as an ethical and sustainable solution to these problems Numerous researchers have developed diverse encapsulation techniques to mitigate toxicity and enhance the efficacy of agrochemicals. MOF is an example of a material that has recently been used to encapsulate agrochemicals, according to Rojas and colleagues. It possesses exceptional sorptive, recognition, and catalytic properties.

The family of porous coordination includes both “inorganic nodes (such as atoms, chains, or clusters)” and “organic linkers (such as nitrogenated, carboxylates, or phosphonates)”. These linkers and nodes form periodic lattices (Rojas et al., 2022).

Figure 1.3 illustrates how MOFs have a wide range of applications and may be used in a variety of contexts. Agrochemical removal through processes including adsorption and photodegradation, as well as sensing, are other applications for MOFs that go beyond their use in controlled release situations. Their complexity highlights the range of their practical contributions to various scientific and technical fields.

Figure 1.3

Application of “Metal-Organic Frameworks (MOFs)” and Agrochemicals in a Variety of Processes, such as Controlled Release, Environmental Cleanup, and Agrochemical Analysis and Quantification

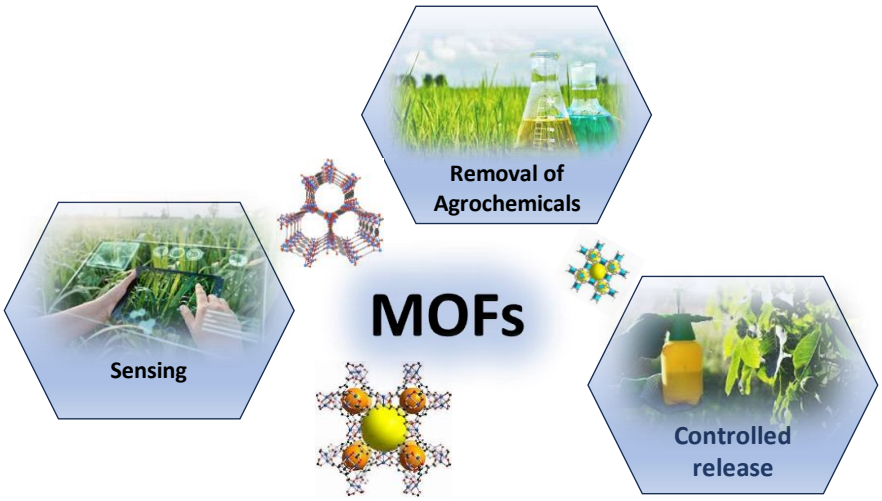

Due to their porous nature, large surface area (up to 6000 $m^2 g^{-1}$), and easily accessible exposed adsorptive sites, MOFs have attracted a lot of interest in tackling these difficulties, particularly in the domain of adsorption (Xu et al., 2020). It offers a wide range of potential applications in ecologically friendly agriculture. Research efforts are currently focused on MOF-based plant feeding and protection platforms (Bindra et al., 2023; Shan, Xu, et al., 2020). Because of their intriguing qualities like ultrahigh

porosity (pore sizes extending up to 4.5 nm), tunable chemical functionality, and low density, MOF-based encapsulated products can help the agricultural sector to achieve better resource management and sustainable crop production (Bindra et al., 2023; Islamoglu et al., 2017; Vasseghian et al., 2022). Basic copper carbonate is transformed into HKUST-1 at room temperature, which results in a product with a high surface area (2089 m^2/g) and cheap manufacturing costs (Riccò et al., 2018). The HKUST-1 converted from natural resources could be an excellent cargo for formulating and delivering agrochemicals.

1.2 Statement of the Problem

More than three billion people eat rice as their primary food. If we are to meet the dietary needs of the rapidly growing global population, yields must double over the next 40 years. "*Magnaporthe grisea"*, the rice blast fungus, causes a loss of 50% of the yearly rice harvest (Skamnioti & Gurr, 2009) and it is found in more than 85 countries (Kato, 2001). Due to the increased demand for agricultural products in terms of both quality and quantity brought about by the growing global population, there has been a significant increase in the use of chemical pesticides to battle crop diseases. (Lahlali et al., 2022). Among the various methods that have been used before, fungicides are most frequently used to control diseases. When used against a pathogen, fungicides can effectively reduce disease, but their frequent and indiscriminate use can also cause air pollution and the emergence of fungicide resistance (Christopher et al., 2010).

A common systemic, broad-spectrum benzimidazole fungicide used to treat rice blast is carbendazim, which is also a metabolite of benomyl. It is also widely used to control other rice diseases including rice bakanae disease and rice sheath blight. Thus, during the entire rice growth season, farmers may have sprayed carbendazim three to four times. This fungicide's control efficacy was reduced or lost because of the pathogens developing fungicide resistance as a result of frequent and extensive treatment. For example, field isolates of *M. oryzae* showed resistance to carbendazim (Zhang et al., 2004). Despite the emergence of resistance, carbendazim is still used, primarily in

combination with other fungicides with various modes of action, to suppress rice blast (Song et al., 2022).

The addition of pesticides, fertilizers, and plant hormones into solid matrices, particularly porous ones, introduces novel prospects for a range of agricultural and environmental benefits. One key benefit is the prolonged duration of these agent's potency, made possible by the controlled release mechanisms built into porous materials. With decreased solubility in water, some pesticides can pose hazards of aquatic toxicity, so this approach provides a way to manage these issues. This technique can reduce the possible ecological impact of these chemicals on aquatic environments by reducing their solubility right after application. Additionally, incorporating light-sensitive chemicals into porous materials has the potential to improve these molecules' stability and durability, hence boosting their overall effectiveness. When a specific pesticide is encapsulated within a metal-organic framework, the release kinetics are inherently sluggish, affording precise control over the release profile. Consequently, this controlled release mechanism enables a reduction in the application frequency of pesticides. In summary, this multifaceted approach encompasses a spectrum of implications for environmentally sustainable practices and the promotion of sustainable agriculture.

1.3 Objectives of the Study

The term "porous materials" refers to a class of materials that contain pores or cavities with a three-dimensional network structure that might be of different sizes and shapes. Recent porous materials called metal-organic framework (or MOFs) facilitate the delivery of agrochemicals. HKUST-1 is a (MOF) made of carboxylate ligands and copper ions, which have pesticidal capabilities. It has a distinctive porous structure in three dimensions, high porosity, and adjustable pore size. HKUST-1 shows promise as a suitable porous material for encapsulating and regulating the release of agrochemicals, thanks to its favorable qualities include large surface area, thermal stability, and efficient gas storage and separation capabilities. It has shown promise for usage in energy storage, sensing, medicinal delivery, and catalysis.

The study's goal is to fabricate Cu-based MOFs (HKUST-1) for the encapsulation of Carbendazim, a systemic, broad-spectrum benzimidazole fungicide, and to see the controlled release. The objectives are mentioned below:

1. Synthesis of carbendazim@HKUST-1 via direct conversion from natural source (copper carbonate).
2. Assessment of the toxicity of HKUST-1 against fungi and plants.
3. In vitro efficacy of carbendazim@HKUST-1 against fungi.
4. Controlled release of carbendazim@HKUST-1 on rice plants and its antifungal properties against blast.

1.4 Scope of the Study

The combination of encapsulated carbendazim within the framework of HKUST-1 presents a novel avenue for agricultural fungicidal intervention and nutrient delivery. This amalgamation offers the potential for targeted fungicidal activity while introducing nutrient supply capabilities. However, thorough toxicological testing and regulatory approval are essential before its deployment. This approach embodies sustainability, augments disease management, and holds promise for enhanced agricultural productivity.

1.5 Limitation of the Study

1. The presence of copper in MOFs raises concerns about potential soil and environmental toxicity due to excessive copper accumulation.
2. The study exclusively assesses MOFs composed of a single element and utilizes only one type of guest chemical (carbendazim), potentially limiting the generalizability of the findings to diverse MOF compositions and guest chemicals.
3. Only two rice varieties and one fungicide were studied simultaneously
4. The experiment's short duration only assessed fungicide impacts up to the seedling stage, precluding observation of effects at the critical fruiting stage, potentially altering results.
5. The study focused solely on controlled environmental conditions within growth chambers, thereby potentially restricting the generalizability of findings to diverse

climates or real-world growing conditions. Conducting field trials would be imperative for broader applicability and additional insights.

CHAPTER 2
LITERATURE REVIEW

“Metal-organic frameworks (MOFs)”, which produce porous frameworks by fusing metal ions/clusters with organic ligands, have proven to be useful for creating nanoplatforms that respond to biotic and abiotic stimuli for controlled agrochemicals delivery (Wang et al., 2023). MOFs are increasingly gaining traction in agronomy due to their expansive and variable surface area, high porosity, scalable synthesis capabilities, and robust soil compatibility. These properties make MOFs promising materials for various agricultural applications. (Rojas et al., 2022). MOF-based agrochemicals are believed to increase agrochemical efficacy and, despite their early stages of research, help reduce toxic emissions. In addition to their systematic manufacture, MOFs' chemical stability has also been criticized (Kumar et al., 2017). The focus of this section will mostly be on the modern uses of MOFs as dispensation agents for agrochemical applications. This inquiry will focus on how fungicidal chemicals are encapsulated within a particular MOF structure. The main goal is to clarify the complex phenomena of controlled release displayed by such fungicides, particularly in relation to their effectiveness in battling a common pathology affecting rice.

2.1 Generalities on Porous Material

Porous materials have demonstrated enormous potential in a variety of applications, including catalysis, energy storage, and targeted and controlled distribution (Hou et al., 2020; Sun et al., 2016). Porous materials are categorized as “microporous (pore sizes under 2 nm), mesoporous (2–50 nm), and macroporous (pore sizes more than 50 nm)” (Su et al., 2011). Regions of vacant space can be found in porous materials, where visitors can be selectively absorbed and occasionally chemically changed. This has made them beneficial in both commercial and residential applications, ranging from heterogeneous catalysis and green chemistry to gas separation, energy storage, and ion exchange (Bennett et al., 2021). It plays a crucial role in new energy and medical technologies as well as in well-established processes like catalysis and molecular

separations. The strongest impact on society has so far been made by porous zeolites, and that sector is currently expanding quickly. “MOFs, covalent organic frameworks (COFs), and porous organic polymers” are some more porous solids that have emerged over the past 20 years (Slater & Cooper, 2015).

From a mechanical standpoint when used in industrial operations, porous materials must be able to withstand stresses including tension, compression, shear, bending, torsion, and impact (Tan & Cheetham, 2011). According to Henke and coworkers, although their synthetic flexibility gives room to create novel materials with greater strength, the mechanical characteristics of "soft porous crystals," a subclass of MOFs, were found to be poor, particularly with regard to shear stresses and fracture propagation. It was advised that the framework connection should be as high as possible to optimize the power of MOFs (Henke et al., 2014). However, the mechanical stability of porous amorphous organic polymers decreases similarly with increasing linker length (Lukose et al., 2012).

Figure 2.1

Pore Channels of an Organic Porous Caged Molecule (Slater & Cooper, 2015)

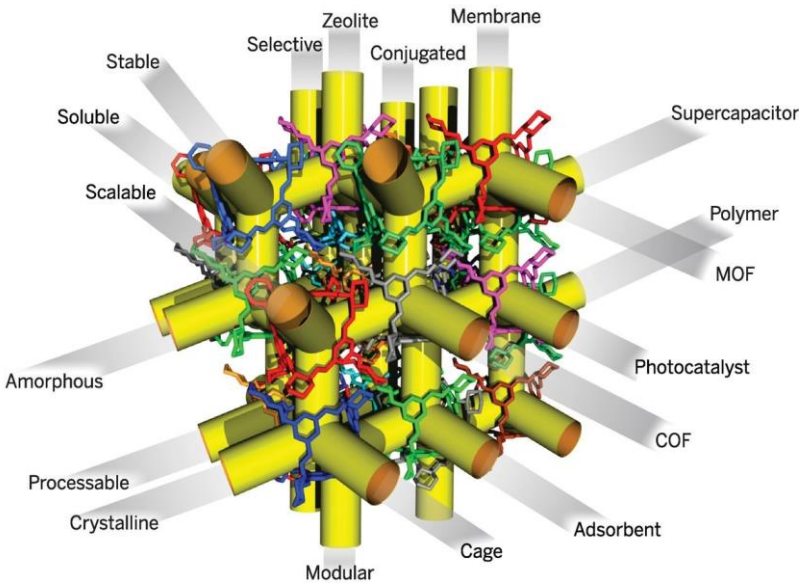

2.2 Metal Organic Framework

In the area of the interaction between molecular coordination chemistry and materials science, metal-organic frameworks (MOFs), also known as “porous coordination polymers (PCPs)”. MOFs are a newly discovered family of porous polymeric materials that are made of metal ions (also known as “secondary building units, or SBUs”) connected by organic bridging ligands (Lu et al., 2014). Because of their structural and functional tunability, MOFs are one of the fastest-growing fields in chemistry (Chen et al.,2017). During the one-pot method for creating MOFs, metal-containing nodes are often generated in situ. While occasionally the ligand may also form during the solvothermal process, it remains a consistent component throughout the reaction. The resulting MOF's topology is influenced by the geometry of the ligand. Typically, functional groups are either pre- or post-synthesized organically and then linked to the ligand. The choice of metal-linker combination also impacts the stability of MOFs. Additionally, the use of a flexible ligand can result in the production of stimuli-responsive or flexible MOFs (Zhou & Kitagawa, 2014)

Figure 2.2

Illustrative Representation Depicting the Formation Process of a “Metal-Organic Framework”.

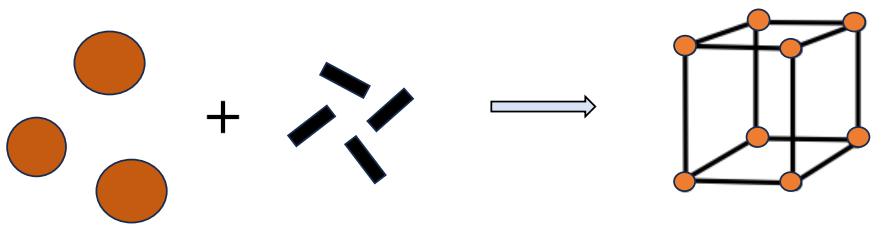

The remarkable properties of MOFs, including their highly accessible “surface areas (which can exceed 6,000 m^2/g), ultrahigh porosity (up to 90% free volume), and chemical tunability”, have spurred researchers to investigate their potential applications in “gas storage, molecular separations, catalysis, drug delivery, biotechnology, and device fabrication” (Riccò et al., 2018; Zhou et al., 2012). Certainly, the versatility of

MOFs is opening up new opportunities in fields like “microelectronics, sensing, ion conductivity, optics, pollutant sequestration, drug delivery, contrast agents, micromotors, and bioreactors”. While their primary applications involve absorbing and separating gaseous molecules like CO2, N2, CH4, and H2, they're quickly finding roles in diverse areas (Ricco et al., 2013).

Figure 2.3

Emerging Applications of Metal-Organic Framework (Ricco et al., 2016)

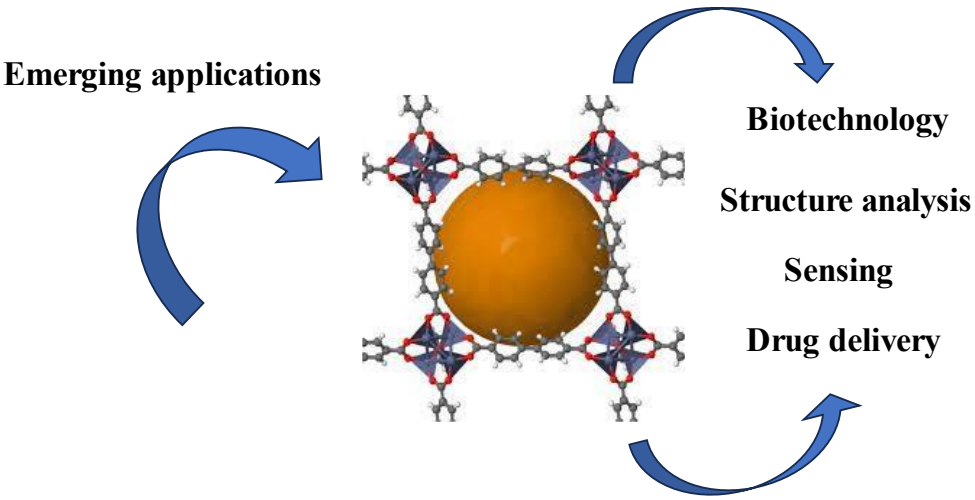

Due to its vast surface area and configurable pores that can be altered to suit particular molecules, MOFs are seeing a significant increase in application for the delivery of pesticides. MOFs are highly relevant in agrochemical applications because of their ability to hold large amounts of pesticides. Their interaction with guest molecules allows for controlled release, influenced by factors like “pore size, surface charge, pesticide pKa, and medium pH” (Furukawa et al., 2010). Additionally, electrostatic forces, π–π interactions, and hydrogen bonds serve as the same driving processes to accomplish maximal loading and extraction capacities (Mahmoud et al., 2022). One additional benefit of utilizing MOFs for pesticide delivery is their adequate stability for agrochemical delivery, which is followed by breakdown. This is advantageous as, at the conclusion of the application, the MOFs' breakdown stops them from building up in the environment.

Figure 2.4

Schematic Diagram of Pesticide Loading in Metal-Organic Framework and its Target Mechanism

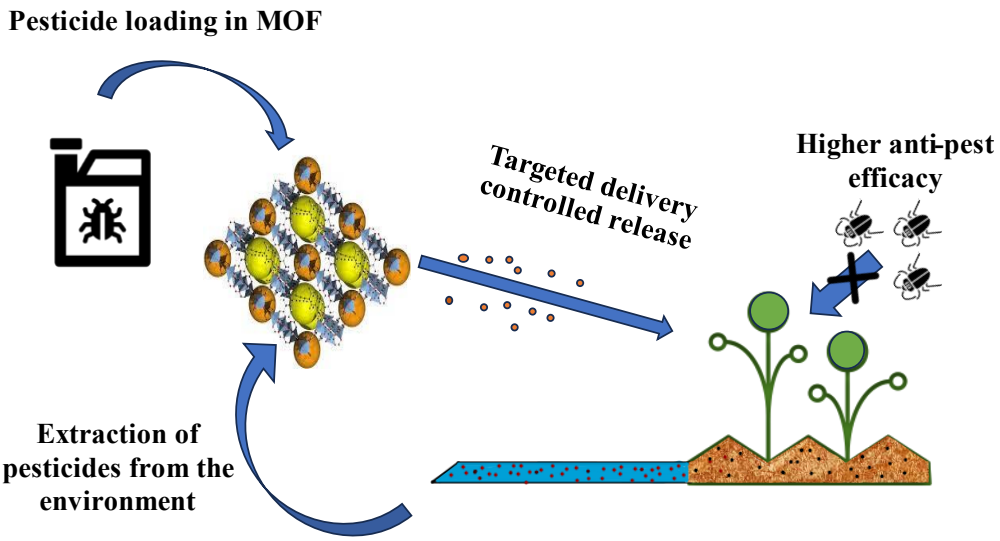

Pretreatment, extraction, detection, and assessment of residues in vegetables, fruits, and water are often used to analyze the primary adverse effect of agrochemicals on human health. MOFs and composites have been widely recommended for extracting and identifying these harmful compounds in food and water, as was to be expected. In 2010, Wen et al. published the first study on the use of MOFs in pesticide detection. A novel MOF was described by the authors as "[Cd(2,2′,4,4′-bptcH_2)] n (2,2′,4,4′-bptcH_4: 2,2′,4,4′ biphenyl-tetracarboxylic acid)" (Wen et al., 2010). Through stripping voltametric measurement, the MOF was able to adsorb and detect organophosphate pesticides with a limit of 0.006 g mL^{-1}. Stripping voltametric analysis is a group of voltammetry-based analytical techniques used to measure ions.

By utilizing the advantages of MOF-based encapsulated products, the agricultural sector can improve resource management and sustain crop production. These products' fascinating characteristics include ultrahigh porosity (pore sizes extending up to 4.5 nm), tunable chemical functionality, and low density (Bindra et al., 2023; Islamoglu et al., 2017; Vasseghian et al., 2022).

2.2.1 Copper Based MOF

Every living organism, including plants, necessitates copper (Cu), a transition metal crucial for various biological functions. It plays vital roles in processes such as "photosynthetic and respiratory electron transport chains, ethylene detection, cell wall metabolism, defense mechanisms against oxidative stress, and the synthesis of molybdenum cofactors". The typical copper content in plant tissues falls between 1 to 5 mg per gram of dry weight, with leaves typically containing around 10 mg per gram of dry weight (Yruela, 2009). On the other hand, a lack of copper can change crucial processes in plant metabolism. Also, excess copper (20 and 100 mg kg^{-1}) (Cruz et al., 2022) in the environment may lead to phytotoxicity, by forming reactive oxygen radicals that harm cells or by interacting with proteins and impairing vital cellular functions, inactivating enzymes, and upsetting protein structure.

To investigate and clarify the fundamental relevance of copper and nano-copper, many academics have engaged in extensive and meticulous research projects. Their continuous and exhaustive research has demonstrated their commitment to increase our grasp of this important field of study. These researchers have studied copper and its nanoscale analogues in great detail, using a wide range of approaches, experimental procedures, and analytical tools to explore the complicated relationships between their characteristics, behaviors, and uses. Their combined efforts highlighted the crucial role of copper in different fields as well as the nuanced characteristics that set nano-copper apart as a topic of utmost significance in the scientific community.

Recently (Fu et al., 2023) described how, in the presence of acetic acid, the interaction between Cu^{2+} ions and 1,3,5-benzenetricarboxylate linkers produced faulty "copper-

based metal-organic frameworks (Cu-MOFs)". These Cu-MOFs demonstrated remarkable organophosphorus pesticide (OP) adsorption capabilities as well as quick adsorption kinetics. The adsorption process' average binding energy was found to be -217.021 kJ mol^{-1}, which points to a very advantageous adsorption mechanism. Notably, "Cu-MOF-6" revealed the highest pesticide absorption capacity and showed superior reusability as an adsorbent. This MOF was distinguished by bigger holes and intrinsic mesoporosity as a result of the MOF's crystallization in acetic acid.

According to (Murinzi et al., 2018), the majority of researchers used the Cu-based MOF HKUST-1 as a matrix because of its good thermal stability, a pore size of (9 Å × 9 Å), and coordinatively unsaturated Cu^{2+} sites that boost its activity. (Chui et al., 1999) initially described the HKUST-1 compound in 1999. It is made up of "1,3,5-benzenetricarboxylate (BTC)" ligands that coordinate copper ions in a cubic lattice (Fm-3m). Cu (II) ions form dimmers in the HKUST-1 framework, with each copper atom being coordinated by four oxygen atoms from BTC linkers as well as water molecules. The potential of obtaining a coordinative vacancy on Cu (II) species has been indicated by the presence of water molecules in the initial coordination sphere of Cu ions (Prestipino et al., 2006).

It has been demonstrated that HKUST-1 can absorb ammonia in both dry and moist conditions. The adsorption sites in HKUST-1 have a high affinity for ammonia and have a Lewis-acid/base coordination of ammonia to accessible open sites on the Cu (II) centers. However, the density of Cu (II) sites (2.2 nm^3) is low in comparison to that of several other MOFs. One of the most Cu (II) sites is present per unit volume in "Cu-MOF-74". The highest volumetric ammonia absorption recorded in 2016 was shown by "Cu-MOF-74" at 80% humidity conditions (Katz et al., 2016).

For the elimination of chlorpyrifos (an organophosphate insecticide) (Kangra et al., 2022), used HKUST-1 as an adsorbent. At pH 7, 20 mg HKUST-1, 30 °C, and 60 minutes, the maximum removal efficiency of 76% was attained. Due to the HKUST-1's significant surface area (635.637 m^2g^{-1}) and pore volume (0.3531 cc/g), the highest

adsorptive capacity of up to 102 mg/g was likely achieved. The occurrence of opposing charges on the surfaces of HKUST-1 and chlorpyrifos was discovered to be associated with the maximum removal effectiveness reported at neutral ph.

Figure 2.5

Diagram showing how Trimesic Acid (1,3,5-benzenetricarboxylic acid, center) reacts with Basic Copper Carbonate (left) to produce HKUST-1 MOF (right) in a Solvent Mixture of Water and Ethanol (Riccò et al., 2018)

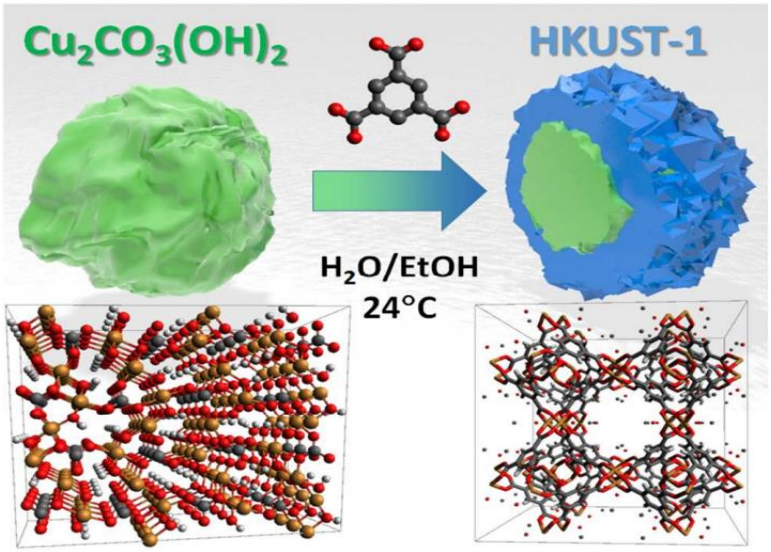

Some examples related to copper nanoparticles are in a recent study, it was found that adding Cu nanoparticles to Venice tomato seeds and distributing them in a polymer matrix boosted the weight of tomatoes by 10.7 percent (Zhao et al., 2021). (Shalaby et al., 2022) proposed that acclimated banana grafts using the biological form of nano-Cu (100 mg L^{-1}), improved the dry weight up to 12.6%. It was also reported that increasing the applied dosages of nano fertilizer to 100 mg L^{-1} boosted the viability rate up to 95.3%.

"Fusarium kuroshium", the causal agent of Fusarium dieback, was tested for the antifungal effectiveness of Cu-NPs at 0.1, 0.25, 0.5, 0.75, and 1.0 mg mL^{-1}. It was found that Cu-NPs were more effective than the cupric hydroxide-based commercial

fungicide used as a positive control in reducing the growth of the pathogen by more than 80%. Significant Cu-NP damage was seen in studies utilizing electron microscopy, mostly to the hyphae surface and the characteristic form of macroconidia. This harm became obvious three days following the immunization (Ibarra-Laclette et al., 2022).

In the literature currently available, little is known about how fungicides like carbendazim can be enclosed within metal-organic frameworks (MOFs). This obvious lack of research on the topic reveals a large gap in our existing understanding and emphasizes the necessity for additional research. The potential use of copper-based MOFs, such as HKUST-1, as a means of encapsulating fungicides is one area where significant study is lacking. Such studies have the potential to advance the study of MOF-based encapsulation systems as well as the sustainable application of fungicides.

2.2.2 Iron Based MOFs

Iron-based metal-organic frameworks (Fe-MOFs) hold great promise in agriculture as versatile materials that can serve as both a means of replenishing plant nutrients and a carrier for pesticide delivery, given the essential role of iron as a micronutrient in crop growth, valued at 1 to 200 mg/L. Plant respiration, nitrogen fixation, and chlorophyll synthesis are all significantly impacted by a Fe deficit. Along with these many benefits, it is nontoxic, inexpensive, has a preferred stability, has a high drug loading, and is well biocompatible (Dable-Tupas et al., 2023; X. Liu et al., 2021; Shan, Cao, et al., 2020).

Fe-MOFs, according to Liu and colleagues, are stable in aqueous and organic solvents because of the strong coordination between the iron (Fe) and oxygen (O) atoms. The ability to modify pore size and internal pore properties makes Fe-MOFs more advantageous than traditional porous materials like zeolites, increasing their potential and capacity to hold guest molecules (Liu et al., 2021).

Fe-MOFs were studied in the lab as novel fertilizers and showed promise for use in the fertilizer industry because of MOFs' ability to administer fertilizer, gases, and pharmaceuticals in a regulated manner (K. Wu et al., 2022). Although there are

numerous ways to create MOFs, including Solvothermal Synthesis, Microwave Synthesis, Hydrothermal Synthesis, Dry Gel Conversion Synthesis, and Liquid-Solid-Solution (LSS) Synthesis (X. Liu et al., 2021), Fe-MOFs were successfully synthesized on a pilot and laboratory scale via hydrothermal synthesis by Wu and colleagues. Notable concentrations of nutrients were present in the Fe-MOFs, including iron (14.69%), phosphorus (14.48%), and nitrogen (6.03%) (K. Wu et al., 2022).

The first Fe-MOF, based on the "oxalate-phosphate-amine triad (OPA-MOF)", was researched as an agrochemical release agent in 2015 (Anstoetz et al., 2016). The characteristics of ferralsol, a urea fertilizer, and triple superphosphate (standard P), a novel fertilizer with a slow-release action, were examined and contrasted (Anstoetz et al., 2016). OPA-MOF hindered plant growth in acidic soil. For fertilizer release, MOF interaction with microorganisms is necessary, with rapid hydrolysis minimizing ammonium conversion to nitrate. Conventionally fertilized plants outperformed those treated with OPA-MOF, showing higher phosphorus absorption and yield. Oxalate solubility is vital for slow-release fertilizer, requiring detectable soil oxalate content meeting 1 mg/L criteria yet remaining low enough to prevent rapid chemical compound alteration. (Anstoetz et al., 2016). The findings revealed that controlled-release fertilizers exhibit a significantly low nitrogen (N_2) content, specifically at 3.1%. Consequently, this limitation restricts their practical application in agriculture.

Guo et al. synthesized "MIL-100(Fe)@CNF-SA", a cellulose-based hydrogel, by combining "MOFs, cellulose nanofibers (CNFs), and sodium alginate (SA)". Because of its porous nature, this hydrogel could store urea for progressive release and had a high water-holding capacity. When "MIL-100(Fe)@CNF-SA" was loaded with only 1.0 g, the water-holding capacity rose concurrently from 27% (control soil without treatment) to 63% (treated soil). Increased germination rate (85.0 ± 1.5%), tillers (38.0 ± 0.7 tillers per plant in 60 d), photosynthetic rate (38.0 ± 0.7 $\mu molCO_2\ m^{-2}\ s^{-1}$ in 60d), and chlorophyll content (43.8 ± 0.8 mg/g in 60 d) all showed a significant improvement in wheat development, indicating that it is a promising option for irrigated farming in water-scarce areas.

MOF-based systems are now being explored for controlled pesticide release, driven by the need for environmentally triggered release. This approach offers benefits like decreased agrochemical usage, improved control effectiveness, and reduced adverse effects. Fe-MOFs hold promise as pesticide delivery systems for eco-friendly plant protection, particularly against fungi, which are inhibited by fungicides (Shan, Xu, et al., 2020). A straightforward octahedral Fe-MOF was created by Shan and Coworkers using trimers with Fe octahedra connected by "1, 3, and 5-benzenetricarboxylate (Fe-MIL-100)". It was created as a vehicle for the fungicide 'azoxystrobin' (Shan, Cao, et al., 2020).

Considering the extensive surface area of 2251 m^2/g, Fe-MIL-100 demonstrates a satisfactory loading capacity for azoxystrobin, reaching up to 16.2% (Shan, Cao, et al., 2020). Fe-MOFs loaded with azaxystrobin (AZOX@Fe-MIL-100) show a pH-responsive initial burst followed by a continual release pattern. Additionally, "AZOX@Fe-MIL-100" has efficacious fungicidal properties against two pathogenic fungi. These are *Fusarium graminearum*-caused wheat head scab and *Phytophthora infestans*-caused tomato late blight. Furthermore, the iron supplement Fe-MIL-100 was found to have a nutritional impact in promoting wheat development (Shan, Cao, et al., 2020). The growth of the wheat was improved by 9.6% and 16.4%, respectively, after applications of 50 mg/L and 300 mg/L Fe-MIL-100.

2.2.3 Zinc Based MOFs

Zinc (Zn) plays a vital role in numerous plant proteins, but excessive amounts can be harmful. Most crops thrive within the optimal range of 30 to 200 µg Zn per gram of dry weight (DW) for their well-being (Kaur & Garg, 2021) . Protein synthesis, cell division, and expansion are just a few of the processes in which zinc, an important micronutrient, plays structural and/or catalytic functions.(Jain et al., 2010). Increased zinc concentrations in soils are phytotoxic, leading to a number of anatomical and functional defects that ultimately impair plant performance. These reactions, however, differ depending on the kind of plant species and its stage of growth (Khudsar et al., 2004; Vaillant et al., 2005). Zinc is mostly taken up by roots feeding the shoots through the

xylem from the soil solution as Zn^{2+}, although it can also be complexed with organic ligands. In high pH soils with low [Zn]bss, it is the most prevalent crop micronutrient shortage (Broadley et al., 2007).

(Mejías et al., 2021) developed a MOF that incorporates two highly promising ortho-disubstituted disulfides, referred to as "zinc zeolitic imidazolate frameworks (ZIF-8)". Through an in-situ method, the disulfide agrochemicals remained present in the medium throughout the MOF production process, enabling the synthesis of the "zinc imidazolate framework (ZIF-8)". The use of "Liédana's method" (Liédana et al., 2012) ensured entrapment of the bioactive compound in the voids present in the icosahedral MOF. DiS-NH_2 was chosen from the disulfide collection because of its ease of synthesis and simplicity. Since most disulfide compounds have structural similarities, they used the knowledge of this molecule's encapsulation to target the most promising herbicides, including acetyl derivatives. DiS-O-acetyl was selected because of its strong growth inhibition capacity against the primary weeds that infect rice, maize, and potato crops, *L. rigidum* and *E. crus-galli* (Oliveira et al., 2019)

Kaur et al. (2022) designed a "Zn-based metal-organic framework (Zn-MOF)" with a hydrophobic-hydrophilic surface characteristic that is water-stable and luminous. By employing a solvothermal technique, pamoic acid (PA) and 5,5′-dimethyl-2,2′-bipyridine (dmbpy) with free functional groups (hydroxyl and methyl groups) were combined to create the produced luminous Zn (II)-MOF

Based on a magnetic graphene oxide composite, Liu et al. (2019) created a "magnetic amino-functionalized zinc metal-organic framework". The framework has a large surface area and a porous structure, effectively adsorbing nitrogen-containing fungicides. The adsorption capacities of various fungicides, including epoxiconazole and pyraclostrobin, were found to be high at equilibrium. Both IRMOF and M-IRMOF have stable NH_2 groups on their surfaces, which are useful for pesticide adsorption. This zinc metal-organic framework shows promise as an adsorbent for extracting and measuring nitrogen-containing fungicides.

2.3 Compatibility of MOFs in Plants:

MOFs, have attracted a lot of attention in the field of materials science due to their remarkable properties and unique structures. However, in order to guarantee the safe production and application of these materials, it is imperative to carry out thorough study on the toxicity and environmental dangers related to MOF compounds (Guan et al., 2021). On the other hand, it is completely unclear how MOF chemicals could impact plant environments. Usually, it is thought that the genesis of soluble MOF toxicity is the liberation of metal ions from MOF materials (Yuan et al., 2022). Prior to large-scale fabrication and consumption, it is imperative to thoroughly investigate the environmental hazards and risks associated with MOF materials at every stage of their lifecycle, including research, development, production, distribution, application, and discharge (Sajid, 2016).

In a study by Guan and colleagues, "MOF-199, also known as HKUST-1", was examined for its phytotoxic effects on pea seedlings. The researchers compared MOF-199's impact with that of its precursor components, "Cu $(NO_3)_2$ and 1,3,5-benzenetricarboxylic acid (H_3BTC)", at equal MOF-199 doses. They assessed various parameters including germination rate, seedling growth, photosynthesis, and structural changes. Low MOF-199 concentrations (0.1 to 10 mg/L) had minimal effects, while high concentrations (100 and 1000 mg/L) were detrimental, affecting root and leaf growth. MOF-199 initially increased photosynthesis at lower doses (10 and 100 mg/L) but had a negative effect at higher concentrations (1000 mg/L). Transpiration rates increased overall, with variations in stomatal conductance. MOF-199's release of Cu^{2+} into the solution led to its bioaccumulation in seedlings, causing oxidative stress and root toxicity (Guan et al., 2021).

The "Fe-MOF" that is based on porous iron was altered by adding "ethylenediamine tetra-acetic dianhydride". Phaseolus vulgaris plants were grown in hydroponic culture using "ferrous-ethylenediamine tetra-acetic acid (Fe-EDTA), Fe-MOF, and Fe-MOF-EDTA". *Phaseolus vulgaris L*., often known as the common bean, is an annual herbaceous plant that is extensively grown for its edible fruit. While the leaves are

utilized for animal nutrition, beans are also regarded as a significant source of protein, vitamins, carbs, and antioxidant components (Granito et al., 2008). *Phaseolus vulgaris* was used to track how Fe sources affected the plant's rate of growth, chlorophyll levels, protein, and antioxidant enzyme activity. The results demonstrated that Fe-MOF-EDTA performed better than other Fe sources, particularly in terms of plant weight, which increased by 9.6% after 96 hours of treatment. Other improvements included protein and enzyme activity, chlorophyll content, and enzyme activity.

Altogether, their findings demonstrated the enrichment impact of the Fe-MOF-EDTA component in nutrient solutions, which may be used as a tactic to enhance the *Phaseolus vulgaris* plants' growth and quality metrics (Abdelhameed et al., 2019).

Agricultural properties, like biomass output, phenolic compound, and physiology, might be impacted by climate change. (N. E. Mahmoud & Abdelhameed, 2022) studied the effects of heat stress on *Sesamum indicum L*. cultivated in El-Wadi El-Gedeed conditions. They used polyamines such as “putrescine (Put), spermidine (Spd), and spermine (Spr)” coupled with a phosphoryl group cross-linker to introduce free amino groups into the network of the “titanium-organic framework (MIL-125-NH2)” in an attempt to counteract the decline in seed yield and oil content. When these modified materials were administered to *S. indicum L.*'s vegetative portion, growth metrics, chemical components, and crop yield were significantly improved. The weight of sesame seeds increased by 1.39, 1.92, and 2.16 times when treated with “Put@MIL-125-NH2, Spr@MIL-125-NH2, and Spd@MIL-125-NH2 compared to the control experiment. These findings support the advancement of sustainable modern agriculture.”

There should be some process through which the toxicity can be minimized. Ma and coworkers suggested that carbonization (the process involves subjecting stabilized precursor fibers to high-temperature pyrolysis (1000-2000°C)), resulting in the removal of hetero atoms and the development of a layered carbon structure. Prior to pyrolysis, the fibers undergo a heat treatment at temperatures of 700-900°C to remove volatiles

and maintain the fiber structure. This carbonation process gradually transforms the organic macromolecular system into a stable carbon material, forming a 3-D network of carbon atoms (Marsh & Rodríguez-Reinoso, 2006)) potentially lessening MOF materials' toxicity (Ma et al., 2021).

To prevent the uncontrolled release of agrochemicals and achieve accurate targeting of the material specifically to the roots, Bindra and colleagues have indicated that some coating can be employed to produce a biocompatible hydrophobic ecosystem surrounding the MOF substances. The researchers conducted research on the MOF-5 with Zeolite composite's (MOFZ) capacity to provide targeted nutrients, specifically urea, to tomato plants. In the study conducted, the MOFZ composite with a chitosan coating demonstrated an impressive loading capacity of 94% for urea, exhibiting sustained release characteristics when compared to uncoated MOF with a loading capacity of 62%. The "Chitosan-coated MOFZ", with its high loading capacity, proved capable of meeting the nitrogen requirements of the tomato plant (*Lycopersicum esculentum*) for a period exceeding 9 days, thus ensuring sustained nourishment (Bindra et al., 2023).

Figure 2.6

A Representation Illustrating the Use of "MOF and MOFZ" Composites for the Effective Loading and Precise Delivery of Urea to Tomato Plants (Lycopersicum esculentum) (Bindra et al., 2023)

2.4 Role of MOF in Disease Management

In research, Bouson and team investigated the antifungal capabilities of a "metal-organic framework (Cu-BTC MOF)" based on copper. With a large surface area ranging from 600 to 1600 m^2g^{-1}, a significant pore volume estimated to be approximately 0.7 cm^3g^{-1}, and excellent thermal stability up to 350°C (Janabi et al., 2015), this MOF is renowned for its water stability and industrial applicability. The efficiency of it against "*Candida albicans*, *Aspergillus niger*, *Aspergillus oryzae*, and *Fusarium oxysporum"* was examined by the researchers.

The Cu-BTC MOF showed substantial inhibitory effects, significantly retarding the development of *C. albicans* while significantly delaying the spore growth of *A. niger*, *A. oryzae*, and *F. oxysporum* (Bouson et al., 2017)**.**Cu-BTC at 100, 200, 300, 400, and 500 ppm was tested for its antifungal properties against a representative of yeasts, *C. albicans,* using the dilution plate count technique on SDA plates over a 60-minute incubation period. Results showed a drastic decrease in colonies with the increased concentrations of Cu-BTC and recorded 96% and 100% growth inhibition at 300 ppm and 500 ppm, respectively (Bouson et al., 2017).

The "HKUST-1 MOF" was effectively utilized as a biocidal agent against representative yeast and mold species. The synthesized MOF demonstrated significant antifungal capabilities against *Saccharomyces cerevisiae*, completely inhibiting its growth, while the growth of *Geotrichum candidum* was reduced from 6.16 to 1.29 CFU mL^{-1}. Over time, the crystalline structure of the material gradually deteriorated, resulting in the formation of surface extra-framework Cu(I). This led to the gradual release of copper ions into the culture medium, thereby inducing the observed antifungal effects (Chiericatti et al., 2012).

Houbraken et al (2015) carried out a study that focused on the use of metal-organic frameworks (MOFs), most especially HKUST-1. "High surface areas, tunable porosity, and microbicidal qualities" are only a few of these MOFs' remarkable qualities. Because they break down slowly in somewhat acidic environments, they are well known for

being suitable as drug release carriers. The researchers used porous HKUST-1 in their work, which quickly reacted with cholinium salt to use as a template and a deprotonation agent. This reaction produced the new antibacterial system known as "Imazalil IL-3@HKUST-1" in an aqueous solution at room temperature. In addition, imazalil is sensitive to sunlight, which results in its short half-life and low utilization efficiency in farming. Imazalil IL-3@HKUST-1 had a synergistic impact in suppressing pathogenic fungus and bacteria, demonstrating great efficacy. Its prolonged release of the essential ingredient, imazalil, over the course of six days following treatment, was especially notable.

Compared to imazalil used alone, this gradual and continuous release demonstrated better sustainability and microbicidal action. Imazalil is a fungicide that is commonly used to treat a variety of plant diseases, such as "rice blast (*Magnaporthe grisea*) and gray mold (*Botrytis cinerea*)". Its chemical name is "4,6-dimethyl-N-phenylpyrimidin-2-amine". Nevertheless, volatilization and photosensitivity are known to cause problems for imazalil, which shortens its half-life and decreases its effectiveness in agricultural applications. (Tang et al., 2019).

Sierra-Serrano et al (2022) have created a novel "2D-MOF (GR-MOF-7)" based on the popular antibacterial and fungicide Cu^{2+} and the herbicide glufosinate. One independent Cu^{2+} ion and one Glu^{2-} ligand molecule makes up the asymmetric unit of "GR-MOF-7", which crystallizes to form a monoclinic P21/c space group. The possible combination of bactericidal and herbicidal impact of GR-MOF-7 was examined in light of the noteworthy antibacterial activity of Cu-based compounds in agriculture. By demonstrating significant antibacterial action against agricultural animal pathogens, such as "*Staphylococcus aureus* and *Escherichia coli"*, GR-MOF-7 outperforms its separate or even physically combined predecessors, "glufosinate and Cu $(NO_3)_2$". Additionally, it works well as a pesticide to stop the invasive species *Raphanus sativus* from germinating and growing on berries and vine crops. This shows that building MOFs with herbicide and antibacterial/antifungal units is a viable method of producing multifunctional agrochemicals. Also it has strong water stability (lasting for five days).

Wang and team developed a novel technique for delivering supramolecular fungicides. They designed and constructed an integrated nano platform using “benzimidazole-modified NH2-MIL-101(Fe)” as carriers loaded with osthole (OS), a natural compound derived from *Cnidium monnieri*. The resulting “β-CD@B-MIL-101(Fe)-OS” system served as a controlled release system with β-cyclodextrin acting as nano valves. This platform demonstrated efficacy in eradicating powdery mildew and gray mold caused by *Botrytis cinerea*. By autonomously releasing ostholein within the oxalic acid microenvironment produced by *B. cinerea,* it effectively protected tomatoes from infection during the maturation phase (Wang et al., 2023).

Figure 2.7

Structure of Osthole

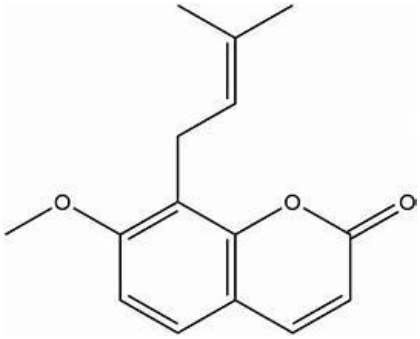

A novel hybrid structure composed of two types of metal-organic frameworks (MOFs), designed for intelligent pest and fungus management, was developed by (Ma et al., 2023). The core of this hybrid consists of “zirconium-based metal-organic framework” nanoparticles known as “UIO”, which were used to encapsulate the insecticide dinotefuran (DNF). Simultaneously, a secondary MOF layer composed of the fungicide tebuconazole (Teb) was formed in situ, effectively creating a satellite structure on the core MOF. This innovative approach to pesticide release is aimed at minimizing unnecessary losses and enhancing the efficiency of pesticide utilization. Moreover, it imparts the MOF-on-MOF hybrid with bioactivity comparable to that of “DNF and Teb”, even when using the same concentration of active ingredients. At 3.0 mg/L, army worm mortality was 87%, and at 4.0 mg/L of MOF-on-MOF hybrid, the inhibition ratio

against fungi was 98%. It offers a clever method for controlling several crop diseases at once and creating multi-agrochemical formulations in a single system with separate stimuli-responsive release properties.

According to (Linxin et al., 2020) the ligands required for "(E)-bis (p-3-nitrobenzoic acid) vinyl ($C_{16}H_{10}N_2O_8$)" were synthesized through a three-step process. Subsequently, the "MOF-$Zn_2(EBNB)_2(BPY)_2 \cdot 2H_2O$" was created using a solvothermal method. This MOF was then examined for its ability to load and release pesticides, with jinggangmycin and avermectin serving as representative models for water-soluble and oil-soluble pesticides, respectively. The findings revealed that the maximum loading capacity of "$Zn_2(EBNB)_2(BPY)_2 \cdot 2H_2O$" for jinggangmycin and avermectin was 0.346 g/g and 0.304 g/g, respectively. The pesticide delivery system exhibited a two-phase mode, and over 84 hours, the cumulative release of jinggangmycin reached 76.8%, while that of avermectin reached 73.8%, indicating a significant slow-release effect. Additionally, when compared to a control group using a "jinggangmycin-avermectin wettable powder", the sustained-release system demonstrated superior efficacy in inhibiting *Rhizoctonia graminearum*.(Wu et al., 2019) synthesized a Zinc metal-organic framework (Zn@MOF) by mixing zinc nitrate hexahydrate and 2-aminoterephthalic acid in N, N-dimethylformamide (DMF). "Thymol" was subsequently loaded into the Zn@MOF at a rate of 3.96%, as determined by thermogravimetric analysis (TGA). The antibacterial effectiveness of thymol-loaded Zn@MOF (T-Zn@MOF) with 0.029 g/100 g active thymol loading was tested against a three-strain mix of E. coli O157:H7 in tryptic soy broth (TSB). E. coli O157:H7 growth in T-Zn@MOF was inhibited, with no exponential growth phase after 24 hours of incubation, likely due to the sustained release of thymol within the porous Zn@MOF through noncovalent interactions.

Xu et al (2023) prepared a "copper-doped ZIF-8 bimetallic MOF nanoparticles (Cu@ZIF-8)" which were created as nanocarriers by in-situ ZIF-8 fabrication. They used to develop "Fludioxonil-loaded Cu@ZIF-8 (Flu@Cu@ZIF-8)" with a 23.9% loading content. These nanoparticles had an average size of about 80 nm.

"Flu@Cu@ZIF-8" demonstrated acid-responsive release, releasing 79.5%, 69.9%, and 43.0% of the payload at pH 5, 7, and 9, respectively, over 48 hours. It displayed similar inhibitory effects on *Fusarium graminearum*, a cereal crop pathogen, compared to free Fludioxonil. *Fusarium graminearum* can cause the development of toxic secondary metabolites, endangering human health and causing financial losses in agriculture (Merhej et al., 2011) . *Fusarium graminearum* thrives in acidic conditions and produces harmful secondary metabolites like deoxynivalenol. The slow release of "Fludioxonil" from "Flu@Cu@ZIF-8" was slightly less effective than free Fludioxonil at concentrations below 0.03 mg L^{-1}. Both Flu TC and Flu@Cu@ZIF-8 had similar fungicidal activity with EC50 values of 0.041 mg L^{-1} and 0.038 mg L^{-1}, respectively. Cu@ZIF-8 exhibited no fungicidal activity at any tested dose.

A versatile approach was used by (Dong et al., 2021) to create smart and biodegradable MOF nano pesticides known as "MIL-101(FeIII)" gated with "FeIII-tannic acid (TA) networks". These nano pesticides offer seven responsive behaviors, including reactions to pH levels, H_2O_2, glutathione, phosphates, ethylenediaminetetraacetate, and near-infrared sunlight. Each of these stimuli corresponds to environmental conditions in agriculture. The nanocarriers are biocompatible and eventually break down, reducing the risk of bioaccumulation in crops. The release mechanisms for these stimuli are well-defined. Furthermore, natural polyphenolic compounds improve the adherence and retention of nano pesticides on the surfaces of hydrophobic plants. Strong antifungal effects against *Fusarium graminearum* (wheat head blight) and *Rhizoctonia solani* (rice sheath blight) were demonstrated by nano pesticides loaded with the fungicide tebuconazole. They are safe for wheat plant growth, seedling emergence, and seed germination. Furthermore, in greenhouse environments, they successfully suppress *Blumeria graminis* caused wheat powdery mildew. These nano pesticides have the potential to increase the yield and quality of agricultural output.

The frequent application of fungicides raises concerns about potential environmental harm in addition to resistance issues. (Kumar et al., 2017) described the synthesis and controlled release study of a carbendazim polymeric nano formulation made with pectin and chitosan. The size of the nanoparticles was usually in the range of 70 to 90 nm. The nano formulated carbendazim showed 100% suppression of *Aspergillus parasiticus* and sustained release of *Fusarium oxysporum* at dosages of 0.5 and 1.0 ppm. On the other hand, commercial products and pure carbendazim showed lower inhibition rates. Furthermore, the phytotoxicity of the nano formulation had less of an impact on the germination and root development of *Cucumis sativa*, *Zea mays*, and *Lycopersicum esculantum* seeds.

2.5 Chapter Summary

The protection of natural resources is the main sustainability issue posed by agrochemical contamination in the modern era. Exploration of innovative Metal-Organic Frameworks (MOFs) with remarkable ion-exchange capabilities is a viable approach to solving this problem. The success of this project in creating MOFs with customized properties hinges on meticulously choosing organic linkers and functional groups, along with appropriate metal ions Additionally, improving the MOF materials' sorption kinetics by the modification of porosity is a smart move. The optimization of porosity is anticipated to enable MOFs to exhibit improved sorption kinetics, thereby bolstering their effectiveness in reducing agrochemical pollution and promoting sustainability in the agricultural sector. These benefits shall be made possible by the application of established synthetic methodologies for MOF design and construction.

The crucial role that MOFs and their related composite materials are set to play in the field of agrochemical encapsulation and release has been confirmed by extensive academic research, exhibiting clear advantages over the currently used commercial approaches. However, considering that the bulk of previous studies have mostly taken place in controlled laboratory settings, it is crucial to emphasize that the stability of MOFs under real-world field circumstances needs intense inspection in upcoming research attempts. Furthermore, considering the agricultural environment in which these materials are meant to function, a thorough assessment of the toxicity and

solubility profiles of the component building blocks and metal nodes employed in the synthesis of MOFs is urgently required. Over the past two to three years, there has been a discernible rise in research articles, the majority of which concentrate on the encapsulation and controlled delivery of pesticides. It is important to highlight that the extensive investigation of fertilizer encapsulation inside MOFs in 2015 marked the beginning of this field. In fact, the number of recent studies brings to light the clear gaps and untapped areas for further study.

Given these factors, it is necessary to provide future recommendations designed to advance this emerging subject into commercial-scale applications. Several MOF opportunities in the agriculture sector deserve careful consideration. The exorbitant cost of MOFs now prevents their large-scale manufacture, necessitating coordinated efforts to create inexpensive ligands and metals for their synthesis. To improve encapsulation effectiveness, stability, and controlled release of agrochemicals, it is also crucial to optimize surface characteristics and increase active sites inside MOFs. Furthermore, a viable method of reducing the problem of agrochemicals' first burst release is the hybridization of MOFs with other materials. Also, it is necessary to improve the procedures for applying MOFs in agriculture and enhance the synthesis processes. In this sense, the current work contributes to the engineering and use of these existing and developing materials for agricultural field-based applications.

CHAPTER 3
METHODOLOGY

3.1 Research Flow Chart

The outline of this research can be expressed in the following Figure 3.1

Figure 3.1

Illustration of the Research Flow Chart

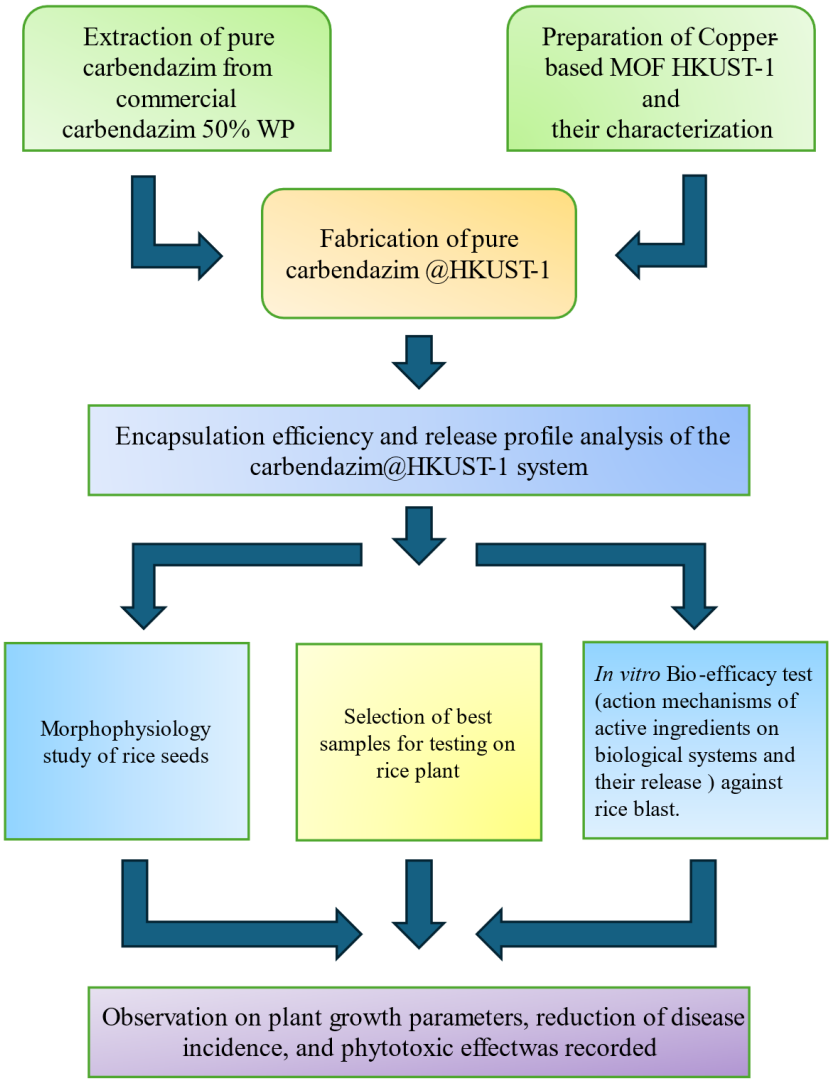

3.2 Materials and Methods

HKUST-1 is a well-known copper-based Metal-Organic Framework (MOF) synthesized utilizing basic copper carbonate (BCC; $Cu_2CO_3(OH)_2$) as the metal sourceand 1,3,5-Benzene tricarboxylic acid (H_3BTC) as the ligand. The reaction was conducted at room temperature in water and ethanol, enhancing its environmental sustainability. In the course of creating HKUST-1, carbendazim, a systemic and broad-spectrum benzimidazole fungicide, was encapsulated. The encapsulation efficiencyand release profiles were assessed. The commercial Carbendazim 50%WP (purchasedfrom the local market) was purified by either extraction with ethanol or crystallization from DMF/H_2O. Then, to create carbendazim@HKUST-1, the active components (pure form of carbendazim) were used as guest molecules. Additionally, as a crucial element of this research, the National Science and Development Agency (a Thai government organization promoting science and technology research and its economic applications) provided the rice varieties "PTT-1(Pathum Thani 1)" is a photoperiod-insensitive, aromatic Thai rice variety that is grown year- round) and "KDML 105 (Khao Dowk Mali 105)" commonly called Jasmine rice. Also, the mother culture of the Rice blast pathogen "*Magnaporthe grisea"* was provided by them. Research and activities concerning pathogens and plants were conducted at this location.

3.2.1 Fabrication of HKUST-1 from Basic Copper Carbonate (BCC)

200 mg BCC (0.90 mmol) and 210 mg of H_3BTC (1mmol) were stirred into 6.5 mL of an EtOH/water 1:1 solvent mixture (Riccò et al., 2018). Following a three-hour incubation period, the samples were undergone a regulated centrifugation procedure that lasts 10 minutes and rotates at a rate of 20 revolutions per minute. After centrifugation, the remaining supernatants must be carefully collected in order to conduct UV-visible spectroscopic analysis to determine whether unreacted H_3BTC molecules may be present. The precipitate, designated as HKUST-1, was thoroughly washed with water and ethanol before being dried for the purpose of further characterization.

Figure 3.2

Diagram for the Preparation of the Copper-Based "Metal-Organic Framework HKUST-1"

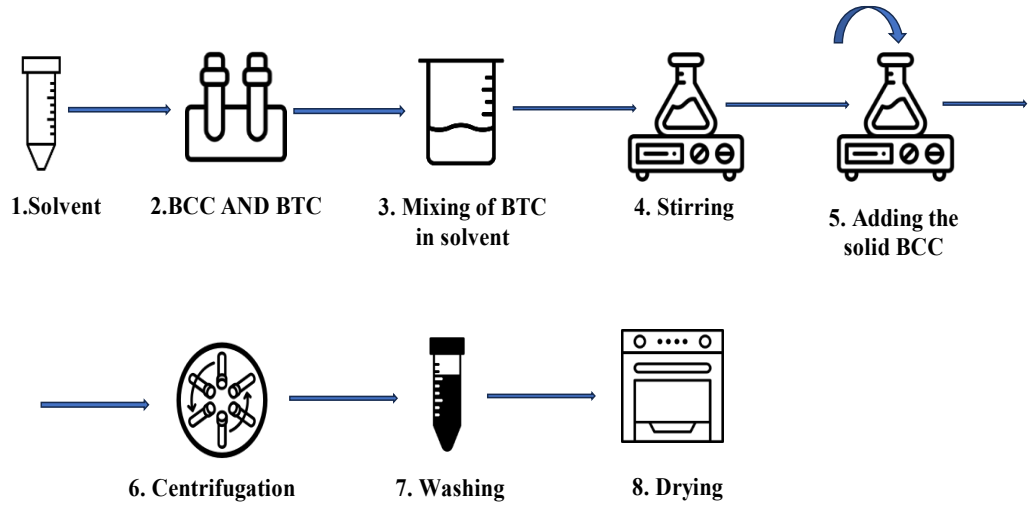

3.2.2 Extraction of Pure Carbendazim from Commercial Carbendazim 50%WP

Carbendazim has a solubility of 5 mg/mL of Dimethylformamide (DMF), however, the commercial formulation is 50%, therefore a double amount was used for extraction. The commercial product (5 g), when suspended in 500 ml N, N-Dimethylformamide (DMF), was stirred overnight, followed by filtration. The non-soluble particles were successfully isolated using this technique. The resulting supernatant was subsequently precipitated by the gradual addition of water (the quantity of which was variable, as precipitation ceased upon saturation), followed by further purification through filtration and washing. This approach enabled the recovery of carbendazim in a noticeably high-purity form by selectively removing the solvent from the supernatant under carefully monitored circumstances. In the context of chemical analysis, this technique was crucial because it guarantees the separation of the required component with an extraordinarily high level of purity.

Figure 3.3

Process Flow Diagram for the Extraction

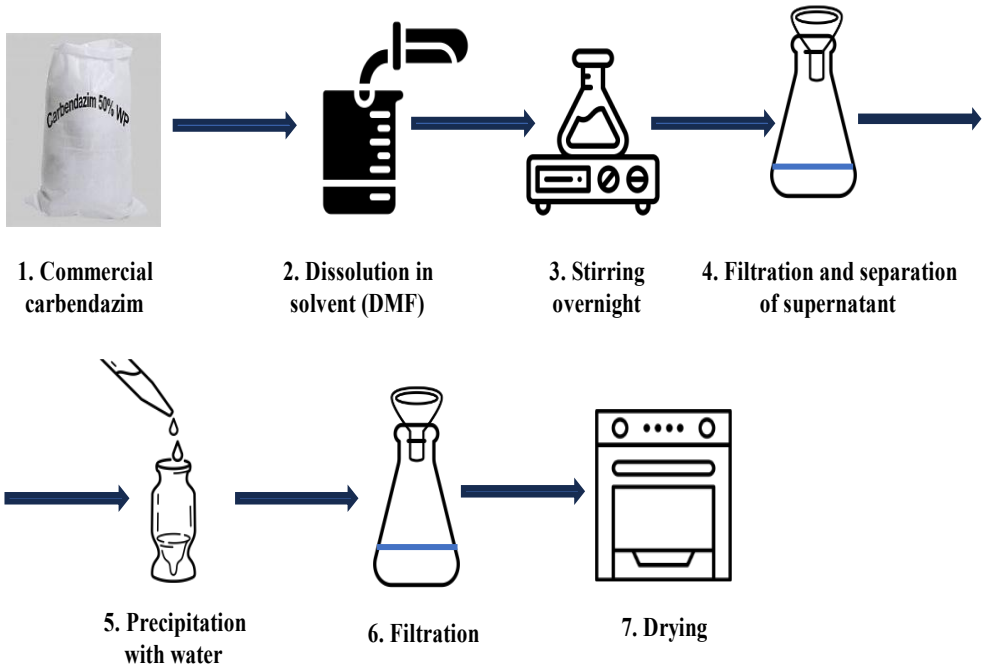

Finally, using the following Eqn. 3.1, the construction percentages were determined

$$\text{Percentage of Agrochemicals} = \frac{Initial\ weight - Final\ weight}{Initial\ weight} \quad (3.1)$$

3.2.3 Fabrication of Carbendazim@HKUST-1 (CB@HKUST-1)

The solvents (ethanol: water=1:1, 25 ml), basic copper carbonate (BCC) (1.0 g), and trimesic acid (H_3BTC) (1.05 g) were used. Then carbendazim was added at molar ratios of 1:2, 1:4, and 1:8 with respect to the ligand BTC. Based on the high encapsulation efficiency, one ratio was finalized. Then, that amount was introduced during the synthesis of HKUST-1. After the fabrication of carbendazim @HKUST-1, the powders were washed with ethanol and water to remove the surface adsorption.

Figure 3.4

Synthesis of Carbendazim @HKUST-1

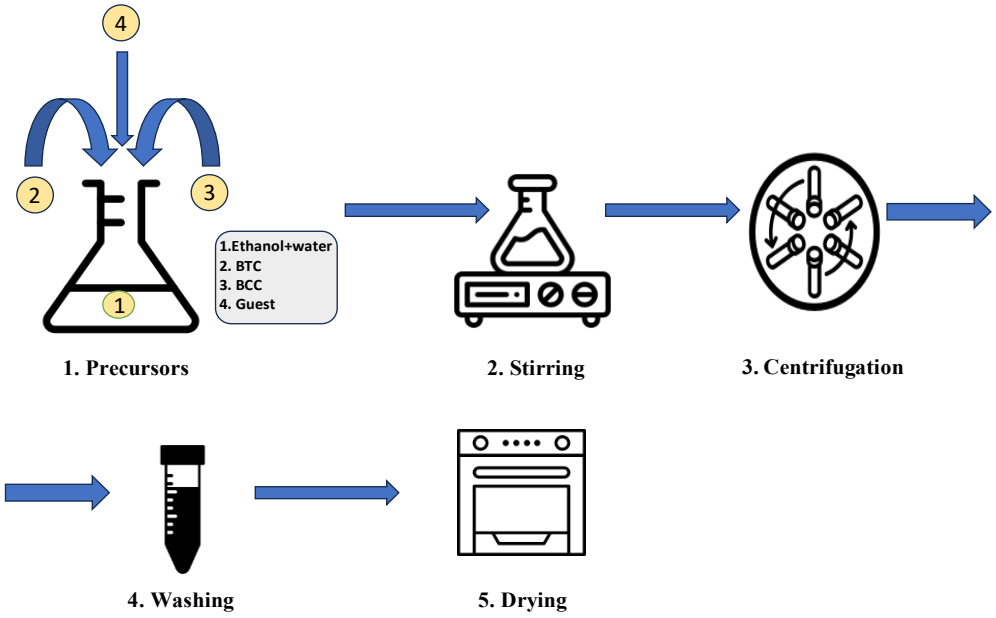

Carbendazim encapsulation was assessed by a stepwise increase of its amount in the reaction mixture. The chosen strategy involved the preparation of three samples in which the precursors' concentrations were kept constant, while carbendazim is added at molar ratios of 1:2, 1:4, and 1:8 with respect to the ligand BTC. The residual carbendazim is monitored by UV-visible analysis before and after the reaction. Samples of the supernatants will be taken at certain intervals, including zero minutes, one hour, three hours, six hours, eight hours, and twelve hours. The U.V. of the supernatants aftercentrifuging will be used to calculate the encapsulation efficiency (EE%). Also, concentrations will be obtained against a calibration curve. The supernatants will offer UV peaks for different sorts of guests at certain wavelengths.

In this experiment, UV spectroscopy will be used to detect the carbendazim. Carbendazim is detected at 280-284nm, indicating their absorbance maxima. Similar types of peaks were found by (Boudina et al., 2003; Meszlényi et al., 1990; Panadés etal., 2000).

The EE% will be calculated using the following Eqn.3.2.

Encapsulation Efficiency (EE%) = $\frac{Ci-Cf}{Ci}$ x 100

(3.2)

Where *Ci* is the initial concentration, and C_f is the final concentration of carbendazim in the supernatant.

3.2.4 Releasing Behavior of Guests

The encapsulation process that was used to analyze the release profiles of encapsulated visitors in the HKUST-1 framework was repeated to analyze the releasing attributes. Several concentrations (3 mg/mL, 2 mg/mL, 1 mg/mL, 0.5 mg/mL, and 0.25 mg/mL) were used in the study to examine how agrochemicals released from the HKUST-1 template. Particular concentration ratio was examined in order to determine an ideal release profile.

The releasing kinetics were clarified by using UV spectrophotometry to measure the concentration of released guests in the solvent. Plotting the release efficiency percentage versus time showed the percentage of encapsulated guests that were released over time. A model called “Korsmeyer-Peppas” was chosen to match the release efficiency curve in a way that would appropriately depict the releasing behavior (Bayer, 2023). In order to provide a thorough knowledge of the encapsulation and release dynamics inside the HKUST-1 framework, this decision was essential for clarifying the underlying kinetics and processes regulating the release process.

3.2.5 Characterization

Table 3.1

Techniques and Uses for Characterization

Techniques	Use
UV Spectroscopy	To obtain the absorbance spectra of a compound
Fourier Transform Infrared Spectroscopy (FTIR)	Identification of the chemical bonds present in the particle
High Performance Liquid Chromatography (HPLC)	To identity and quantify a particular analyte or compound.
X-Ray Diffraction (XRD)	To identify the crystallographic structure of a material.
Inductively Coupled Plasma Atomic Emission Spectroscopy (ICP)	To analyze the release of copper ions.

3.3 Application of Fungi and Rice Plants

3.3.1 Cleaning and Sterilization of Glass Wares for Fungi Inoculation

All glassware that will be used in this experiment must first go through a stringent cleaning procedure that includes treatment with an acid solution including aqua regia (a mixture of “nitric acid and hydro chloric acid, diluted sulfuric acid, chromic acid solutions piranha solution and fuming sulfuric acid”), a subsequent rinse with distilled water, and careful air drying at room temperature. After being thoroughly cleaned, theglassware must be properly sterilized. This involves wrapping each piece in brown paper and placing it in an autoclave (SX-700 230V). The process of sterilization must be carried out at 121 ℃ for 20 minutes while maintaining a 1 bar pressure. The disinfected glassware should then go through an additional 2 hours of sterilization in ahot air oven (Equitron, Oven Stream Series) set at 180 °

3.3.2 Preparation of Media (Rice Polish Agar Media)

It is necessary to carefully measure and fill a one-liter beaker with a 500 ml aliquot of distilled water. The beakers were then be filled with 20 g of rice polish before the mixture was gently boiled in water for 20 minutes. In addition, a second one-liter beaker containing 500 ml of distilled water was heated. Within this beaker, precisely weighed quantities of yeast extract (2 g) and agar (15 g) were to be meticulously incorporated and thoroughly homogenized.

3.3.3 Isolation, Purification, and Preservation of the Pathogen

Biotech Laboratory of "The National Science and Technology Development Agency (NSTDA)" in Thailand provided a pure culture, which was used to aseptically isolate the pathogenic organism (*Magnaporthe grisea*). The hyphal tip method, a precise and well-known approach in the field of microbiological practice, was used in the purification procedure and carried out under strict and regulated laboratory circumstances. On specialized petri plates that were supplemented with RPA (Rice PolishAgar) growth medium, the painstakingly acquired pure pathogenic culture was reproduced and preserved in order to maintain genetic integrity. This was provided the best circumstances for its growth.

Sub-culturing intervals of 30 days were followed periodically to preserve the axenic integrity of the culture. This sub-culturing procedure used both slant cultures and Petriplate cultures. These sub cultured derivatives were carefully stored in a special refrigeration unit at a temperature of 4°C in order to protect the pathogenic culture's long-term vitality and stability. The pathogenic microorganism, thus conserved and authenticated, were subsequently served as a valuable and controlled resource for ongoing and forthcoming research endeavors, contributing to the advancement of scientific knowledge in the field.

3.3.4 Effect of Pure Carbendazim, HKUST-1 and Carbendazim@HKUST-1 on Germination of Rice Seeds

To determine the impact of pure CB, HKUST-1, and CB@HKUST-1 on the ability of rice seeds to germinate, rice (cultivar- PTT-1) was selected. It was collected from Biotech Laboratory, NSTDA, Thailand. All these products were prepared in different concentrations ranging from 1, 10, 50, 100, 200, 300, 400, 500, 750, and 1500 µg/ml respectively, and comparison was made with commercial carbendazim 1500 µg/ml, along with the control having sterile distilled water. All treatments were replicated four times. The seeds were treated with different concentrations of pure carbendazim for 6 hours. The treated seeds were placed in petri plates having sterile filter paper. Observation of seed germination percentage, root and shoot length, speed of germination, vigor index, etc. were recorded. The treatment combinations with four replications used for this study is described in the table 3.2.

Table 3.2

Treatments of Pure Carbendazim, HKUST-1, and CB@HKUST-1 on Germination of Rice Seeds

Pure carbendazim	**HKUST-1**	**Carbendazim@HKUST-1**
T1: Seeds alone (Control)	T1: Seeds alone (Control)	T1: Seeds alone (Control)
T2: T1 + CB @1 µg/ml	T2:T1 + HKUST-1@ 1µg/ml	T2: T1+CB@HKUST-1@ 1 µg/ml
T3: T1 + CB@10 µg/ml	T3:T1 + HKUST-1@ 10µg/ml	T3: T1 + CB@HKUST-1@ 10 µg/ml
T4:T1 + CB@50µg/ml	T4: T1 + HKUST-1@ 50µg/ml	T4: T1 + CB@HKUST-1@ 50 µg/ml
T5: T1 + CB@100 µg/ml	T5: T1 + HKUST-1@ 100 µg/ml	T5: T1 + CB@HKUST-1@ 100 µg/ml
T6: T1 + CB@200 µg/ml	T6: T1 + HKUST-1@ 200 µg/ml	T6: T1 + CB@HKUST-1@ 200 µg/ml
T7: T1 + CB@300 µg/ml	T7: T1 + HKUST-1@ 300 µg/ml	T7: T1 + CB@HKUST-1@ 300 µg/ml

Pure carbendazim	HKUST-1	Carbendazim@HKUST-1
T8: T1 + CB@400 µg/ml	T8: T1 + HKUST-1@ 400 µg/ml	T8: T1 + CB@HKUST-1@ 400 µg/ml
T9: T1 + CB@500 µg/ml	T9: T1 + HKUST-1@ 500 µg/ml	T9: T1 + CB@HKUST-1@ 500 µg/ml
T10: T1 +CB@750 µg/ml	T10: T1 + HKUST-1@ 750 µg/ml	T10: T1 + CB@HKUST-1@ 750 µg/ml
T11: T1 + CB@1500 µg/ml	T11: T1+HKUST1@ 1500 µg/ml	T11: T1 + CB@HKUST-1@ 1500 µg/ml
T12: T1 + CB@2000 µg/ml	T12: T1 + HKUST-1@ 2000 µg/ml	T12: T1 + CB@HKUST-1@ 2000 µg/ml
T13: T1 + CB@3000µg/ml	T13: T1 + HKUST-1@ 3000 µg/ml	T13: T1 + CB@HKUST-1@ 3000 µg/ml
T14: T1 + commercial CB @ 1500 µg/ml	T14: T1 + commercial CB @ 1500µg/ml	T14: T1 + commercial CB @ 1500 µg/ml

"Germination percentage (GP)" was calculated by using the following formula

$$\text{Germination Percentage \%} = \frac{\textit{Number of seeds germinated}}{\textit{Total number of seeds}} \text{x100} \quad (3.3)$$

"Accumulated germination rate (AGR)" and "daily germination rate (DGR)" in each petri is calculated by the following two equations

$$\text{AGR} = \frac{(\sum \textit{GPi})}{\textit{i}} \text{ where i is the day after seed set in these chambers} \quad (3.4)$$

DGR= The newly germinated seed number per day/10 in each Petri dish. (3.5)

To calculate the vigor index following formula was used.

Vigor Index (VI) = Germination (%) x Seedling length (cm) (3.6)

3.3.5 In Vitro Efficacy of HKUST-1 and Precursors against Rice Blast

The efficacy of HKUST-1 and CB @HKUST-1 against *Magnaporthe grisea* was evaluated in vitro using the poisoned food technique as described by (Hajano etal., 2012). The growth media RPA was used for the experimentation. The media was sterilized in an autoclave at 15psi (121°C) for 20 min. The experiments were conducted in a UV-sterilized laminar airflow cabinet. Different concentrations (375, 500, 750, 1000, and 1500 μg ml^{-1}) of HKUST-1 and CB @HKUST-1 against *Magnaporthe grisea* μg ml-1 were added to the media using a pipette.

The media was poured into sterilized petri plates, allowed to solidify, and inoculated with an actively growing mycelial disc of 5 mm diameter size using a flame-sterilized inoculation loop. The plates were then sealed with parafilm strips. Incubation of the fungal pathogens were carried out at a temperature of 28±2°C with a relative humidity of 60±5%. Commercial fungicides CB 50% WP, at concentrations of 1500 μg/ ml,was used for comparison. The radial growth of the fungi was measured after the controlplates achieved full growth, and the inhibition percentage was calculated using the formula (Suryadi et al., 2013)

$$\text{Inhibition Percentage, } I = \frac{C-T}{C} \times 100 \qquad (3.7)$$

Where, I= percent Inhibition, C is radial growth/diameter in control (cm), and T is radial growth/diameter in treatment (cm).

3.3.6 Effect of HKUST-1 and CB@HKUST-1 on Rice Plants under a Controlled Environment

The efficacy of HKUST-1 and CB@HKUST-1 were evaluated during the Dec 2023-Feb 2024 against the rice blast disease caused by *Magnaporthe grisea*, a dreadful foliar rice disease prevalent in Thailand and all over the rice-growing countriesof the world. A susceptible variety of rice PTT-1 and a resistible variety KDML 105 were used for the study. Controlled environment chambers were used for the experiments.

A total of 3 concentrations were selected from the invitro efficacy test and based on those concentrations of HKUST-1 and CB@HKUST-1 foliar spray (FS) was used against negative control (only pathogen inoculated), absolute control (water spray), and commercial fungicides (CB 50% WP @ 1500 mg L^{-1}) with five replications in Randomized Completely Block Design (RCBD) were studied.

The treatment combinations with five replications were used for this study as shown in the table 3.3.

Table 3.3

Treatments of HKUST-1 and CB@HKUST-1 on Rice Plants under a Controlled Environment

HKUST-1	**CB@HKUST-1**
T1: Control (spray with water only) + *M. grisea*	T1: Control (spray with water only) + *M. grise**a***
T2: Foliar Spray (FS) of HKUST-1@ "X" µg/ml+ 48 hrs. after of inoculation of *M. grisea*	T2: FS of CB @HKUST-1@ **"**X" µg/ml + 48 hrs. after inoculation of *M. grisea*
T3: FS of HKUST-1@ "Y" µg/ml + 48hrs. after inoculation of *M. grisea*	T3: FS of CB @HKUST-1@ **"**Y" µg/ml + 48 hrs. after inoculationof *M. grisea*
T4: FS of HKUST-1@ "Z" µg/ml + 48 hrs. after inoculation of *M. grisea*	T4: FS of CB @HKUST-1@"Z" µg/ml + 48 hrs. after inoculation of *M. grisea*
T5: FS of CB @1500 µg/ml + 48 hrs. after inoculation of *M. grisea*	T5: FS of CB @1500 mg/ml + 48 hrs. after inoculation of *M. grisea*

3.3.7 Mass Multiplication and Preparation of Inoculums

To prepare the inoculum of *M. grisea*, RPA media was utilized. Once the fungal growth becomes darker spore concentration were measured with a Hemocytometer and inoculum concentration $1x10^6$-$1x10^8$ spore per ml were used for inoculation in the treated pot and in control at 8 days after transplanting in controlled environmental conditions. The inoculum was sprayed after 48 hours of the chemicals (HKUST-1 and CB @HKUST-1) sprayed. Observation on disease incidence and reduction of disease were calculated as per disease scale 0-9 of IRRI (Aslam Khan et al., 2011).

3.3.8 Morphological Analysis of the Rice Plants

Following a 12-day chemical treatment regimen, morphological assessments were conducted on both diseased and non-diseased plants for both of the rice varieties. Parameters including root length and shoot length were measured to gauge the impact of the treatment. Moreover, root and shoot biomass were determined through the meticulous collection and subsequent oven-drying of roots and shoots separately over a period of 48 hours. Furthermore, the enumeration of leaf numbers was carried out for both diseased and non-diseased specimens, thereby enriching the comprehensive analysis of the experimental outcomes. Again, the disease index was calculated based on the disease scoring. The typical symptoms of blast disease generally started to appear around 3-4 DAI. To evaluate the effectiveness of CB @HKUST-1 in managing disease, disease data were periodically recorded. Disease scoring was conducted twice on the 7th and 15th DAI using a 0-9 scale, as outlined in Table 3.4. The "percent disease index (PDI) or severity" was calculated using the formula provided by (Naveenkumar et al., 2022)

$$\text{Percent Disease Index} = \frac{Sum\ of\ all\ ratings}{Total\ number\ of\ observation\ X\ Maximum\ rating\ scale} \text{ X } 100$$

Table 3.4

Disease Rating Scale (1-9) of Rice Blast (Aslam Khan et al., 2011)

Scale	Description	Host Behavior
0	No lesions observed.	Highly resistant
1	Small brown speaks of pinpoint size	Resistant
2	Small roundish to slightly elongated necrotic grey spots about 1-2 mm in diameter with distinct brown margins. Lesions are mostly foundon lower leaves	Moderately resistant
3	Lesion type is the same as in scale 2, but a significant number of lesions are one on upper leaves.	Moderately resistant
4	Typical susceptible blast lesion, 3 mm or longer infecting lesions than 2% of leaf area.	Moderately resistant
5	Typical blast lesion infecting 2-10% of the leaf area	Moderately resistant
6	Typical blast lesion infecting 11-25% of the leaf area	Susceptible
7	Typical blast lesion infecting 26-50% of the leaf area.	Susceptible
8	Typical blast lesion infecting 51-75% of the leaf area many leaves are dead	Highly Susceptible
9	More than 75% leaf are affected	Highly Susceptible

3.3.9 Physiological Analysis of the Rice Plants

In the realm of physiological analysis encompassing both diseased and non-diseased varieties of rice plants, leaf greenness served as a pivotal parameter, quantified meticulously via the SPAD (Soil Plant Analysis Development) meter. This measurement facilitated the discernment of nuanced physiological responses of the plants to the experimental treatments applied. Furthermore, in-depth investigation delved into the realm of phytochemical analysis, focusing particularly on phenolic compounds and flavonoids. Measuring phenolic compounds and flavonoids holds significant importance in plant physiology and agricultural research due to their multifaceted roles and potential implications as defense mechanisms against pathogens,

regulation of plant growth and development. A meticulous procedural approach was adopted for each analysis, ensuring accuracy and reliability in the obtained results. The leaf samples underwent initial preservation by storage at -20°C for a duration of 48 hours to maintain sample integrity. Subsequently, to facilitate efficient extraction of phenolic compounds and flavonoids, the preserved leaf samples were finely ground using liquid nitrogen. This cryogenic grinding method ensures rapid and effective disruption of cell structures, allowing for the release of target compounds from the plant matrix while minimizing degradation.

Following grinding, the leaf material was carefully weighed to obtain a standardized sample size of 50 mg, ensuring consistency and accuracy across analyses. The extraction process, outlines the subsequent steps involved in isolating phenolic compounds and flavonoids from the prepared leaf samples. This systematic procedure serves as a critical foundation for downstream analyses aimed at quantifying and characterizing the bioactive constituents present in the plant material. The process is mentioned below.

a. Collect 50 mg of dried sample of rice leaf.
b. Mix the sample with 1 ml of 60% ethanol
c. Sonicate the mixture for 15 minutes.
d. After cooling down, centrifuge the mixture at 500 rpm for 10 minutes.
e. Incubate the resulting solution at 60 °C for 15-30 minutes

Following the completion of the extraction process, the subsequent phase entailed the analysis of phenolic compounds. This stage comprised a systematic sequence of constituents extracted from the leaf samples. The methodological framework delineated in following steps served as a comprehensive guide throughout the analytical process, meticulously crafted to uphold standards of reproducibility and accuracy, thereby enhancing the reliability of the obtained results.

a. Take 50 µl of extracted supernatant.
b. Add 250 µl of 10% Folin–Ciocalteu.
c. Incubate the mixture in the dark for 5-10 minutes.
d. Add 700 µl of 7.5% Na_2CO_3.
e. Incubate the mixture in the dark for at least 30 minutes.
f. Check the absorbance at 765 nm using UV spectroscopy.

To establish a standard curve, it is imperative to utilize various concentrations of Gallic acid monohydrate as the standard. Subsequently, these concentrations should be correlated with the corresponding absorbance values obtained from spectrophotometric analysis. This allows for the determination of a linear relationship between concentration and absorbance, facilitating the quantification of phenolic compounds present in the sample. Upon obtaining absorbance readings, the concentration of phenolic compounds can be calculated by dividing the absorbance values by the mass of the sample subjected to grinding, thereby yielding the final concentration of phenolic compounds in the solution. This meticulous procedure ensures the accuracy and reliability of the phenolic compound quantification process.

Following the extraction process, a systematic procedure was adhered to for the analysis of flavonoids, as elucidated in the following steps This procedure delineated a sequence of steps aimed at discerning and quantifying the flavonoid constituents extracted from the leaf samples.

a. Take 100 µl of extracted supernatant.
b. Add 300 µl of 10% methanol (99.99%).
c. Add 20 µl of 10% AlCl3.
d. Add 20 µl of 1M potassium acetate.
e. Add 560 µl of distilled water (DI H2O).
f. Incubate the mixture for at least 30 minutes at room temperature.
g. Check the absorbance at 415 nm using UV spectroscopy.

In the determination of flavonoids, a standard curve must similarly be constructed utilizing varying concentrations of Quercetin as the reference standard. Through this process, absorbance values corresponding to each concentration can be measured using spectrophotometric techniques. This facilitates the establishment of a linear relationship between concentration and absorbance, enabling the accurate quantification of flavonoids within the sample. Following absorbance measurements, the calculation of flavonoid concentrations entails dividing the absorbance values by the mass of the sample subjected to grinding, yielding the final concentration of flavonoids present. This systematic approach ensures precision and reliability in the quantification of flavonoid content within the analyzed sample.

CHAPTER 4
RESULTS AND DISCUSSION

This chapter outlines the research findings and provides a thorough analysis and discussion of their consequences. The way the results are presented and explained is designed to make it easier for readers to understand the findings and how they relate to the body of existing research on the topic. These newly discovered insights have the potential to greatly advance knowledge regarding the distribution and composition of pesticides. The academic conversation in agricultural science is noteworthy because it has expanded to include the encapsulation of agrochemicals in HKUST-1 materials as a new area of study. The principal objective of this research is to contribute to the sustainability of agricultural practices by mitigating the adverse environmental impacts associated with agrochemicals, all the while augmenting their stability and effectiveness. This chapter has been segmented into 4 sections: 4.1 Fabrication of HKUST-1 from Basic Copper Carbonate (BCC); 4.2 Extraction of pure Carbendazim (CB); 4.3 Encapsulation of pure CB; 4.4 Release Study 4.5 Characterization of materials; 4.6 Effect of pure CB, HKUST-1, and CB@HKUST-1 on germination of rice seeds; 4.7 In vitro efficacy evaluation of HKUST-1, their precursors BCC and BTC, and CB @HKUST-1 against pathogen causing blast of rice; 4.8 Effect of HKUST-1 and CB@HKUST-1 on rice plants under a controlled environment.

4.1 Fabrication of HKUST-1 from BCC

The techniques according to (Riccò et al., 2018) was used to fabricate the “Metal-Organic Framework called HKUST-1”. The identification and validation of the synthesized compound were established through UV analysis. The experimental observations reveal that HKUST-1 exhibits a distinctive blue coloration at the ambient standard room temperature. As the temperature increases, a discernible transition occurs, transforming the hue into a deeper indigo shade, with pronounced effects observed beyond 130 °C. Remarkably, the reversion to the initial coloration at standard room temperature transpires rapidly within a matter of seconds. This dynamic alteration in coloration serves as a notable indicator of the compound's responsiveness to

temperature variations and underscores its potential utility in temperature-sensitive applications.

Figure 4.1

Alteration of Color in HKUST-1 in Response to Varying Temperatures a) Fabricated HKUST-1 in the Room Temperature, b) HKUST-1 at 135 °C, c) Temperature-Dependent Color Shift in HKUST-1

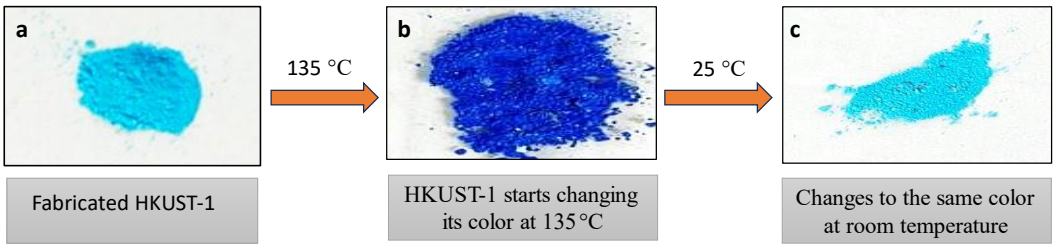

4.2 Extraction of Pure Carbendazim (CB)

During this investigation, carbendazim was extracted from the commercial product with an organic solvent (DMF).and the pure compound analyzed by the UV-Vis spectrophotometry. Although the manufacture declared an amount of carbendazim as 50%, the isolated product was only 32.2% (3.22 g extracted from 10 g of formulation).

4.3 Encapsulation of Pure Carbendazim (CB)

Extracted carbendazim was added at molar ratios of 1:2, 1:4, and 1:8 with respect to the ligand BTC. The guest was added immediately after stirring 200 mg of BCC (0.90 mmol) and 210 mg of H_3BTC (1 mmol) into a 6.5 mL solution of ethanol/water (1:1). In this experimental framework, UV spectroscopy served as the method of choice for detecting CB, with its characteristic absorbance maxima at 280-284 nm. Similar absorbance peaks have been identified in prior studies conducted by (Boudina et al., 2003; Meszlényi et al., 1990; Panadés et al., 2000). Notably, the comparative study of the three molar ratios showed that, in comparison to the 1:2 and 1:8 ratios, the 1:4 ratio performed better and produced the maximum encapsulation efficiency. To determine and track the encapsulation efficiency, a standard calibration curve and a linear fitting

graph for pure CB were created. In order to do this, different concentrations of CB were systematically used and then exposed to UV analysis.

Figure 4.2

Calibration Curve of a) Absorbance of CB b) Linear Fitting of CB

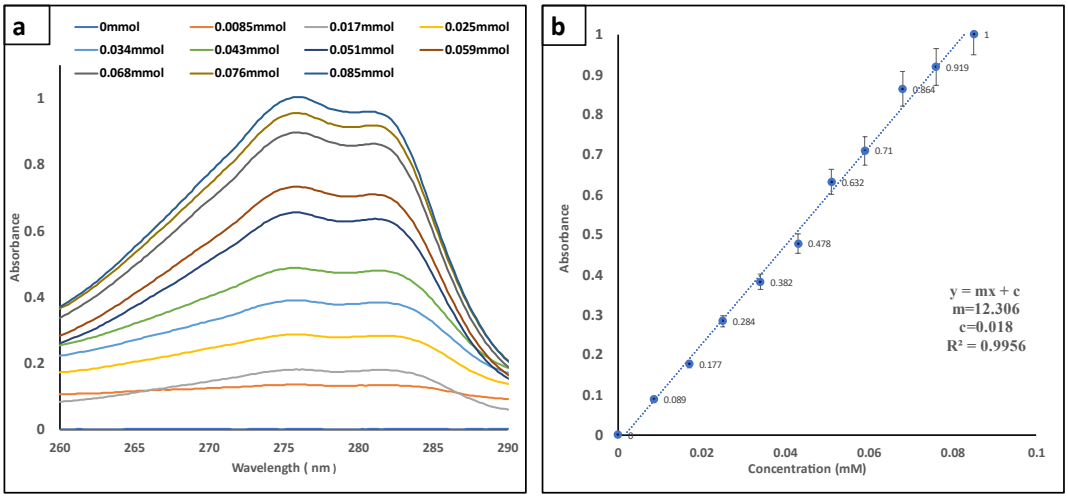

The UV spectroscopy analysis of pure CB showed two broad and overlapping peaks. However, for the experimental objectives, emphasis was placed solely on one peak with the wavelength of 284 nm for subsequent calculations and analysis. By using this single peak to represent the compound's absorbance maximum, the concentration of carbendazim in the sample could be accurately determined. The term "encapsulation efficiency of CB" in HKUST-1 describes the amount of pure CB that is successfully introduced into the material's pores. The efficiency of HKUST-1 encapsulation may be affected by a number of significant variables, including as the synthesis conditions, the choice of precursor materials, the intrinsic properties of the agrochemical, and the size and shape of the pores.

The encapsulation efficiencies of CB within HKUST-1 were systematically evaluated at varying initial amounts of CB (200 mg, 400 mg, and 800 mg). For the 200 mg dosage, an encapsulation efficiency of 94.02% was achieved, resulting in the incorporation of 184.27 mg of CB per gram of HKUST-1. Likewise, with 400 mg of CB, the encapsulation efficiency reached 78.1%, leading to the encapsulation of 243.3 mg per gram of HKUST-1. In the case of 800 mg of CB, the encapsulation efficiency was 40.39%, corresponding to the integration of 251.65 mg per gram of HKUST-1.

These findings illuminate a trend wherein the encapsulation efficiency decreases as the initial amount of CB increases. Notably, the results suggest that the encapsulation efficiency achieved with 400 mg of CB surpasses that of both 200 mg and 800 mg. This observation is substantiated by the graphical representation of the data in the figure 4.3, highlighting the superior performance of the 400 mg dosage in the encapsulation process. It is noteworthy that while the encapsulation efficiency appears higher for 200 mg, potential vacancies in the structure are indicated, prompting the exploration of the 400 mg dosage to optimize encapsulation efficacy.

Figure 4.3

Encapsulation Efficiency % Concerning Time under Different Concentrations of Pure CB for Encapsulation.

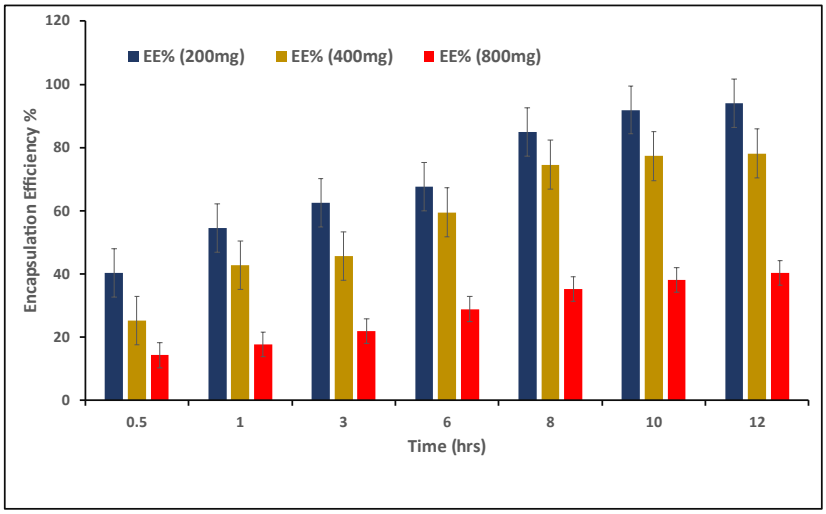

In accordance with the culmination of prior experimental investigations, the optimal loading capacity of HKUST has been ascertained, revealing a pivotal threshold at 400 mg for the encapsulation of CB. This measured value, obtained from the previous experiment, provides a fundamental framework for the subsequent encapsulation procedures.

The experimental investigation revealed a notable trend in the encapsulation efficiency over time, demonstrating a discernible augmentation from the initial 30-minute interval, progressively escalating until reaching a zenith at the 12-hour mark as shown in the figure 4.4. After then, stability continued for longer than previously stated. This time series highlights a dynamic encapsulation process in which efficiency seems to be closely related to the length of the encapsulation time. The phenomena that have been observed implies a complex temporal dependence, confirming the crucial role that time plays in determining the encapsulation efficiency in the experimental setup.

Figure 4.4

Encapsulation Efficiency of Pure CB (400mg) inside HKUST-1

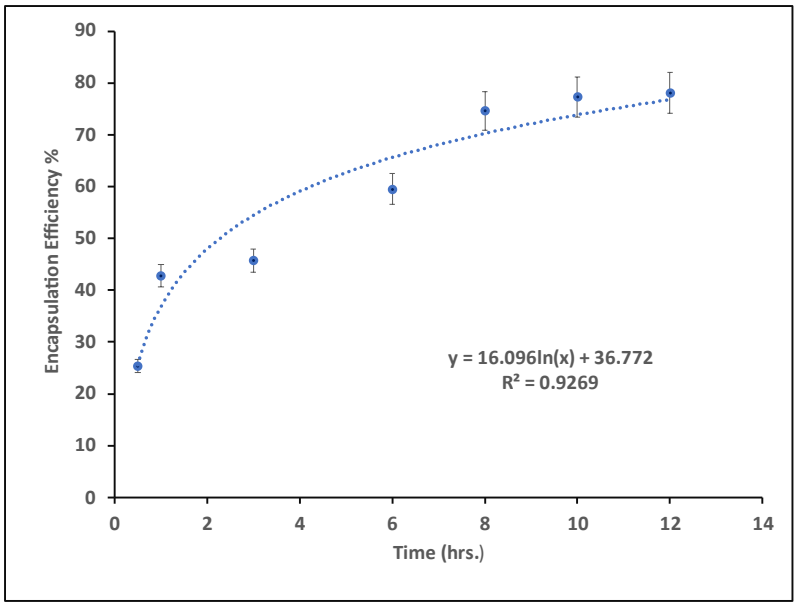

4.4 Release Study

The primary objective of this study was to examine the environmental behavior of agrochemicals after their release from HKUST-1. The investigation focused on the release of agrochemicals from the porous structure of HKUST-1 using tap water and deionized water (DI water) as the solvents. The research was conducted under conditions of constant stirring at room temperature. Notably, the pH levels of both tap water and deionized water were found to be congruent with the pH of the rice leaf surface. Consequently, the use of buffers was deemed unnecessary in this experimental setup, ensuring that the study accurately reflects the natural pH conditions of the rice leaf environment.

Figure 4.5

Releasing Behavior of Encapsulated Pure CB inside HKUST-1

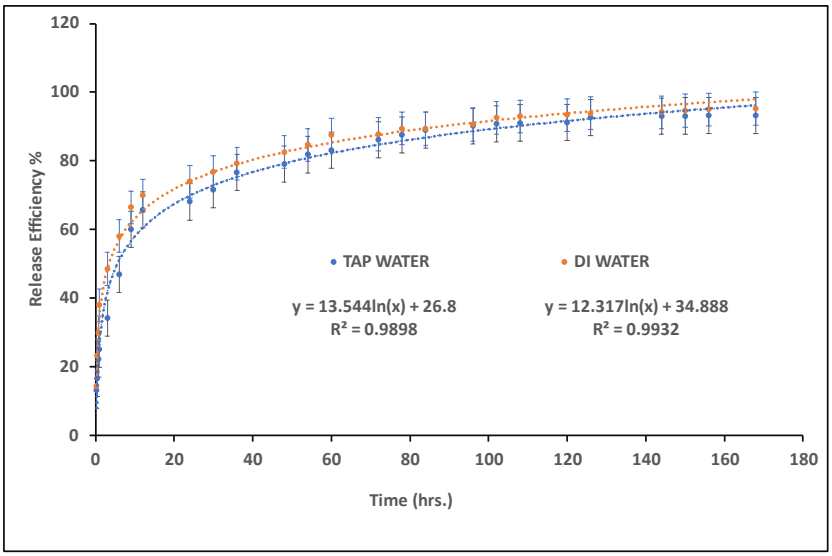

The release kinetics of encapsulated CB are depicted in figure 4.5, with distinct comparisons drawn between its behavior in both DI water and tap water. Notably, despite the differing solvent compositions, the release profiles exhibit striking similarities.In this study, the experimental data collected from dynamic dialysis studies

were analyzed by applying Equation 4.1, which is commonly referred to as the "Korsmeyer-Peppas (KP)" equation.

$$\frac{M_t}{M_\infty} = \mathrm{K}.\, t^n \qquad (4.1)$$

The fractional permeated drug, represented by M_t/M_∞, is dependent on time (t), the transport constant (K), and the transport exponent (n). The transport exponent (n) is dimensionless and typically ranges between 0.5 and 1.0. Its value provides insight into the mechanism of drug release: Fickian diffusion occurs when n=0.5, while non-Fickian or anomalous transport is indicated when n falls between 0.5 and 1.0.

Among the mathematical models used to interpret non-linear diffusion profiles, the "Higuchi and Korsmeyer-Peppas models" are the most commonly utilized. The "Korsmeyer-Peppas" model, in particular, has proven successful in describing drug release kinetics from porous materials in previous studies (Bayer, 2023; Wu et al., 2019) The study involved fitting the data to a mathematical model using non-linear regression techniques, which allowed the researchers to delve into the drug's release kinetics from HKUST-1 and gain deeper insights. Table 4.1 displays the fitted parameters derived from this analysis.

Table 4.1

Korsmeyer-Peppas Equation (Eqn.4.1) Fitted Data Points

Material	**DI water**			**Tap water**		
CB@HKUST-1	K	R^2	n	K	R^2	n
	31.1	0.9793	0.23	38.30652	0.9822	0.20

When the parameter n=0.2 in the Korsmeyer-Peppas equation, it signifies that the drug release mechanism from the controlled-release formulation adheres to the Fickian diffusion process. This observation underscores the significance of diffusional processes in governing drug release kinetics (Bayer, 2023). Specifically, it suggests that the rate of drug release is primarily influenced by the concentration gradient of the drug within the matrix, aligning with the fundamental principles of Fickian diffusion.

In DI water, the release of the fungicide commences after an incubation period of 15 minutes, gradually progressing thereafter. Noteworthy was the observed sustained release, characterized by a gradual and steady liberation of the active compound. This release kinetics display a discernible plateau phase, observed between 144 to 168 hours, indicative of an attainment of saturation equilibrium. Such equilibrium suggests a cessation of further release, highlighting a critical aspect of the encapsulation system's performance. In contrast, when comparing the release behavior in tap water to that in deionized (DI) water, there are distinct differences. Tap water shows a slower initial release phase compared to DI water. However, similar to DI water, the release kinetics eventually stabilize into a consistent pattern, reaching a plateau phase that indicates saturation equilibrium.

The way by which encapsulated carbendazim from HKUST-1 releases into water is dependent on a number of factors, including solubility, surface chemistry, water quality (DI vs. tap water), pH impacts, and possible ion exchange mechanisms (McGuire & Forgan, 2015; Zacher et al., 2011). Both strong and weak interactions may occur between encapsulated carbendazim and HKUST-1 or between carbendazim and water molecules. Robust interactions, including coordination connections between carbendazim functional groups and metal ions in the MOF, can support the stability of the encapsulated complex. By altering the solvation and diffusion processes, weak interactions like the hydrogen bonding between carbendazim and water molecules can have an impact on the release kinetics.

So the notable finding was the significant difference in release efficiency between DI the release efficiency of the fungicide from the MOF matrix is notably higher in DI water than in tap water because the presence of different ions in tap water might stop the guest from being released. This difference highlights the complex relationship between solvent composition and release kinetics, suggesting potential opportunities for improving release efficiency based on the specific environmental conditions.

4.5 Characterization of HKUST-1 and CB@HKUST-1

Figure 4.6

"Fourier Transform Infrared Spectroscopy" of HKUST-1, CB and CB@HKUST-1

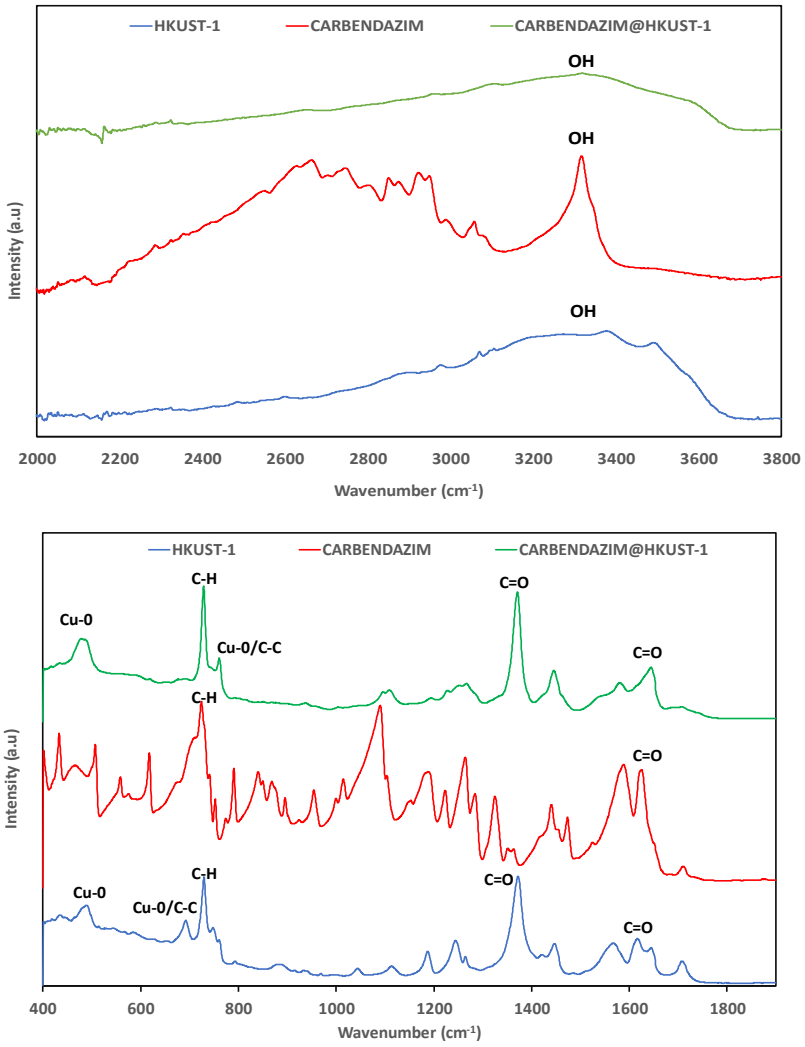

FTIR spectroscopy has been utilized to get further insight into the vibrational modes of the different functional groups as shown in in the Figure in the HKUST-1, CB, and the composite material CB@HKUST-1. The infrared (IR) absorption spectra within the wavenumber range of 1700-1500 cm^{-1} were attributed to the stretching modes of asymmetric (COO-) functional groups, while those within the range of 1500-1300 cm^{-1} were attributed to the stretching modes of symmetric (COO-) functional groups.

Moreover, spectral features around 1450 cm^{-1} were observed, which were ascribed to a combination of the stretching and deformation modes associated with the benzene ring moiety (Borfecchia et al., 2012) .

The discernible shifts observed in the stretching vibration of the C=O acid ligand, transitioning from 1690 cm^{-1} to 1640 cm^{-1}, provided clear evidence of the deprotonation of the C=O carboxyl group associated with BTC, subsequently forming coordination bonds with Cu^{2+} ions to generate the HKUST-1 framework. There was a band at 728 cm^{-1} that was identified as the stretching vibration of the Cu-O/C-C loop. These outcomes showed that the Cu^{2+} ions had been coordinated by the 1,3,5-BTC ligands. The band joining forces with carbendazim to explain the intensity of the 728 cm^{-1} peaks in CB@HKUST-1. The broad peak spanning the wavenumbers of 3300-3400 cm^{-1} is indicative of the OH stretching absorption characteristic of the carboxyl group. This peak undergoes a notable shift from approximately 3400 cm^{-1} to 3600 cm^{-1} upon the formation of HKUST-1, suggesting the loss of water molecule bonds within the HKUST-1 structure (Yu Tsivadze et al., 2016).

The FTIR spectra of HKUST-1 indicated a predominantly is bidentate nature of the -COO group, as evidenced by peaks observed at 1651, 1618, 1451, and 1375 cm^{-1}, which signify the characteristic binding mode (Loera-Serna et al., 2016). However, validation of HKUST-1 was achieved through the identification of characteristic bands between 650 and 1150 cm^{-1} (BTC), 730 cm^{-1} (C-H) and 1350 and 1700 cm^{-1} (Cu coordination) (Riccò et al., 2018; Mohammadabad et al., 2020). The molecule's bulk grew with the presence of guest molecules, initially causing the peak's apex to move in the direction of lower wave numbers due to a negative correlation between the mass of the vibrating molecule and the vibration's frequency. As a result, as molecular density decreases, a molecule's vibratory frequency and wave numbers rise. The peaks corresponding to CB at 417,750 1189, 1223, 1263, 1324, 1440, 1588,1620, and1710 cm^{-1} are discernible within the CB@HKUST-1 composite material. Notably, certain peaks exhibit overlapped with those originating from the intrinsic peaks of HKUST-1.

Figure 4.7

a) "High Performance Liquid Chromatogram" of CB Standard Solution (5ppm) b) Chromatogram of MeOH c) Chromatogram of Sample 0 min d) Chromatogram of Sample 15mins e) Chromatogram of Sample 30mins

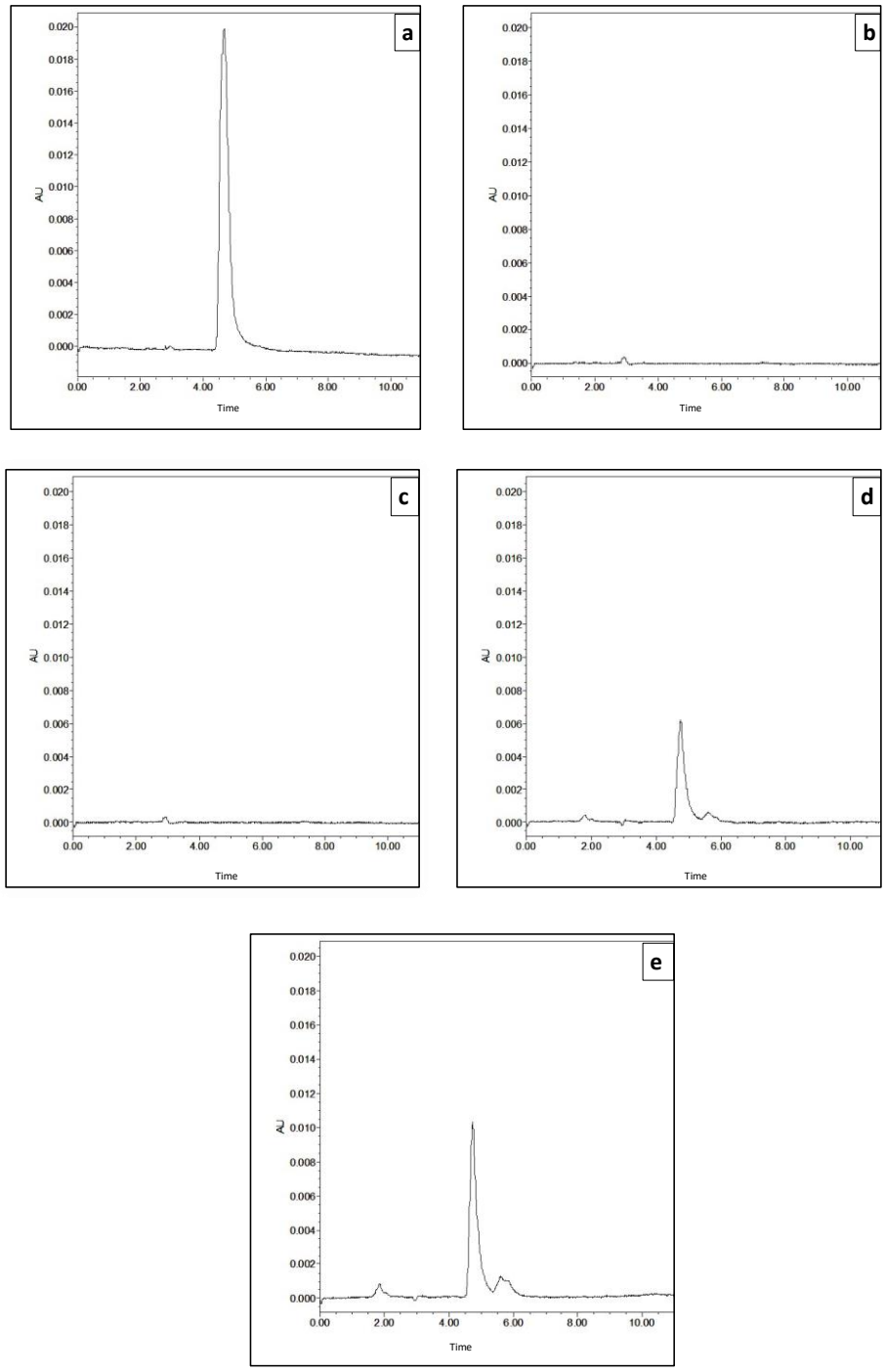

In the “high-performance liquid chromatography (HPLC)” analysis conducted, a standard solution of CB served as the reference, while methanol was employed as the blank sample. Upon examination of the chromatographic figure, a distinct and well-defined peak corresponding to CB was evident, mirror findings reported by (Lin et al., 2013; Phansawan & Prapamontol, 2015) . Notably, no discernible peak was observed upon analysis of the sample collected at the initiation of the experiment (0 minutes). However, subsequent analysis of the sample collected at 15 minutes revealed a peak congruent in position with that observed in the standard solution. Furthermore, examination of the sample collected at 30 minutes exhibited a more pronounced peak intensity. These observations collectively suggest that the release of encapsulated CB initiates from the 15-minute mark onward.

Figure 4.8

“XRD” Analysis of Basic Copper Carbonate, HKUST-1, CB@HKUST-1 and CB@HKUST-1 (Released)

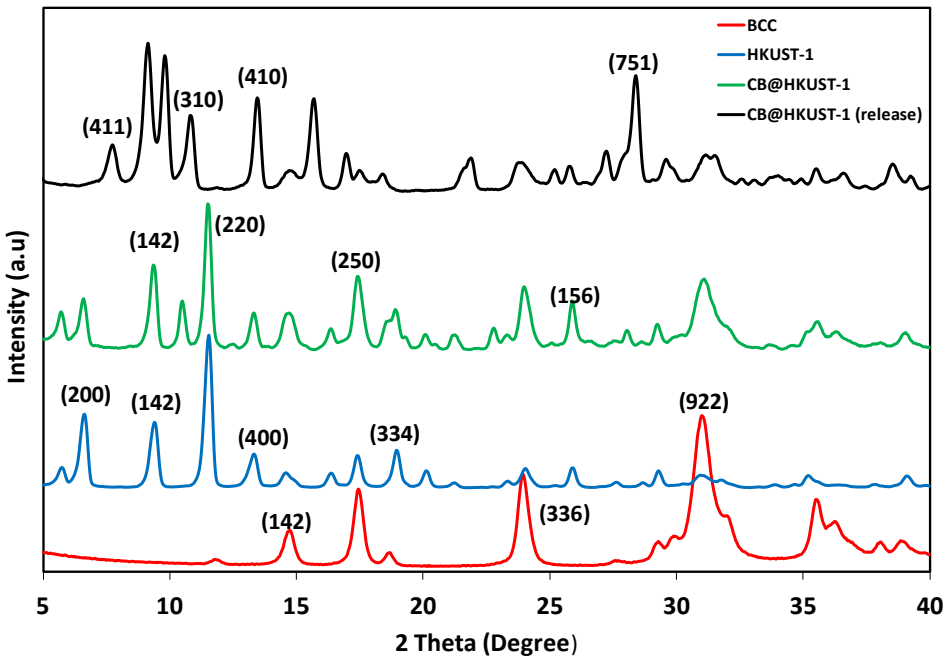

X-ray diffraction analysis was done for the samples Basic copper carbonate, HKUST-1, CB@HKUST-1 and CB@HKUST-1(released). X-ray diffraction assessments were conducted on the porous materials to verify the presence of highly pure crystalline phases within the HKUST-1 MOF material. As per published research (Panella et al., 2006), the intense peaks seen in Figure 4.8 at modest 2θ angles are indicative of micro-porous materials that have a large number of microscopic holes or cavities. The discernible presence of a sharp peak (hkl) in the XRD pattern of HKUST-1 serves as confirmation of its crystalline nature. In contrast, upon juxtaposition with HKUST-1, it becomes evident that the peak in the latter exhibits a broadening, suggestive of a diminished degree of crystallinity within the structure. The patterns seen in HKUST-1 and its composites with CB, when compared, indicate that the host material's crystal structure was maintained during the drug loading and release phases. This conclusion is derived on the peak position similarities found in the parent HKUST-1 and its composites. On the other hand, the Basic Copper Carbonate sample has a unique pattern that suggests a different crystal structure.

Figure 4.9

"Inductively Coupled Plasma Atomic Emission Spectroscopy (ICP)" of Cu ions from HKUST-1

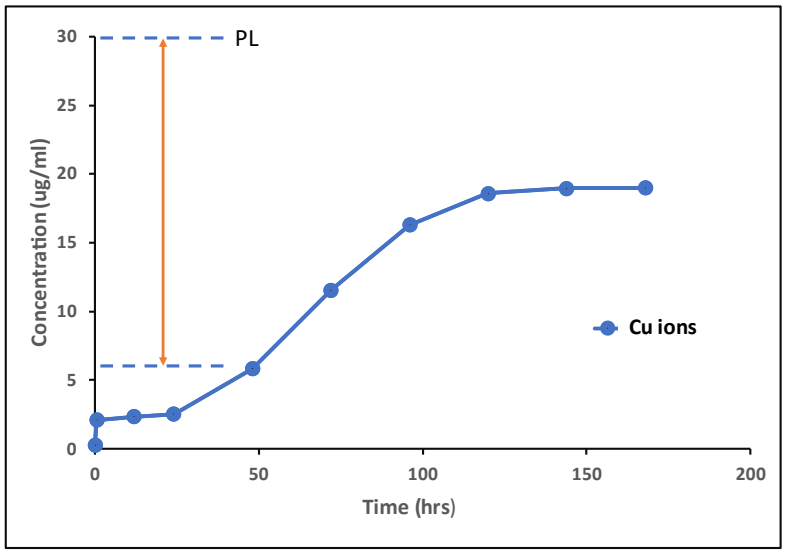

To investigate the release phenomenon of copper from HKUST-1, the methodology outlined by (Ren et al., 2015) was followed. A standard curve was established using elemental stock solutions of copper, facilitating the calculation of copper concentrations released from HKUST-1 over various time intervals, as depicted in Figure 4.9. The findings indicate a gradual release pattern: initially, copper release was notably slow within the first 24 hours. Subsequently, however, there was a progressive increase in release concentration, peaking at 18.59 µg/ml on the 5th day. Following this peak, the release concentration plateaued, with minimal change observed until the 7th day. Notably, the difference in copper release between the 5th and 7th days was calculated to be 0.39 µg/ml. These observations delineate the temporal dynamics of copper release from HKUST-1, highlighting distinct phases of release kinetics over the monitored time frame.

The investigation's current results show that the levels of copper ions in the solution escalated notably, ranging from the 5th day onwards, eventually reaching approximately 20 ppm by the 7th day. This concentration is within the range generally considered suitable for plant growth, as outlined in existing literature (Kumar et al., 2021; Xiong & Wang, 2005), typically falling between 5-30 ppm (Plant Limit). However, it's important to note that concentrations above this range can harm plants, so we need to be careful and examine them closely.

A release rate of about 20 ppm was reported in a case where HKUST-1, was dissolved in a solvent at a ratio of 1:1 and delivered at a concentration of 50 mg per 50 mL for seven days. This result establishes a critical threshold for plant safety when compared to the existing plant tolerance limit of 30 ppm for copper toxicity. In particular, it shows that, as long as the release of HKUST-1 stays below the critical toxicity threshold, it is safe to use up to 1500 ppm of the compound under the investigated circumstances. However, there is a chance for negative consequences above this concentration, which emphasizes the significance of monitoring concentrations to guarantee the best possible health and growth for plants.

Significant morphological alterations were seen in the treated plants, particularly at higher copper ion concentrations. There are questions regarding possible physiological and biochemical consequences on the treated plants due to the significant release of copper ions into the solution. Determining the copper threshold of the soil may not be necessary for this investigation because the treatments were applied directly to the leaves.

4.6 Effect of Pure CB, HKUST-1, and CB@HKUST-1 on Germination of Rice Seeds

Figure 4.10

Rice Seed Treatment a) Experimental Setup b) Arrangement of the Seeds in the Petri Dish c) Germination of the Rice Seeds d) Seed Length Measurement

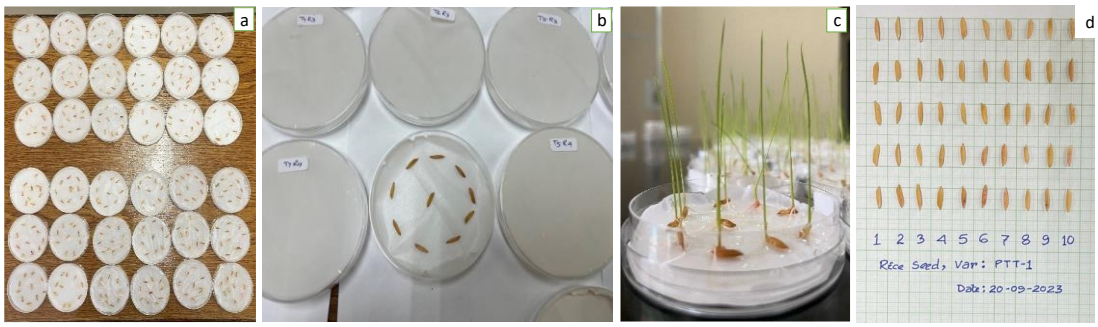

Table 4.2

Characteristics of the Rice Seeds

Source	VR	SG (%)	SC	1000 GW (g)	L(mm)	W (mm)	T (mm)	MC (%)
NSTDA, Thailand	PTT 1	100	Light yellow	29.21	11.3	3.2	2.4	9.4

NSTDA: 'National Science and Technology Development Agency', VR: Variety, SG: Standard Germination, SC: Seed Color, GW: Grain Weight, L: Length, W: Width, T: Thickness, MC: Moisture Content

In the case of pure CB treatments, a 100% germination rate was observed on the 6th day after seed sowing, indicating a positive impact at the low concentrations on the rice seedlings. Notably, the results demonstrated low germination rates and vigor index at high concentrations. For HKUST-1, a reduction in the number of days required for achieving a 100% germination rate was observed compared to pure CB. Despite exhibiting enhanced germination rates at all concentrations in comparison to pure CB, the vigor index showed a decline. It is noteworthy that at higher concentrations of HKUST-1, both the rate of germination and vigor index decreased.

In the case of CB@HKUST-1, a notably faster 100% germination rate was achieved in just 4 days. Additionally, both the rate of germination and vigor index surpassed those of both pure CB and HKUST-1. Similar to HKUST-1, higher concentrations of CB@HKUST-1 resulted in decreased rates of germination and vigor index, although they remained higher than those observed for pure CB and HKUST-1.

Figure No. 4.11 is a vital resource that offers a comprehensive summary of the comparison research that was conducted, therefore consulting it is required for an in-depth analysis of the experimental data. The intricate relationships between HKUST-1, pure CB, and CB@HKUST-1 concentrations and the germination kinetics and vigorousness of PTT-1 rice seedlings are depicted in this figure. The knowledge gathered from these investigations goes much beyond simple numerical data and greatly advances our understanding of the intricate relationships between these treatments and the physiological reactions of the rice seedlings. This comparative analysis sheds light on the many effects that manifest at various concentration ranges, offering a more nuanced picture. This aids in choosing farming practices that will optimize the emergence and vigor of seedlings.

Figure 4.11

Effect of different Concentrations of HKUST-1, Pure CB, And CB@HKUST-1 on the Germination and Vigor of PTT-1 Rice Seedling on a) Rate Of Germination b) Vigor Index.

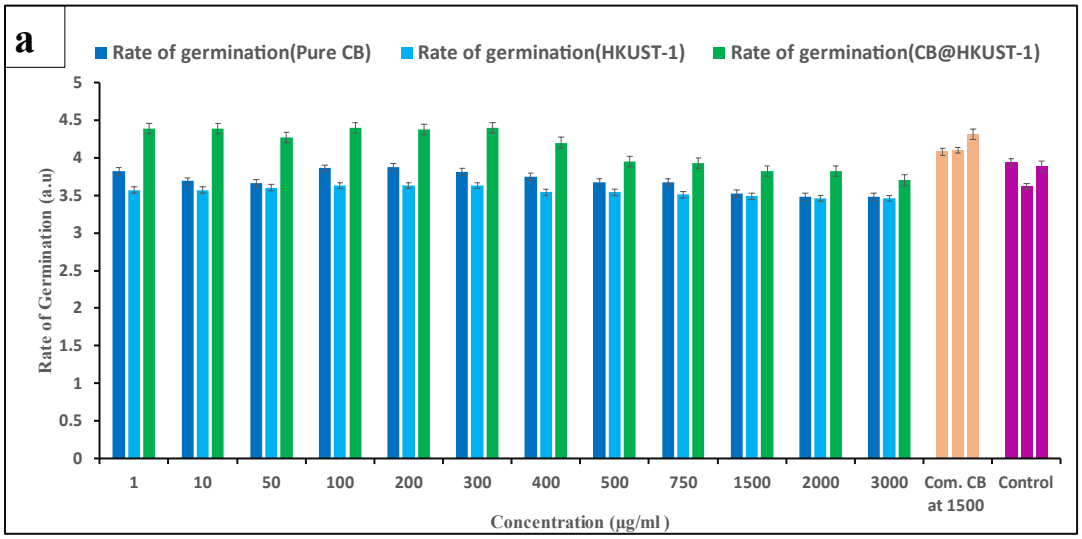

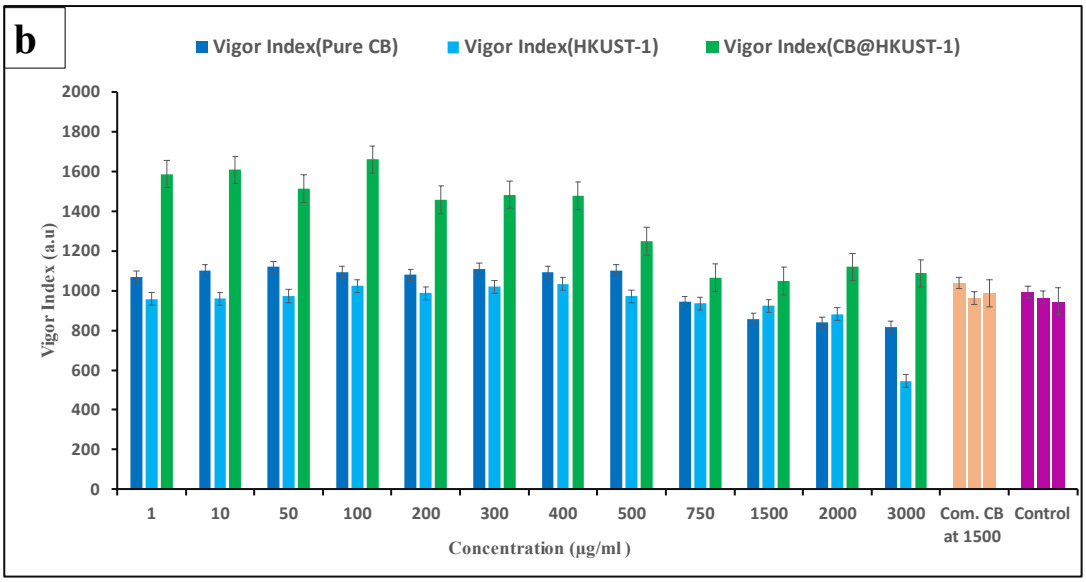

4.7 In Vitro Efficacy Evaluation of HKUST-1, their Precursors BTC and BCC, and CB @ HKUST -1 against Pathogen causing Blast of Rice

The National Science and Technology Development Agency (NSTDA) was the main source of the microbial culture used in this experimental study. Subsequent to the collection of the mother culture from this esteemed institution, a meticulous process of sub-culturing is undertaken to propagate and sustain the microbial strains for further experimental analyses.

Figure 4.12

a) Mother Culture of the Pathogen Magnaporthe grisea b) Sub-Culture of the Pathogen c) Multiplication of the Pathogen

The in vitro efficacy assessment for hyphal inhibition as shown in the figure 4.13 involved the utilization of specific concentrations of HKUST-1, alongside its precursors such as BTC and BCC, and the encapsulated formulation CB@HKUST-1. Even though the control plates required about 7 days for the hyphae to fully mature, the author chose to collect the data on the eighth day in order to get more clarity and contrast. This intentional decision guarantees a sharper separation of hyphal development traits. Notably, the data collected on the eighth day served as the reference point for all comparisons made across different concentrations, creating a stable temporal baseline for the analytical framework. During this experimental phase, these compounds' ability to suppress the hyphae of the pathogenic organism *Magnaporthe grisea* was thoroughly assessed. The results led to the computation of inhibition percentages.

Interestingly, the data showed a concentration-dependent trend for HKUST-1, showing a clear absence of inhibitory action on the pathogen's hyphae from low to high concentrations. Interestingly, hyphal inhibition did not occur at any of the different doses of HKUST-1, indicating that this compound has a natural restriction on the ability to impede the growth of *Magnaporthe grisea* hyphae. Moreover, an interesting finding surfaced at greater HKUST-1 concentrations, when a phenomenon was seen. Inversely, a decrease in the inhibition % indicated that the hyphae were somewhat resistant to the material. This is a fascinating result that emphasizes how crucial it is to identify concentration thresholds because too high of HKUST-1 concentrations seemed to cause a reduced inhibitory response.

Similar to HKUST-1, the precursor substances BTC and BCC were evaluated for their efficacy in inhibiting the hyphae of the pathogenic organism. Intriguingly, akin to HKUST-1, both BTC and BCC demonstrated a lack of inherent capacity to impede the growth of *Magnaporthe grisea* hyphae. But in the instance of BTC, a noteworthy exception occurred, as a clear inhibitory impact was noted at a certain dose. BTC had a significant ability to block the pathogen's hyphae at 1500 ppm. This effectiveness that is dependent on concentration emphasizes BTC's complex nature and emphasizes its potential use as a hyphal inhibitor at a certain threshold.

In the context of CB@HKUST-1, the evaluation of its efficacy against the hyphae of the pathogenic organism presents compelling results. Remarkably, even at low concentrations, the inhibition rate of the pathogen's hyphae by CB@HKUST-1 proves to be highly substantial, surpassing an impressive 80% inhibition percentage. Furthermore, at elevated concentrations, specifically at 1000 and 1500 ppm, the inhibitory effect reaches completeness, indicating a robust and comprehensive suppression of the pathogen's hyphal growth. This outcome underscores the potent inhibitory capacity of CB@HKUST-1, even at minimal concentrations, establishing it as a highly effective agent against the targeted pathogenic hyphae.

In conclusion, CB@HKUST-1's demonstrated inhibitory performance, which is marked by a notable effect at low concentrations and total inhibition at higher concentrations, supports the drug's potential as a strong and adaptable inhibitor against the pathogen's hyphae. These results highlight the potential involvement of CB@HKUST-1 in hyphal inhibition, even at low concentrations, and offer insightful information on the drug's range of activity.

Figure 4.13

In-Vitro Efficacy Test by using Different Concentrations of BTC, BCC, HKUST-1 and CB@HKUST-1 against the Hyphae of the Pathogen

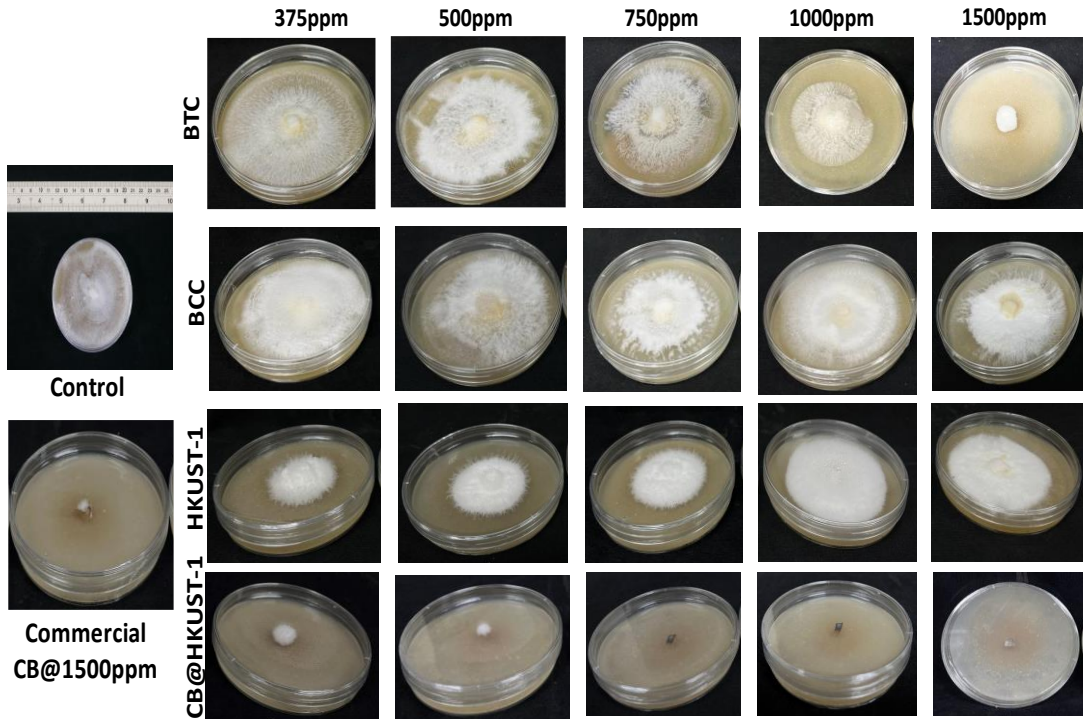

Figure 4.14

Inhibition Percentage of BTC, BCC, HKUST-1 and CB@HKUST-1 against the Pathogen.

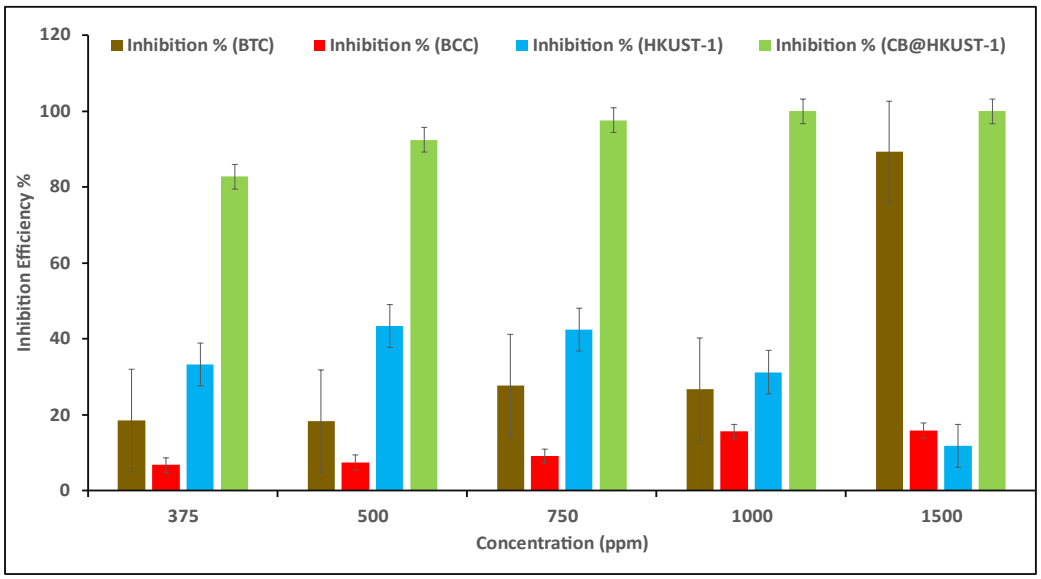

As a result of CB@HKUST-1's remarkable effectiveness, which was most noticeable at 375 ppm, it was decided to carry out an inhibition test that was directed at the pathogen's spores. The use of several lower doses was employed in the following study to determine the corresponding inhibitory percentages. The results of this investigation helped to determine the concentrations to use in the plant experiments.

For the in vitro assessment against the spores, germination represents a pivotal phase. This process was meticulously executed under dark conditions at ambient room temperature. The germination process for the spores took almost 7 days. After the spores successfully germinated, spore quantification was performed using a hemocytometer as shown in the figure 4.15, and the results showed that there were $1.74x10^5$ cells (aggregated from two plates). Considering that the required volume is in the range of 10^6 cells, the experiment must be conducted across a total of 20 plates in order to satisfy the requirements. And accordingly, spore count from 20 plates was found to be $2.14x10^6$/ml.

Figure 4.15

a) Germination of Spores b) Spindle Structured of Spores c) Spore Count using Hemocytometer in Compound Microscope

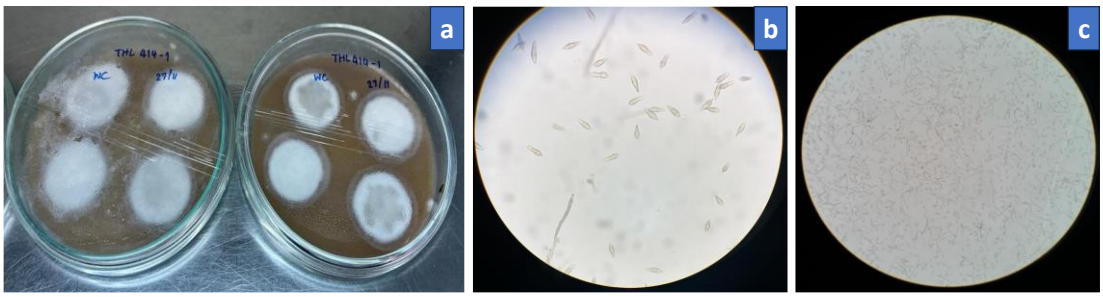

Following the first inoculation and incubation phase, in which the spores proliferated at different rates on each of the petri plates, a careful inspection was conducted. Surprisingly, a different result surfaced, explaining a spore growth phenomenon that was only seen at the 50 ppm concentration threshold. Further investigation, as seen in Figure 4.16, demonstrated a critical turning point at which the inhibition rate rapidly increased to 100%.

This fascinating finding highlights the strong inhibitory action of concentrations beyond 50 ppm, indicating a strong regulating effect on the dynamics of spore formation. These results provide insight into the complex interactions between environmental cues and spore growth, and they also raise the possibility of using tailored control techniques to reduce the spread of microorganisms.

Figure 4.16

In-Vitro Efficacy Test by using Different Concentrations of CB@HKUST-1 against the Spores of the Pathogen

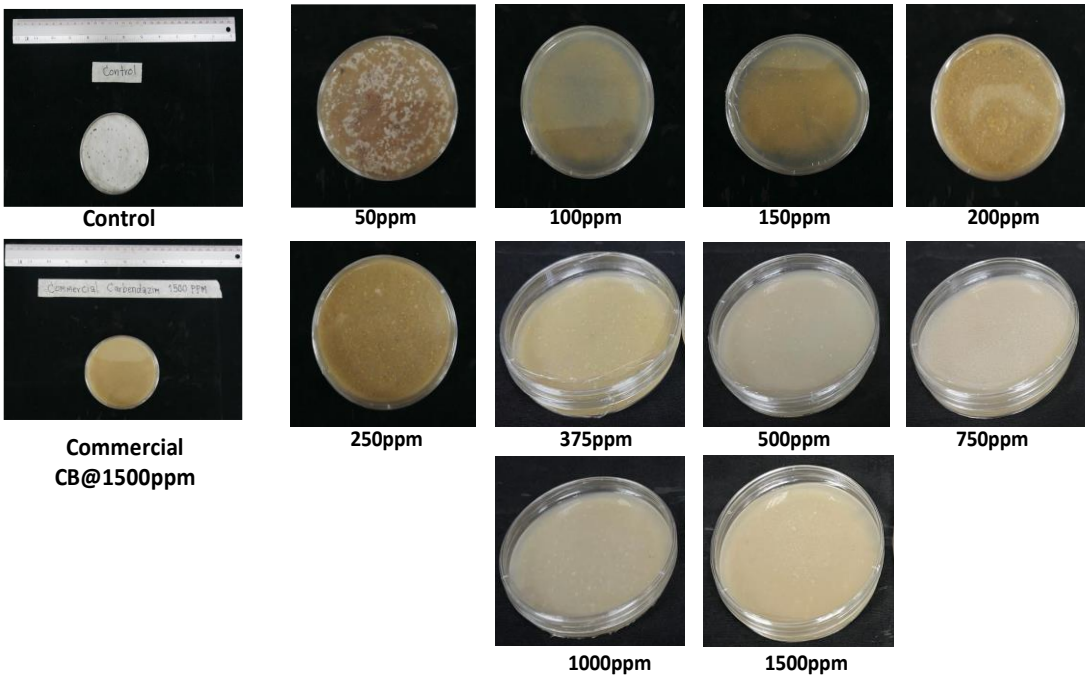

4.8 Effect of HKUST-1 and CB@HKUST-1 on Rice Plants under a Controlled Environment.

KDML 105 (Khao Dawk Mali 105) and PTT-1 (Pathum Thani 1), two well-known indigenous rice varieties from Thailand, were carefully chosen for analysis in the interest of a thorough investigation. The rice seedlings were transplanted following an 8-day incubation period, which started with the original planting phase. After that, the plants received an application of calibrated spores exactly eight days after transplantation, with a precise measurement of the spore concentration of 2.14×10^6/ml taken.

Derived from insights gleaned from prior in vitro experimentation, a discerning selection of optimal concentrations for two distinct substances, HKUST-1 and CB@HKUST-1, was methodically conducted. Concentrations of 500, 1000, and 1500

ppm were specifically selected for HKUST-1 in order to correspond with the observed inhibition rates that were thought to be the most promising in terms of antifungal effectiveness. Lesser concentrations (125, 250, and 500 ppm) of CB@HKUST-1 were carefully chosen due to their proven ability to impede spore formation inside the boundaries of the in vitro paradigm.

Then 48 hours after the spore treatment, chemicals were methodically sprayed on the rice plants while strictly following the quantities that had been specified. The consistent application amount of 40 milliliters per plant, which guarantees consistency in treatment dose across the trial units, is noteworthy. This methodological rigor is essential to the creation of controlled environments and enables a more sophisticated assessment of the ensuing effects of the compounds used on the development dynamics of the chosen rice types, KDML 105 and PTT-1.

4.8.1 Morphological Analysis

A comprehensive set of morphological analyses was conducted, including a wide variety of parameters such as root length, shoot length, number of leaves, biomass, and disease index. These evaluations were carried out after both non-inoculated and inoculated rice plants had a carefully monitored 14-day chemical treatment.

Within the broad framework of Table 4.3, a thorough description distinguishes between significant and non- significant characteristics about the interaction between treatment and disease was revealed. Additionally, the table clarifies the combined effect that was produced by the complex interplay of various variables over a range of morphological features. It explores the subtleties of root length, shoot length, root biomass, and shoot biomass in particular, illuminating the dynamic interactions present in the experimental setting.

Table 4.3

*Significance Levels in Individual and Interactive Effect of Different Morphological Parameters in Two Different Rice Varieties***.**

	Root length	**Shoot length**	**Biomass root**	**Biomass shoot**
Variety KDML				
Factor				
Treatment(T)	**	**	**	**
Disease(D)	**	**	**	**
T×D	NS	**	**	*
Variety PTT-1				
Factor				
Treatment(T)	**	**	**	**
Disease(D)	**	*	**	**
T×D	NS	**	*	*

***, * and NS indicate P ≤0.01, P ≤0.05, and non-significant respectively*

4.8.1.1 Root and Shoot Length Analysis of Rice Variety: KDML 105

Figure 4.17 illustrates the developmental path of plant growth by showing the root and shoot length under different treatments, including varying concentrations of HKUST-1 (500, 1000, 1500 ppm) and carbendazim (125, 250, 500 ppm), applied to both non-inoculated and inoculated rice plants. This visualization facilitates the examination of treatment effects on rice plant root growth, thereby enriching the understanding of the factors influencing plant development in this study. Additionally, it allows to observe any potential toxic effects on plant growth.

Figure 4.17

Analysis of the Root and Shoot Length for the Rice Variety KDML 105 a) Without Inoculum and b) With Inoculum.

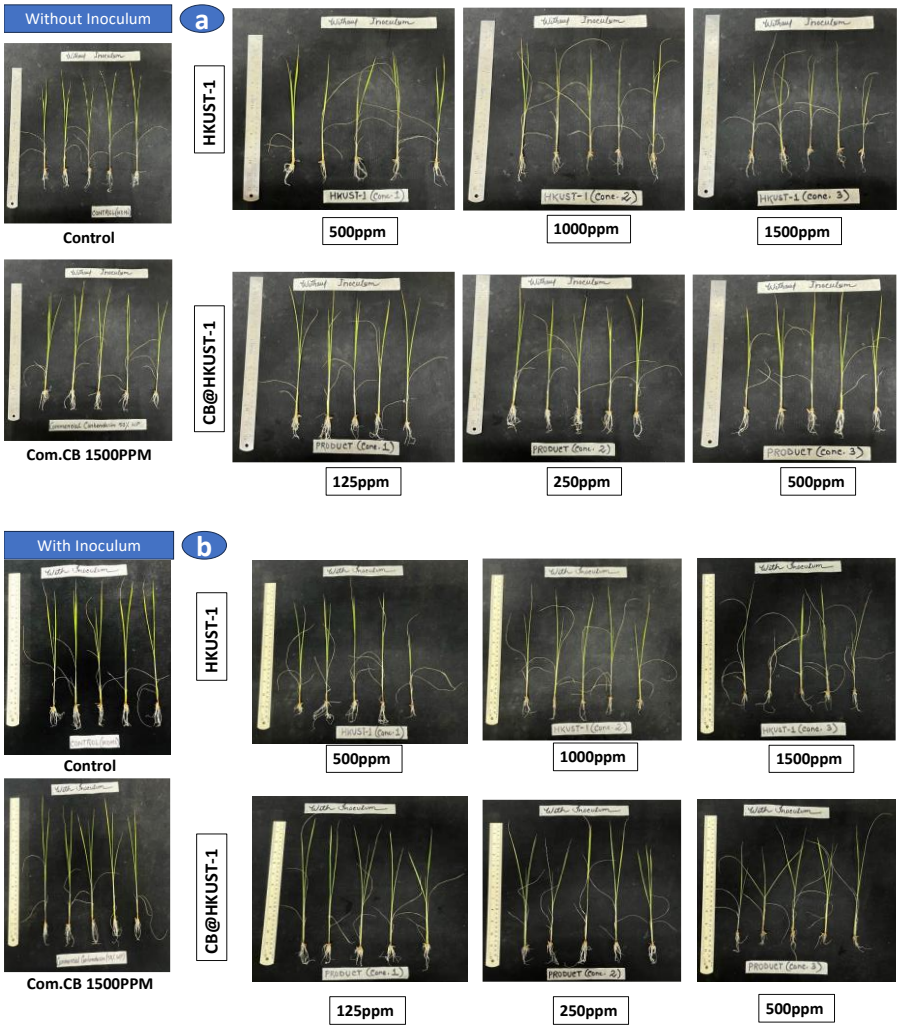

In the context of root length measurements, statistical analysis via ANOVA revealed a non-significant interaction between the two factors considered. As depicted in Figure 4.18, examination of the initial graph indicates that at concentration 1 of HKUST-1, there exists no discernible impact on root length, akin to the control group. However, at higher concentrations, observable decreases in root length suggest a potential toxic effect. Furthermore, analysis of CB@HKUST-1 indicates the concentration 2 exhibited notably favorable effects on root length enhancement. Concentration 1 exhibited a

similar effect to the control group, while Concentration 2 resulted in a reduction in root length. Moving to the second graph, a notable discrepancy emerges between diseased and non-diseased rice plants in terms of root length. This disparity underscores a statistically significant distinction between the two groups, implicating a potential influence of disease status on root morphology and growth dynamics.

Figure 4.18

Changes of Root Length by the a) Effect of Different Concentrations (500,1000,1500ppm) of HKUST-1 and (125,250,500ppm) CB@HKUST-1(P) a) Effect of Diseased(W) and Non-Diseased (WO) on Rice Plants.

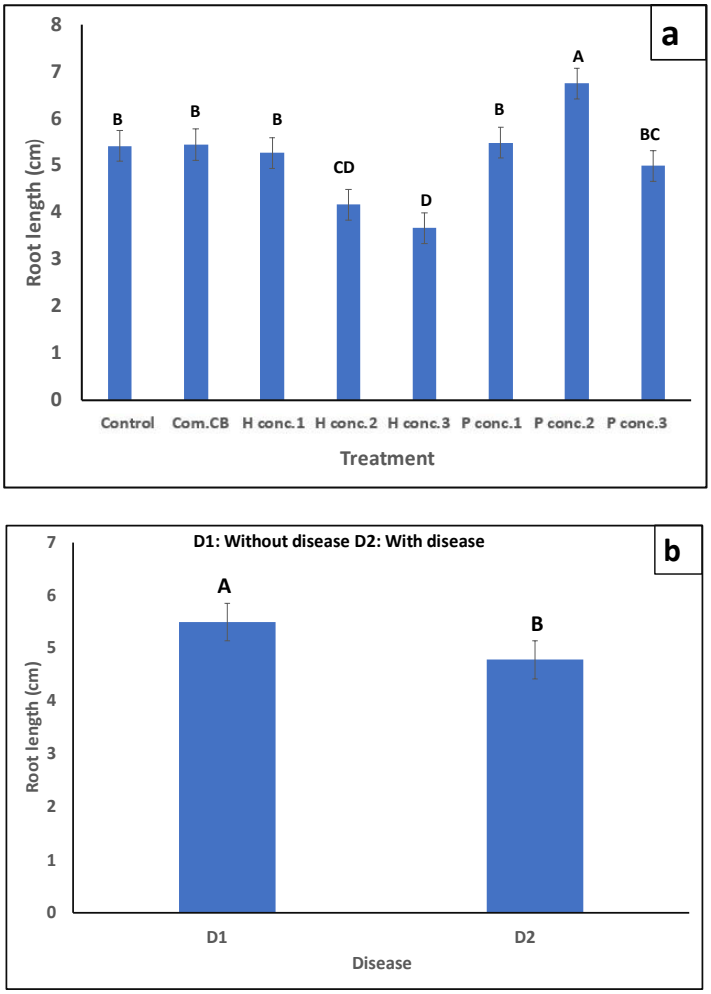

In assessing shoot length, distinct trends were observed among the various concentrations of HKUST-1 and CB@HKUST-1 in both diseased and non-diseased rice plants as shown in figure 4.19.

For HKUST-1, concentrations 1(500 ppm) and 2 (1000ppm) exhibited no significant deviation in shoot length compared to the control group, regardless of the plant's health status. However, concentration 3 (1500ppm) notably hindered shoot length in both diseased and non-diseased plants.Conversely, in the case of CB@HKUST-1, concentrations 1(125 ppm) and 2 (250 ppm) displayed notable increases in shoot length compared to the control group, indicating a positive impact on plant growth. Furthermore, concentration 3 (500ppm) did not exhibit any detrimental effects on shoot length, suggesting its compatibility with plant development.

Figure 4.19

Changes of Shoot Length in the Diseased(W) and Non-Diseased (WO) Rice Plants due to the Response of Different Concentrations (500,1000,1500ppm) of HKUST-1 and (125,250,500ppm) CB@HKUST-1(P).“Values are Means of Five Replications. Vertical Bars Represent Standard Error.Bar Columns with Different Uppercase Letters are Statistically Significant Based on Tukey’s Honest Significant Difference Test at P<0.05”.

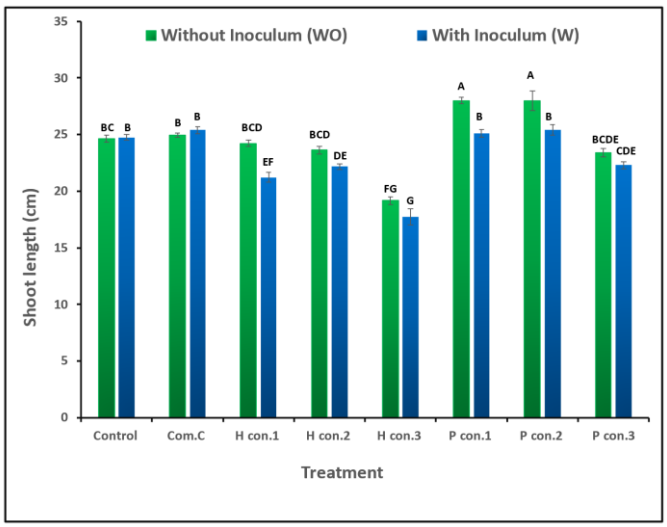

4.8.1.2 Root and Shoot Analysis of Rice Variety: PTT-1

In pursuit of comprehending the developmental trajectory of plant growth, an analysis akin to that conducted for the KDML variety was undertaken for the PTT-1 variety. Figure 4.20 serves as a visual representation of root length and shoot length dynamics across diverse treatments administered to both non-inoculated and inoculated rice plants of the PTT-1 variety. This graphical portrayal facilitates an examination of the influence of different treatments on the root growth of rice plants, thereby enriching our insights into the factors shaping plant development within the scope of this investigation.

Figure 4.20

Analysis of the Root and Shoot Length for the Rice Variety PTT-1 a) Without Inoculum and b) With Inoculum.

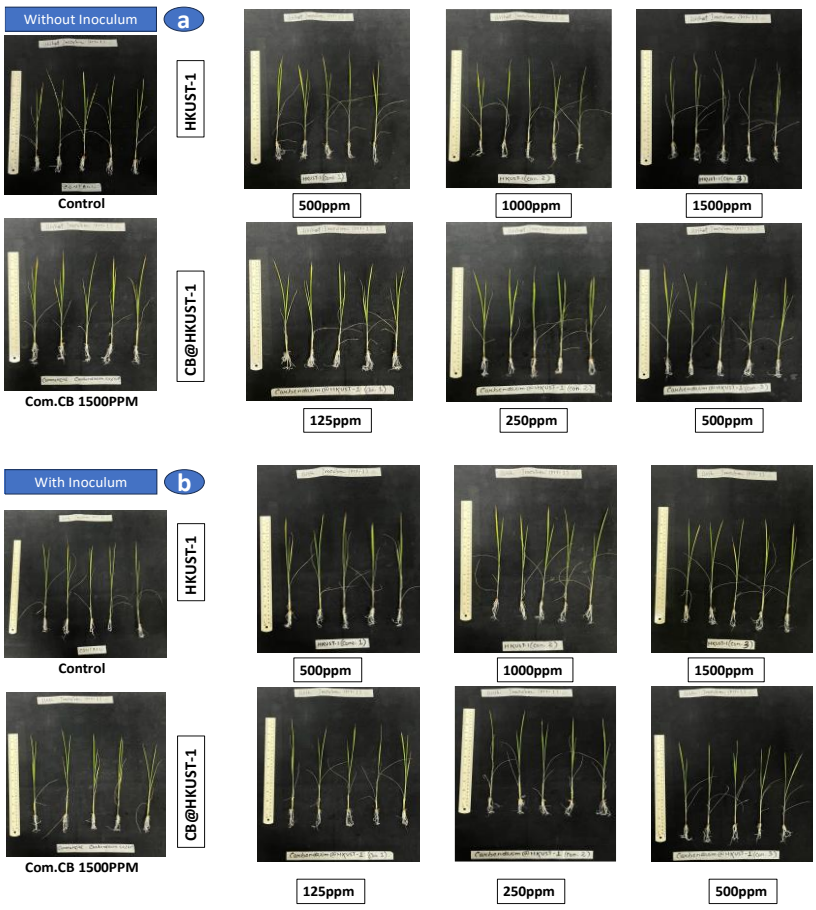

In the context of root length measurements for the PTT-1 variety, statistical analysis utilizing ANOVA revealed a non-significant interaction between the two factors under consideration.

The first graph in Figure 4.21 amply demonstrates that the PTT-1 rice plants consistently have a beneficial effect on root length at all HKUST-1 concentrations. This indicates that roots often develop longer when HKUST-1 is treated, regardless of the amount utilized. This implies that HKUST-1 influences these rice plants' root growth in a dependable and advantageous way, which may be helpful for enhancing the general health and production of the plants.

It is clear from a closer look at CB@HKUST-1 in Figure 4.21 that the PTT-1 rice plants' roots grew longer at all concentrations of this substance. This suggests that there has been a constant beneficial impact at all tested doses. But as compared to other concentrations, concentration 2 (250ppm) stands out as being especially notable because of its substantial improvement in root length. This implies that CB@HKUST-1 concentration 2 may have a more powerful or focused impact on root growth in these rice plants, which makes it a good candidate for more research or possible use in farming techniques meant to enhance root development.

In the second graph, there is a clear difference in root length between rice plants that are infected and those that are not. This difference indicates a statistically significant difference between the two groups, suggesting that the disease state may have an impact on the growth dynamics and root shape.

Figure 4.21

Changes of Root Length by the a) Effect of Different Concentrations (500,1000,1500ppm) of HKUST-1 and (125,250,500ppm) CB@HKUST-1(P) and a) Effect of Diseased(W) and Non-Diseased (WO) on Rice Plants.

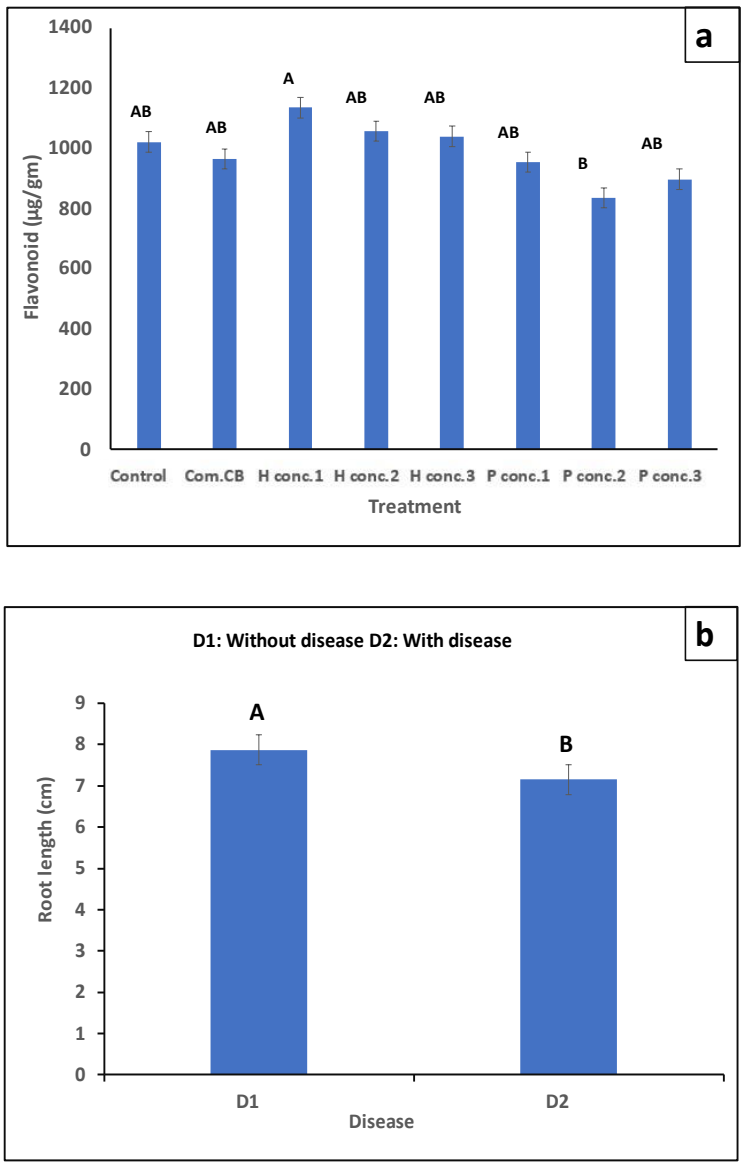

When shoot length was assessed, patterns were observed in both diseased and unaffected rice samples at different HKUST-1 and CB@HKUST-1 concentrations. Regarding HKUST-1, plants that were non-diseased and were subjected to Concentrations 1 (500 ppm) and 2 (1000 ppm) showed similar patterns of shoot length

to the control group, regardless of the state of health of the plants. Nonetheless, a decrease in shoot length was noted at Concentration 3 (1500 ppm). On the other hand, diseased plants subjected to all three concentrations showed shorter shoot lengths, with Concentration 2 showing a more noticeable effect.

Contrary to HKUST-1, CB@HKUST-1 showed significant enhancements in shoot length for both non-diseased and diseased rice plants across all concentrations, except for Concentration 3 (500 ppm), which inhibited shoot development in diseased specimens.

Figure 4.22

Changes of Shoot Length in the Diseased(W) and Non-Diseased (WO) Rice Plants due to the Response of Different Concentrations (500,1000,1500ppm) of HKUST-1 and (125,250,500ppm) CB@HKUST-1(P). "Values are Means of Five Replications. Vertical Bars Represent Standard Error. Bar Columns with Different Uppercase Letters are Statistically Significant Based on Tukey's Honest Significant Difference Test at P<0.05"

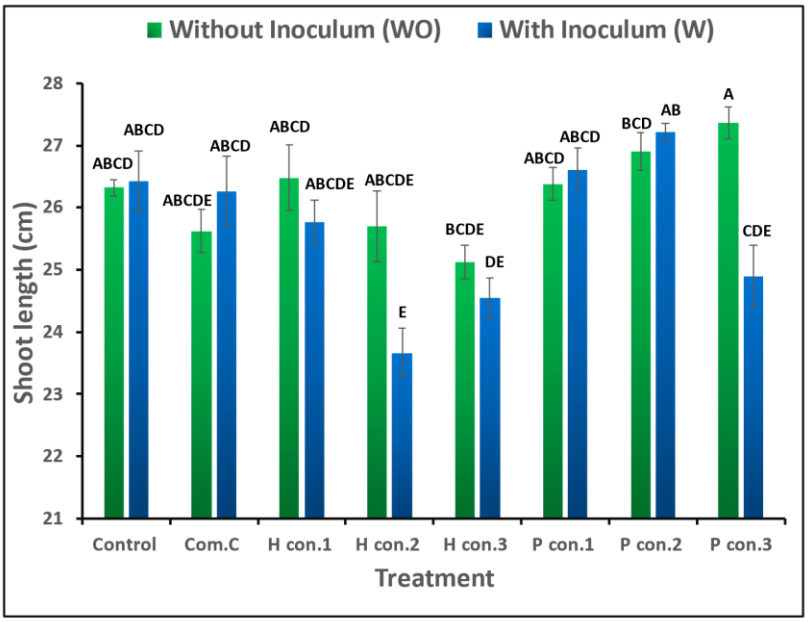

4.8.1.3 Analysis of Leaf Number

Given the controlled conditions of growth within a growth chamber, it's understandable that the morphological characteristics of both of the rice varieties, such as the average number of leaves, may not vary significantly. Typically, in such controlled environments, the maximum number of leaves per plant is limited. In this study, it was observed that the maximum number of leaves in each plant for the rice varieties did not exceed 3. This consistency in leaf number across plants underscores the uniformity of growth conditions within the growth chamber, minimizing variations in plant morphology that might arise under more heterogeneous field conditions.

4.8.1.4 Analysis of Biomass for the Rice Variety: KDML 105

Analysis of biomass is crucial because it serves as a reliable indicator of a plant's growth and development over time. In the examination of biomass, encompassing both root and shoot metrics across diseased and non-diseased plant specimens, a discernible pattern emerged concerning the influence of HKUST-1 and CB@HKUST-1's concentrations.

Notably, in the analysis of root biomass, a pronounced decrement was observed, as elucidated in Figure 4.23. It became evident that escalating concentrations of HKUST-1 corresponded with a marked reduction in root biomass, irrespective of the health status of the plants. The consistent decline in root biomass with higher HKUST-1 concentrations emphasizes a significant aspect in this thesis. In the examination of CB@HKUST-1's impact on root biomass in both diseased and non-diseased rice plants, notable findings emerged. Specifically, concentrations of 125 ppm and 250 ppm exhibited a significant elevation in root biomass compared to the control group. However, this positive trend was not sustained at higher concentrations, notably 500 ppm, where a discernible decline in root biomass was observed. This observation underscores a nuanced relationship between CB@HKUST-1 concentration levels and their influence on root biomass.

Figure 4.23

Changes of Root Biomass in the Diseased(W) and Non-Diseased (WO) Rice Plants due to the Response of Different Concentrations (500,1000,1500ppm) of HKUST-1 and (125,250,500ppm) CB@HKUST-1(P).“Values are Means af Five Replications. Vertical Bars Represent Standard Error. Bar Columns with Different Uppercase Letters are Statistically Significant Based on Tukey’s Honest Significant Difference Test At P<0.05”

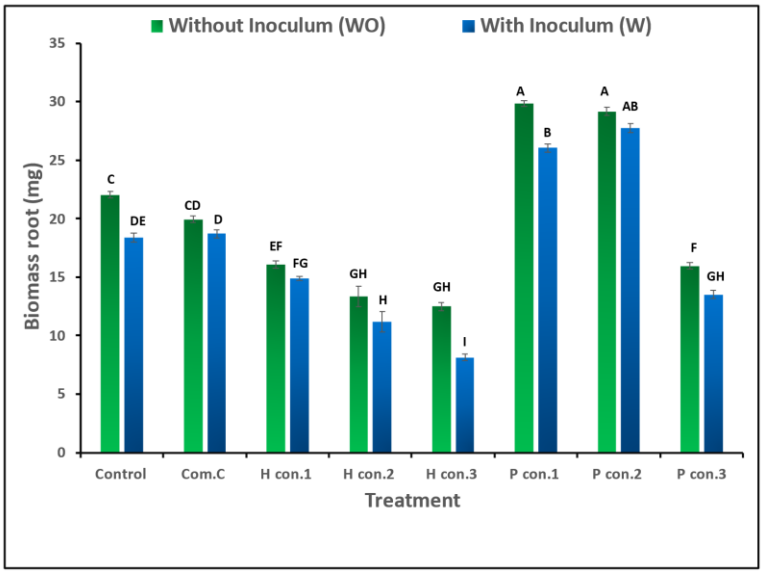

The variation in shoot biomass between rice plants with and without disease was analyzed, with a focus on the effects of different doses of HKUST-1 on this aspect of plant development. The findings presented in Figure 4.24 indicate that the influence of HKUST-1 on shoot biomass was comparatively less significant than that on root biomass.

A little decrease was seen in shoot biomass at 500 ppm and 1000 ppm in comparison to plants that were not affected by the disease, but the difference from the control group was not very noticeable. Although there was still a drop in shoot biomass at 1500 ppm when compared to plants that were not afflicted, it was not as noticeable as it was in the

control group. This implies that increased HKUST-1 concentrations could provide some defense against the normal disease-related decline in shoot biomass.

In contrast, analysis pertaining to CB@HKUST-1 revealed a consistently positive influence across all concentrations. Notably, at concentration 2 (250 ppm), a substantial increase in shoot biomass was noted. Consequently, it can be inferred that higher concentrations of HKUST-1 may exert adverse effects on plant development. However, the encapsulated variant CB@HKUST-1 demonstrated safety up to 500 ppm, with a concentration of 250 ppm emerging as optimal for promoting robust growth and development in plants.

Figure 4.24

Changes of Shoot Biomass in the Diseased(W) and Non-Diseased (WO) Rice Plants due to the Response of Concentrations (500,1000,1500ppm) of HKUST-1 and (125,250,500ppm) CB@HKUST-1(P). "Values are Means of Five Replications. Vertical Bars Represent Standard Error. Bar Columns with Different Uppercase Letters are Statistically Significant Based on Tukey's Honest Significant Difference Test at P<0.05"

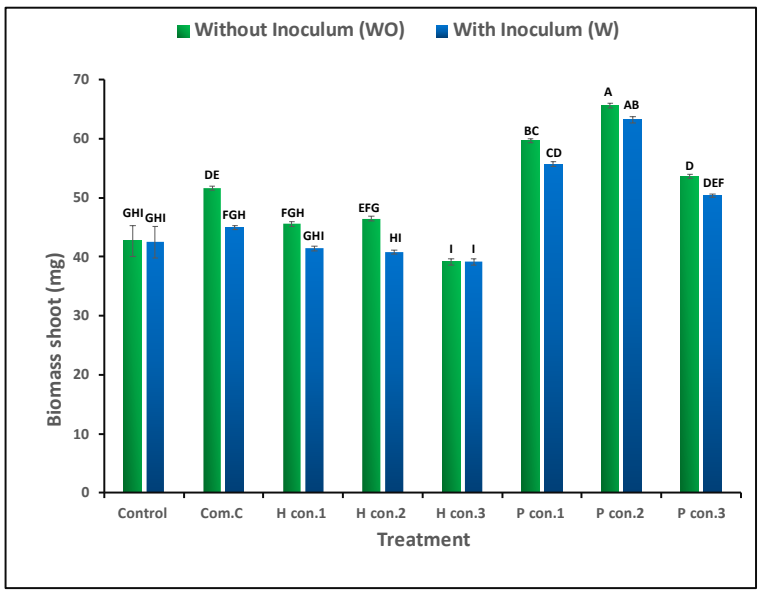

4.8.1.5 Analysis of Biomass for the Rice Variety: PTT-1

The analysis of biomass assumes paramount significance as it serves as a reliable indicator of a plant's growth and developmental trajectory over time. Through a comprehensive examination of biomass, encompassing both root and shoot metrics across diseased and non-diseased plant specimens, discernible patterns emerged regarding the impact of varying concentrations of HKUST-1 and CB@HKUST-1. Remarkably, in the evaluation of root biomass, it was observed that across non-diseased plants, all three concentrations of HKUST-1 exhibited a similar impact, albeit slightly lower than the control group. However, in diseased plants, Concentration 2(1000ppm) displayed a drastic decrease in root biomass compared to the other concentrations.

Upon scrutinizing CB@HKUST-1's effect on root biomass in both diseased and non-diseased rice plants, notable findings emerged. Specifically, in non-diseased plants, concentrations of 125 ppm and 500 ppm demonstrated a noteworthy elevation in root biomass compared to the control group. Additionally, a distinctly positive trend was observed at concentrations, particularly at 250 ppm, where a discernible increase in root biomass was noted. However, in the case of diseased plants, Concentration 1 exhibited a similar impact to the commercial product, while Concentrations 250 and 500 ppm showed similarity to the non-diseased control plants. This observation underscores a nuanced relationship between CB@HKUST-1 concentration levels and their influence on root biomass, suggesting potential implications for agricultural practices and emphasizing the need for tailored approaches based on plant health status.

Figure 4.25

Changes of Root Biomass in the Diseased(W) and Non-Diseased (WO) Rice Plants due to the Response of Different Concentrations (500,1000,1500ppm) Of HKUST-1 and (125,250,500ppm) CB@HKUST-1(P). "Values are Means of Five Replications. Vertical Bars Represent Standard Error. Bar Columns with Different Uppercase Letters are Statistically Significant Based on Tukey's Honest Significant Difference Test at P<0.05"

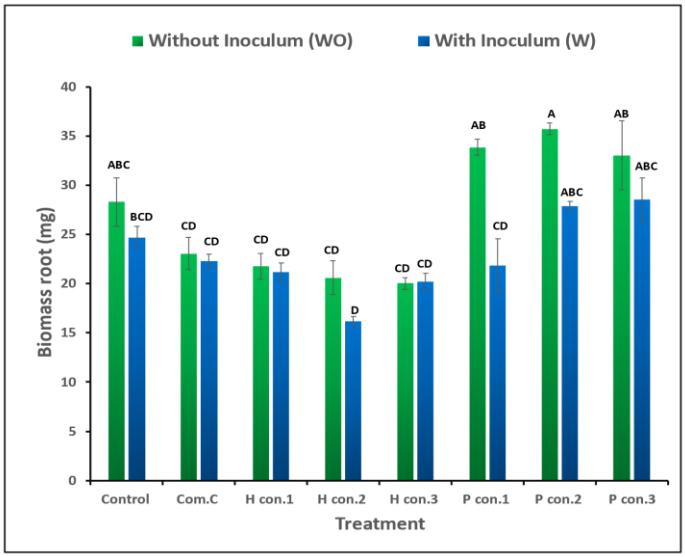

In the examination of shoot biomass variation between diseased and non-diseased plants, it was observed that concentrations of HKUST-1 exhibited relatively modest fluctuations in comparison to root biomass. Specifically, at concentrations of 500 ppm and 1500 ppm, although a reduction in shoot biomass was discerned, the disparity with the control group was marginal, as depicted in Figure 4.26. Conversely, at a concentration of 1000 ppm, while a decrease in shoot biomass relative to non-diseased plants was evident, the reduction was more pronounced when compared to the control group.

After more investigation, the CB@HKUST-1 research revealed a consistently beneficial effect at different concentrations. The noteworthy increase in shoot biomass

at concentration 2 (250 ppm) indicated a significant improvement in plant development. This crucial discovery implies that although HKUST-1 at greater concentrations may have detrimental effects on plant growth, the encapsulated form, CB@HKUST-1, demonstrated an exceptional safety margin up to 500 ppm. This finding emphasizes CB@HKUST-1's promise as a workable strategy for encouraging robust and sustained plant development. Furthermore, the concentration of 250 ppm was shown to be the ideal dose, producing the strongest benefits in promoting plant growth and vitality. This comprehensive knowledge provides important insights for upcoming agricultural applications and environmental sustainability initiatives by illuminating the complex dynamics between nanoparticle concentrations and their effects on plant biology.

Figure 4.26

Changes of Shoot Biomass in the Diseased(W) and Non-Diseased (WO) Rice Plants Due to the Response of Different Concentrations (500,1000,1500ppm) Of HKUST-1 and (125,250,500ppm) CB@HKUST-1(P); "Values are Means of Five Replications. Vertical Bars Represent Standard Error. Bar Columns with Different Uppercase Letters are Statistically Significant Based on Tukey's Honest Significant Difference Test at P<0.05"

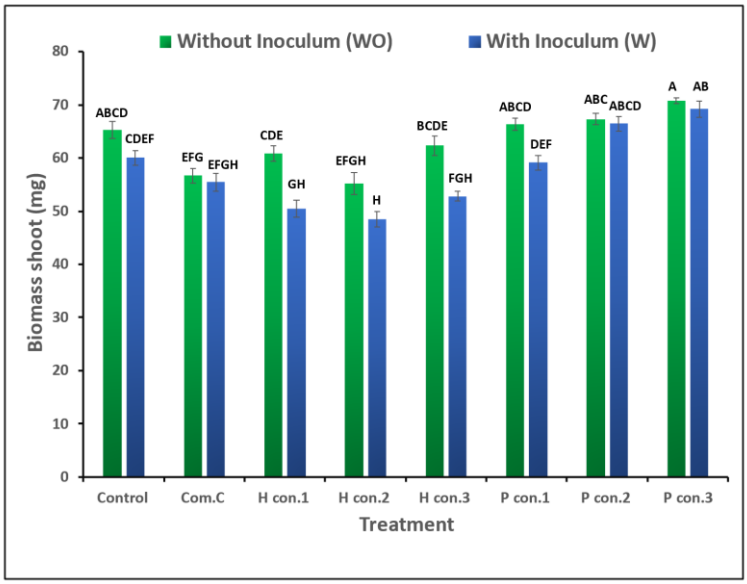

4.8.1.6 Analysis of Disease Index for the Rice Variety: KDML 105

After 14 days of chemical treatment, the rice plants were harvested in order to be thoroughly examined. After the first seven days of therapy, the writer it was reported no symptoms at all. But by the tenth day of the observation, mild but noticeable symptoms started to appear, albeit not very obviously, as Figure 4.27 shows. The KDML variet y demonstrated a noteworthy resistance against rice blast infection, as seen by the very modest development of symptoms and delayed start that the authors scrupulously noted. This discovery highlights the KDML variety's innate resistance and provides insight into its possible use in lessening the effects of rice blast disease in agricultural environments.

Figure 4.27

a) Diseased Rice Plants, b) Non-Diseased Rice Plants

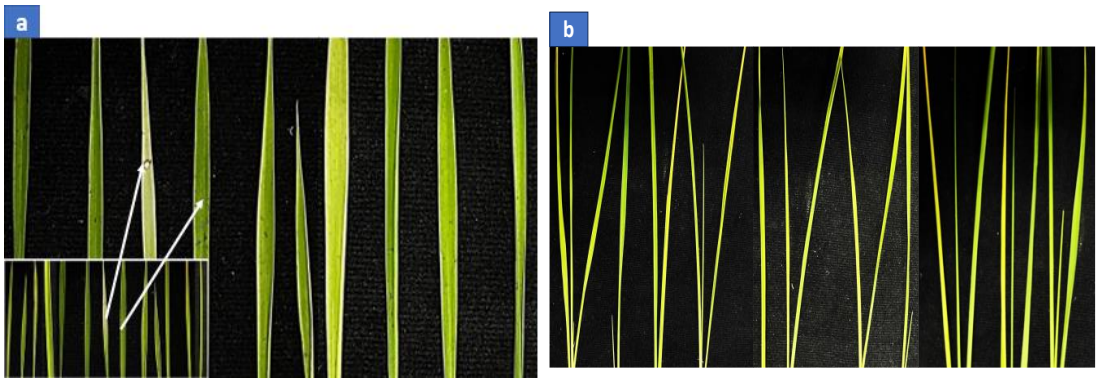

Moreover, during the inoculation process, where spores were administered at a rate of 40 ml per plant, it became evident that this dosage was insufficient for effectively challenging the resilience of the KDML variety against the rice blast pathogen.

In the context of the three concentrations of HKUST-1 applied it appears that they do not possess the efficacy to effectively mitigate the diseases under study. As a consequence, the disease index associated with these concentrations are almost similar to that of the control group. This observation suggests that despite the application of

HKUST-1, the progression or severity of the diseases remains unimpeded, possibly indicating a lack of disease control potential at the tested concentrations. Indeed, for CB@HKUST-1, the author reported a notable absence of symptoms across all concentrations tested. This observation is substantiated by a disease index of 0 for each concentration, indicating a complete lack of symptoms associated with the diseases under investigation. Such findings suggest that CB@HKUST-1 exhibits remarkable efficacy in disease suppression, as evidenced by its ability to entirely prevent symptom development at all tested concentrations. This underscores the potential of CB@HKUST-1 as a highly effective and reliable agent for disease management in rice plants. The percent disease index for each treat

Table 4.4

Percent Disease Index (KDML 105)

Treatments	Percent Disease Index
Control	15.92 ± 0.06%
Commercial CB (1500 ppm)	11.48 ± 0.06%
HKUST-1	
Conc.1 (500 ppm)	14.44 ± 0.03%
Conc.2 (1000 ppm)	15.72 ± 0.06%
Conc.3 (1500 ppm)	15.54 ± 0.06%
CB@HKUST-1	
Conc.1 (125 ppm)	NA
Conc. 2 (250 ppm)	NA
Conc. 3 (500 ppm)	NA

4.8.1.7 Analysis of Disease Index for the Rice Variety: PTT-1

Figure 4.28

a) Diseased Rice Plants, b) Non-Diseased Rice Plants

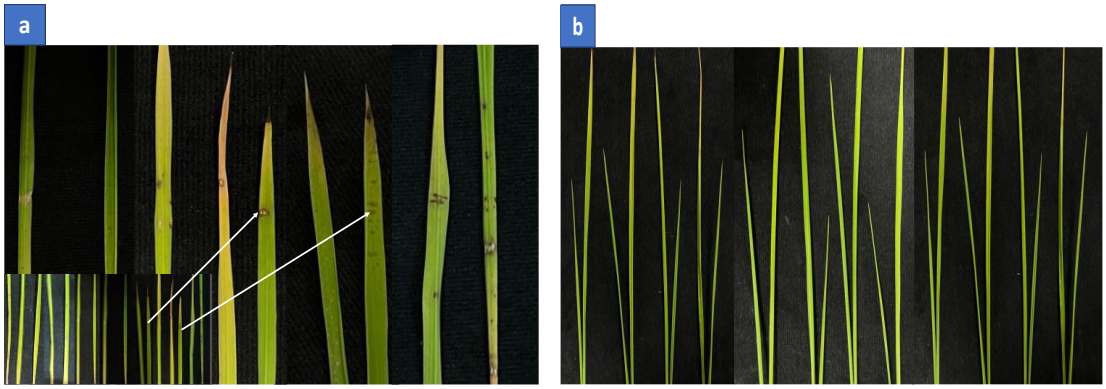

Following a 14-day interval subsequent to chemical treatment, the rice specimens were gathered for assessment. Initial symptomatology became perceptible by the 4th day, albeit in a subdued manner. However, by the 6th day, symptom expression became notably conspicuous. The authors underscored the notable susceptibility of the PTT-1 variety to rice blast infection, substantiated by the rapid progression of symptoms observed.

Regarding the application of the three concentrations of HKUST-1, initial observations suggest that the lowest concentration lacked the efficacy to adequately mitigate the targeted diseases. Conversely, the subsequent two concentrations of HKUST-1 demonstrated marginal inhibitory effects when compared to the control group.

Notably, CB@HKUST-1 exhibited a remarkable absence of symptoms across all tested concentrations, albeit minor symptoms were discerned at the lowest concentration. This observation was supported by a disease index of 0 for the other two concentrations, indicative of a complete absence of disease symptoms. Such compelling findings suggest that CB@HKUST-1 manifests noteworthy efficacy in disease suppression, as

manifested by its ability to entirely forestall symptom development at all examined concentrations. This underscores the promising potential of CB@HKUST-1 as a highly efficacious and dependable agent for the management of diseases in rice plants.

Table 4.5

Percent Disease Index (PTT-1)

Treatments	Percent Disease Index
Control	31.3± %1.3
Commercial CB (1500 ppm)	23.704 ±1.9 %
HKUST-1	
Conc.1 (500 ppm)	31.788± 1.1%
Conc.2 (1000 ppm)	19.982± 1.8%
Conc.3 (1500 ppm)	12.582± 1.8%
CB@HKUST-	
Conc.1 (125 ppm)	3.322±4.3%
Conc. 2 (250 ppm)	NA
Conc. 3 (500 ppm)	NA

4.8.2 Physiological Analysis

A comprehensive set of physiological investigations was conducted, encompassing measurements of leaf greenness, phenolic compound, and flavonoid content, following a 14-day chemical treatment administered to both non-inoculated and inoculated rice plants

Table 4.5 delineates the discernible attributes, both significant and non-significant, pertaining to the dual factors under consideration: treatment and disease. Moreover, it elucidates the collective impact engendered by the interaction of these factors across various physiological parameters.

Table 4.6

Significance Levels in Individual and Interactive Effect of Different Physiological Parameters in Two Different Rice Varieties

	Leaf greenness	Phenolic compound content	Flavonoid content
Variety KDML			
Factor			
Treatment(T)	**	**	*
Disease(D)	**	**	**
TxD	**	*	NS
Variety PTT-1			
Factor			
Treatment(T)	**	**	**
Disease(D)	**	**	**
TxD	*	**	*

***, *, and NS indicate $P \leq 0.01$, $P \leq 0.05$, and non-significant respectively*

4.8.2.1 Analysis of Leaf Greenness for the Rice Variety: KDML 105

An analysis of leaf greenness (SPAD) was conducted for both diseased and non-diseased plants. As per physiological understanding, plants experiencing stress typically exhibit a decrease in leaf greenness, while those not under stress tend to show an increase. However, contrary to this expectation, the author reported that leaf greenness was higher in the diseased plants compared to the non-diseased ones. This finding aligns with previous literature by (Nemeskéri et al., 2018)., which suggests that under certain circumstances, such as observed in the diseased plants in this study, plants may exhibit heightened chlorophyll production as a response to stress.

The impact of HKUST-1 and CB@HKUST-1, administered at various concentrations, on the leaf greenness of rice plants, both diseased and non-diseased, was investigated as shown in the figure 4.29. Regarding HKUST-1, it was noted that a concentration of 500ppm elicited no significant alteration in leaf greenness compared to the control group. However, concentrations of 1000ppm and 1500ppm resulted in a notable decrease in leaf greenness across both diseased and non-diseased rice plants. Conversely, the application of CB@HKUST-1 exhibited distinctive effects on leaf greenness. Specifically, concentrations of 125ppm and 250ppm induced an increase in leaf greenness relative to the control group. However, at a concentration of 500ppm, a decline in leaf greenness was observed in both diseased and non-diseased rice plants.

Figure 4.29

Changes of Leaf Greenness in the Diseased(W) and Non-Diseased (WO) Rice Plants due to the Response of Different Concentrations (500,1000,1500ppm) of HKUST-1 and (125,250,500ppm) CB@HKUST-1(P). "Values are Means of Five Replications. Vertical Bars Represent Standard Error. Bar Columns with Different Uppercase Letters are Statistically Significant Based on Tukey's Honest Significant Difference Test at P<0.05".

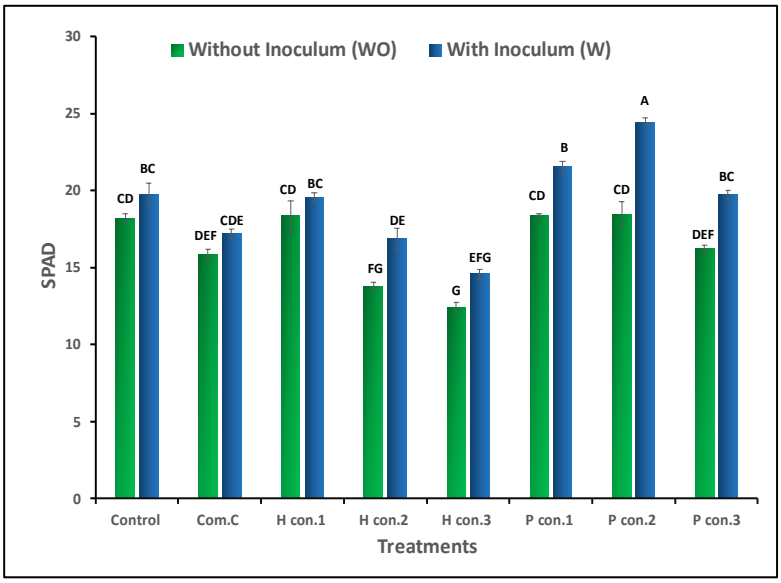

4.8.2.2 Analysis of Leaf Greenness for the Rice Variety: PTT-1

For rice variety PTT-1, akin to the observations made with KDML, a similar phenomenon was noted wherein diseased plants exhibited heightened leaf greenness compared to their healthy counterparts as shown in the figure 4.30. Meanwhile, in the case of HKUST-1, it was discerned that a concentration of 500 parts per million (ppm) elicited no significant alteration in leaf greenness in comparison to the control group. However, concentrations of 1000 ppm and 1500 ppm yielded a noticeable decline in leaf greenness across both diseased and non-diseased rice plants. Conversely, the application of CB@HKUST-1 manifested distinct effects on leaf greenness. Specifically, concentrations of 125 ppm and 250 ppm induced an augmentation in leaf greenness relative to the control group. Nonetheless, at a concentration of 500 ppm, a reduction in leaf greenness was observed in both diseased and non-diseased rice plants.

Figure 4.30

Changes of Leaf Greenness in the Diseased(W) and Non-Diseased (WO) Rice Plants due to the Response of Different Concentrations (500,1000,1500ppm) of HKUST-1 and (125,250,500ppm) CB@HKUST-1(P). "Values are Means of Five Replications. Vertical Bars Represent Standard Error. Bar Columns with Different Uppercase Letters are Statistically Significant Based on Tukey's Honest Significant Difference Test at P<0.05"

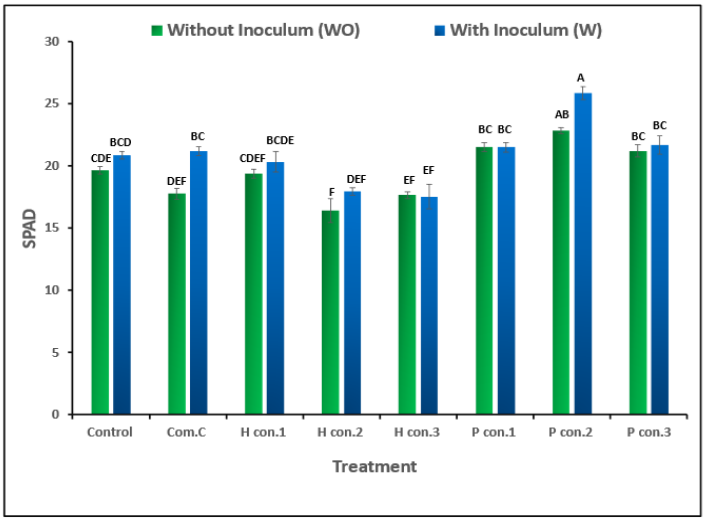

4.8.2.3 Analysis of Phenolic Compound and Flavonoids for the Rice Variety: KDML 105

For the assessment of physiological parameters, namely phenolic compounds and flavonoids, in both the KDML and PTT-1 rice varieties, standard curves were prepared to facilitate accurate measurement. The standard curve, as depicted in Figure 4.31, served as a crucial tool in quantifying these parameters.

Figure 4.31

Standard Curve for Assessment of a) Phenolic Compounds and b) Flavonoids

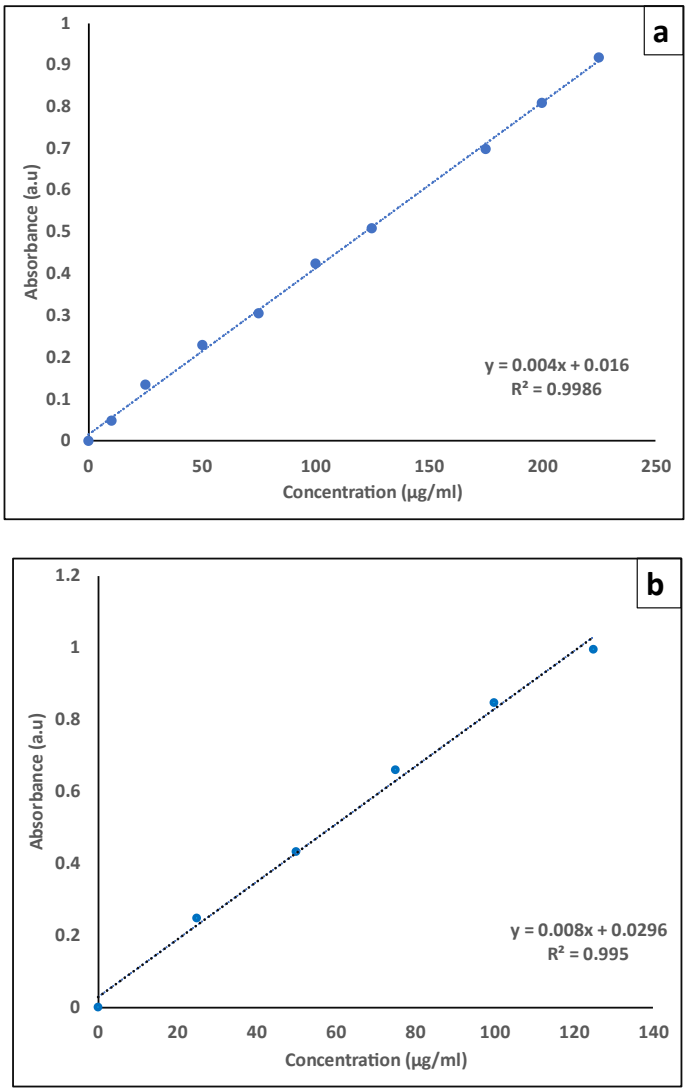

In the evaluation of phenolic compound concentrations within the KDML variety, it was observed that diseased plants exhibited a reduction in phenolic compound levels compared to their non-diseased counterparts. This observation aligns with previous research findings, specifically corroborated by (Toan et al., 2017). This congruence underscores a consistent trend linking disease manifestation with decreased phenolic compound concentrations.

Conversely, in the case of HKUST-1, across all three concentrations, non-diseased plants displayed uniform phenolic compound levels, indicating a consistent impact comparable to the control group. However, in diseased plants, concentrations 1 and 2 yielded similar effects, demonstrating levels of phenolic compounds comparable to the control group. Intriguingly, at concentration 3, a substantial increase in phenolic compound levels was observed. This divergence in concentration 3 suggests an unexpected elevation in phenolic compound concentration, diverging from the trend observed in concentrations 1 and 2. Such findings highlight a nuanced response to HKUST-1 treatment, wherein higher concentrations induce an unexpected surge in phenolic compound concentration within diseased plants.

In the context of CB@HKUST-1, it is noteworthy that diseased plants displayed uniformity in phenolic compound levels across all three concentrations especially for the concentration 1, albeit at levels lower than the control group. Conversely, in non-diseased plants, a discernible reduction in flavonoid release was evident across all concentrations, with particular prominence observed at concentration 2. This observed incongruity underscores a pronounced contrast in the response to CB@HKUST-1 treatment between diseased and non-diseased plants

Figure 4.32

Influence of Diseased and Non- Diseased Plants on Phenolic Compound Content due to the Response of Different Concentrations (500,1000,1500ppm) of HKUST-1 and (125,250,500ppm) CB@HKUST-1(P). "Values are Means of Five Replications. Vertical Bars Represent Standard Error. Bar Columns with Different Uppercase Letters are Statistically Significant Based on Tukey's Honest Significant Difference Test at P<0.05

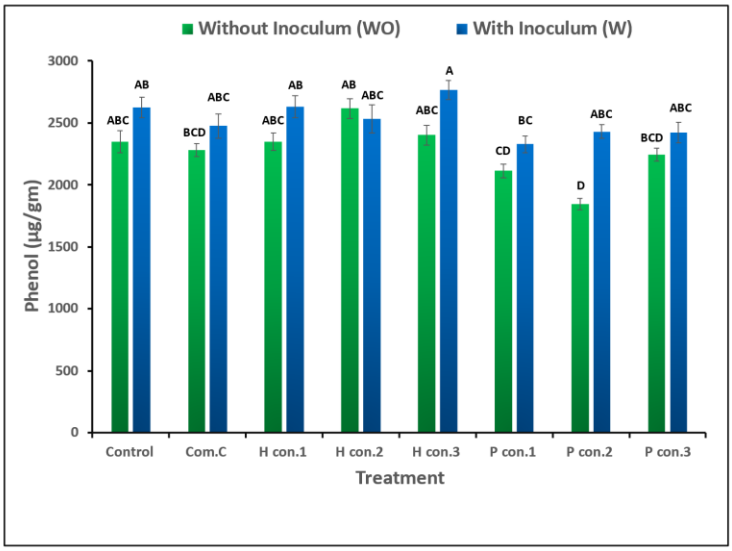

Similarly to phenolic compounds, in the assessment of flavonoid concentrations, diseased plants exhibited a reduction in flavonoid levels compared to their non-diseased counterparts. This consistency further reinforces the association between disease susceptibility and diminished flavonoid levels.In the assessment of flavonoid content, statistical analysis employing ANOVA indicated a lack of significance in the interactive interaction between the two factors under consideration. Examination of Figure 4.33 reveals notable patterns: in the initial graph, concentration 1 of HKUST-1 induced an increased release of flavonoids compared to the control group, whereas higher concentrations led to a decline in flavonoid release. Similarly, for CB@HKUST-1, all concentrations exhibited relatively low levels of flavonoid release, with concentration 2 demonstrating a particularly pronounced decrease.

Furthermore, the second graph unveiled a significant disparity between diseased and non-diseased rice plants, with a discernible elevation in flavonoid release observed in the former. This finding underscores a noteworthy divergence in flavonoid dynamics between the two groups, suggesting a potential influence of disease status on the regulatory mechanisms governing flavonoid biosynthesis and release in rice plants.

Figure 4.33

Influence on Flavonoid Content by the a) Effect of Different Concentrations (500,1000,1500ppm) of HKUST-1 and (125,250,500ppm) CB@HKUST-1(P) and b) Effect of Diseased(W) and Non-Diseased (WO) on Rice Plants.

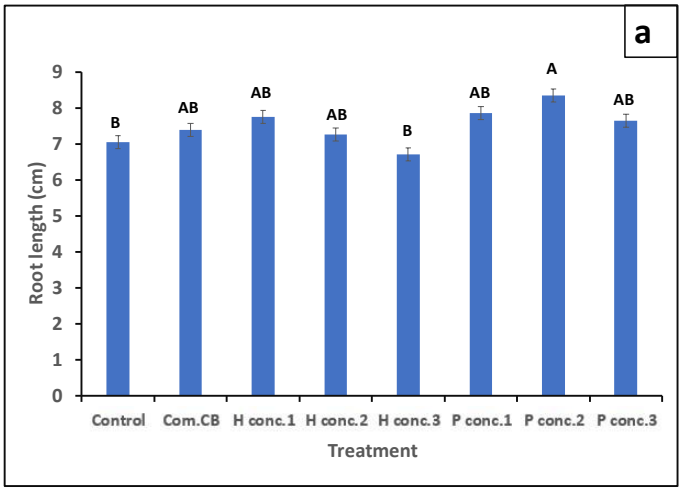

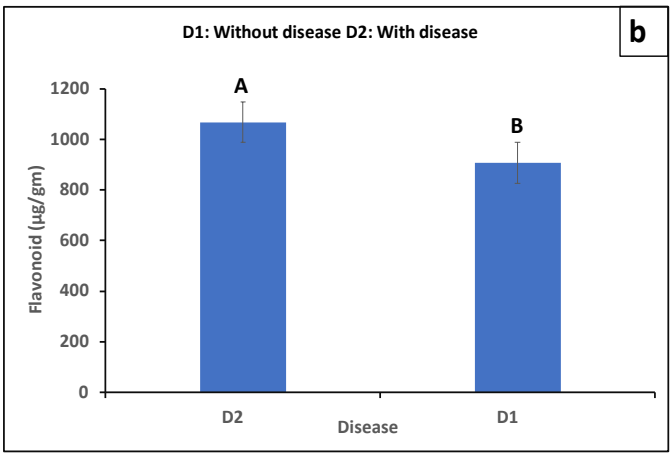

4.8.2.4 Analysis of Phenolic Compounds and Flavonoids for the Rice Variety: PTT-1

In the assessment of phenolic compound concentrations within the PTT-1 rice variety, it was again observed that diseased plants exhibited a reduction in phenolic compound levels relative to their non-diseased counterparts, akin to previous findings in the rice variety KDML (Toan et al., 2017). This alignment with prior research underscores a consistent association between disease manifestation and diminished phenolic compound concentrations.

Conversely, in the case of HKUST-1 treatment, non-diseased plants demonstrated comparable phenolic compound levels to the control group at concentration 1 (500 ppm), while concentrations 2 (1000 ppm) and 3 (1500 ppm) exhibited an increase. However, in diseased plants, concentrations 1 and 3 elicited similar effects, yielding elevated phenolic compound levels akin to the control group. Notably, concentration 2 showed a substantial elevation in phenolic compound concentration, deviating from the trends observed in concentrations 1 and 3. Such disparities highlight a nuanced response to HKUST-1 treatment, wherein moderate concentrations induce an unforeseen surge in phenolic compound concentration within diseased plants.

Regarding CB@HKUST-1, it is pertinent to note that diseased plants displayed uniformity in flavonoid levels across all concentrations, particularly noticeable at concentration 1 (125 ppm), albeit at levels lower than the control group. Conversely, non-diseased plants exhibited a discernible reduction in flavonoid release across all concentrations, with notable prominence observed at concentration 2 (250 ppm). This observed incongruity underscores a pronounced disparity in the response to CB@HKUST-1 treatment between diseased and non-diseased plants.

Figure 4.34

Influence of Diseased and Non-Diseased Plants on Phenolic Compound Content due to the Response of Different Concentrations (500,1000,1500ppm) of HKUST-1 and (125,250,500ppm) CB@HKUST-1(P). "Values are Means of Five Replications. Vertical Bars Represent Standard Error. Bar Columns with Different Uppercase Letters are Statistically Significant Based on Tukey's Honest Significant Difference Test at P<0.05"

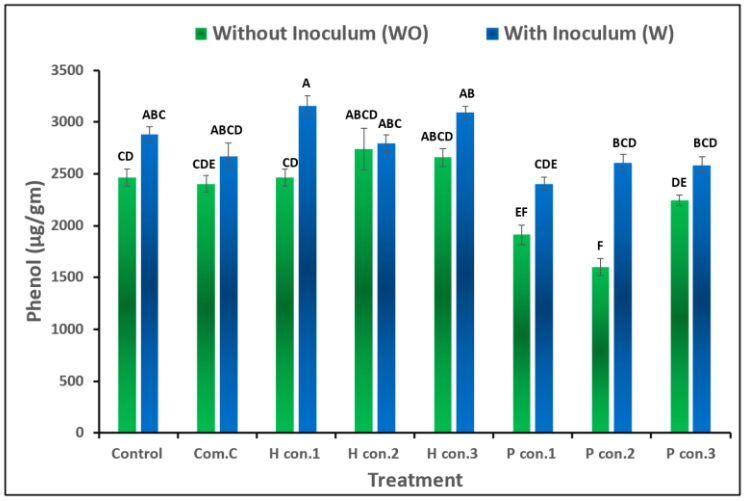

In parallel with the evaluation of phenolic compounds, the appraisal of flavonoid concentrations reveals a congruent trend wherein diseased plants manifest diminished flavonoid levels relative to their non-diseased counterparts. This consistent finding serves to fortify the established correlation between disease susceptibility and the attenuation of flavonoid content.

In the context of HKUST-1 treatment, non-diseased plants display uniform flavonoid levels across concentrations 1 (500 ppm) and 3 (1500p ppm), suggestive of a consistent impact reminiscent of the control group. However, at concentration 2 (1000 ppm), a discernible increase is observed. Conversely, in diseased plants, concentrations 2 and 3 exhibit comparable effects, yielding flavonoid levels akin to the control group. Intriguingly, concentration 1 incites a notable elevation in flavonoid levels, deviating from the observed trends in concentrations 2 and 3. This divergence underscores a

nuanced response to HKUST-1 treatment, particularly accentuated at the lowest concentration.

Concerning CB@HKUST-1, within diseased plants, concentrations 2 (250 ppm) and 3 (500 ppm) showcase consistent flavonoid levels analogous to the control group, albeit with a minor increase observed in concentration 1 (125ppm). Conversely, in non-diseased plants, a decrement in flavonoid release is noted across all three concentrations, with a more pronounced decrease notably observed at concentration 2. This observed discrepancy underscores a distinct response to CB@HKUST-1 treatment between diseased and non-diseased plants, thereby necessitating further inquiry into the underlying mechanisms governing this observed phenomenon.

Figure 4.35

Influence of Diseased and Non-Diseased Plants on Flavonoid Content due to the Response of Different Concentrations (500,1000,1500ppm) of HKUST-1 and (125,250,500ppm) CB@HKUST-1(P). "Values are Means of Five Replications. Vertical Bars Represent Standard Error. Bar Columns with Different Uppercase Letters are Statistically Significant Based on Tukey's Honest Significant Difference Test at P<0.05"

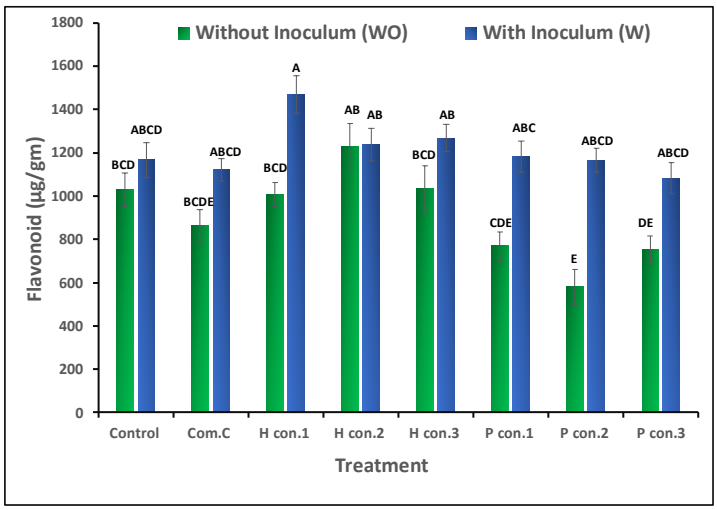

The morphological and physiological parameters' individual effects on rice varieties KDML 105 and PTT-1 are delineated in Table 4.7 and 4.8, respectively, denoting Mean ± SE value

Table 4.7

Individual Effect on Different Parameters by using the Treatment on Diseased and Non- Diseased Rice Plants for the Variety KDML 105

Variety KDML 105	Leaf greenness (SPAD)	Root Length (cm)	Shoot Length (cm)	Biomass Root (cm)	Biomass Shoot (cm)	Phenolic compound (µg/gm)	Flavonoid (µg/gm)
Control (WO)	18.19±0.3CD	5.8±0.3	24.63±0.3BC	22.05±0.3C	42.75±2.5GHI	2348±87.6ABC	955.4±88.6
Control(W)	19.79±0.7BC	5.02±0.3	24.74±0.2B	18.38±0.4DE	42.49±2.7GHI	2627±81.6AB	1086.9±124
Commercial CB (WO)	15.84±0.3DEF	5.76±0.3	24.97±0.2B	19.934±0.3CD	51.66±0.3DE	2282.1±51.7BCD	912.3±60.1
Commercial CB (W)	17.18±0.3CDE	5.12±0.4	25.4±0.3B	18.726±0.3D	44.93±0.3FGH	2476.5±98.2ABC	1018.1±88.4
HKUST-1 (con.1) (WO)	18.34±0.9CD	5.524±0.3	24.22±0.3BCD	16.066±0.3EF	45.54±0.3FGH	2349.4±69.9ABC	923.1±100.5
HKUST-1 (con.1) (W)	19.56±0.3BC	5±0.2B	21.22±0.4EF	14.898±0.2FG	41.41±0.4GHI	2632.2±89.1AB	1348.4±66.7
HKUST-1 (con.2) (WO)	13.76±0.3FG	4.38±0.4	23.62±0.3BCD	13.34±0.8GH	46.38±0.6EFG	2617.2±81.1AB	1056.3±64.5
HKUST-1 (con.2) (W)	16.88±0.6DE	3.94±0.2	22.17±0.2DE	11.18±0.9H	40.76±0.3HI	2531.2±114.1ABC	1058.9±74.6
HKUST-1 (con.3) (WO)	12.38±0.4G	3.74±0.3	19.17±0.3FG	12.501±0.4GH	39.15±0.4I	2402.1±77.8ABC	963±47.1
HKUST-1 (con.3) (W)	14.57±0.3EFG	3.58±0.2	17.76±0.7G	8.144±0.3I	39.13±0.5I	2766.5±76.5A	1116.3±27.9
CB@HKUST-1(con.1) (WO)	18.34±0.2CD	5.976±0.3	28±0.2A	29.841±0.2A	59.636±0.3BC	2115.7±55.2CD	868.6±51.2
CB@HKUST-1(con.1) (W)	21.54±0.4B	4.98±0.3	25.08±0.3B	26.032±0.4B	55.7±0.4CD	2329.1±69.1BC	1041.1±93.8
CB@HKUST-1(con.2) (WO)	18.46±0.8CD	7.16±0.3	27.98±0.8A	29.17±0.3A	65.657±0.3A	1846.5±46.6D	756.5±54.7
CB@HKUST-1(con.2) (W)	24.44±0.3A	6.32±0.3	25.42±0.5B	27.748±0.4AB	63.206±0.5AB	2432.1±54.0ABC	914.7±64.9
CB@HKUST-1(con.3) (WO)	16.21±0.2DEF	5.66±0.3	23.42±0.4BCDE	15.95±0.3F	53.57±0.4D	2247.1±52.4BCD	826.8±82.2
CB@HKUST-1(con.3) (W)	19.73±0.3BC	4.32±0.4	22.29±0.3CDE	13.522±0.3GH	50.395±0.3DEF	2424.9±81.9ABC	968.3±87.6
ANOVA (p-value)	0.0004	0.7585	0.0016	0.0034	0.0331	0.0317	0.4836

Table 4.8

Individual Effect on Different Parameters by using the Treatment on Diseased and Non- Diseased Rice Plants for the Variety PTT-1

Variety PTT-1	Leaf greenness (SPAD)	Root length (cm)	Shoot Length (cm)	Biomass Root (cm)	Biomass Shoot (cm)	Phenolic compound (µg/gm)	Flavonoid (µg/gm)
Commercial CB (WO)	17.781±0.4DEF	7.52±0.2	25.62±0.3ABCDE	23.06±1.7CD	56.7±1.4EFG	2402.7±79.1CDE	859.9±77.2BCDE
Commercial CB (W)	21.189±0.4BC	7.28±0.3	26.26±0.6ABCD	22.32±0.6CD	55.46±1.7EFGH	2667±130.7ABCD	1122.3±50.8ABCD
HKUST-1 (con.1) (WO)	19.397±0.3CDEF	7.88±0.5	26.48±0.5ABCD	21.74±1.3CD	60.88±1.4CDE	2462.5±83CD	1007±54.1BCD
HKUST-1 (con.1) (W)	20.327±0.8BCDE	7.66±0.4	25.76±0.4ABCDE	21.16±0.9CD	50.5±1.6GH	3153.2±98.7A	1468.9±86.4A
HKUST-1 (con.2) (WO)	16.42±0.9F	7.72±0.4	25.7±0.6ABCDE	20.6±1.7CD	55.22±2.0EFGH	2739.8±201.9ABCD	1229.1±107.8AB
HKUST-1 (con.2) (W)	17.957±0.3DEF	6.82±0.2	23.66±0.4E	16.16±0.5D	48.48±1.4H	2789.7±87.6ABC	1238.3±75.1AB
HKUST-1 (con.3) (WO)	17.653±0.3EF	6.92±0.1	25.12±0.3BCDE	20.02±0.6CD	62.32±1.8BCDE	2658.6±87.3ABCD	1033.3±106.4BCD
HKUST-1 (con.3) (W)	17.527±0.9EF	6.54±0.2	24.54±0.3DE	20.18±0.9CD	52.8±0.9FGH	3092.4±59.3AB	1267.7±62.5AB
CB@HKUST-1(con.1) (WO)	21.527±0.3BC	8.72±0.2	26.38±0.2ABCD	33.84±0.8AB	66.38±1.2ABCD	1910.8±94.6EF	768.4±66.8CDE
CB@HKUST-1(con.1) (W)	21.493±0.4BC	7.02±0.3	26.6±0.4ABCD	21.8±0.8CD	59.12±1.4DEF	2403.5±66.5CDE	1180.8±72.2ABC
CB@HKUST-1(con.2) (WO)	22.84±0.2AB	8.46±0.4	26.9±0.3BCD	35.72±0.6A	67.32±1.0ABC	1599.4±83.9F	581.1±80.9E
CB@HKUST-1(con.2) (W)	25.847±0.5A	8.28±0.4	27.22±0.1AB	27.88±0.5ABC	66.46±1.4ABCD	2607.7±78.9BCD	1165±56.1ABCD
CB@HKUST-1(con.3) (WO)	21.207±0.5BC	8.52±0.4	27.36±0.2A	33.02±3.5AB	70.78±0.5A	2241.8±52.4DE	754.4±59.4DE
CB@HKUST-1(con.3) (W)	21.693±0.8BC	6.78±0.3	24.9±0.5CDE	28.522±2.2ABC	69.22±1.5AB	2584.1±77.9BCD	1081.5±71.9ABCD
ANOVA (p-value)	0.0459	0.1838	0.0031	0.0235	0.0112	0.0028	0.0249

CHAPTER 5
CONCLUSION AND FUTURE RECOMMENDATION

5.1 Conclusion

In conclusion, this research exemplifies how agrochemicals can be encapsulated within HKUST-1, resulting in a slow and controlled release. It is however important to note that the maximum time taken for the release of carbendazim loaded from the system is 6 days. These results demonstrate the potential of HKUST-1 as an effective carrier of agrochemicals with controlled release properties. The experiments conducted on rice plants illustrate their significant implications for agriculture processes and crop defense techniques.

High performance liquid chromatography (HPLC) findings support that carbendazim is released as depicted. These findings show also that HKUST-1 reduces mutated cells caused by UV radiations, as well as protecting pesticides from the atmosphere such as air or moisture. This is an indication of the potential use of agrochemical encapsulation in HKUST-1 in agriculture. Thus, this technology enables efficient and sustainable distribution of agrochemicals to crops with minimal environmental impact. Therefore, it represents a great leap towards promoting environmentally friendly agricultural practices thereby ensuring the effectiveness and sustainability of crop protection measures.

Furthermore, significant insights were provided through the comparison of the encapsulated carbendazim within a metal-organic framework and the standard recommended dose of commercial carbendazim. The encapsulated carbendazim showed its effectiveness even in low concentrations (100 ppm). As well, at above 500 ppm copper toxicity might have been induced in the plants.

These findings came from controlled plant trials done under controlled conditions and also in vitro efficacy testing. Through methodical evaluation of morphological and

physiological attributes, complex relationships between different HKUST and Carbendazim@HKUST product concentrations on rice plants were cleared up thereby underscoring the need for dose optimization for maximum efficacy and minimum environmental levels of destruction. Therefore, this study's results contribute significantly to our understanding about agrochemical encapsulation and sustained release with particular reference to suitability of HKUST-1 as a material that may serve this function in future

Also, there is potential for reducing environmental damage caused by excessive application of pesticides through use of these containers leading to reduced amounts required on farms which will benefit farmers financially as well. In conclusion, these results demonstrate how modern-day encapsulation technologies have the ability to revolutionize farming practices into more sustainable ones that are ecologically aware in future.

5.2 Future Recommendation

Further studies in the area could mostly be concerned about refining encapsulation methods and observing release kinetics for diverse agrochemicals. This research could strive to find more eco-friendly and efficient ways of delivering pesticides. Such results signal a milestone in the development of effective, long-acting pesticide delivery technologies. It is worthy to note that successful synthesis of agrochemicals with sustainable slow-release properties and defense against environmental damage at HKUST-1 encapsulation indicates major advancement towards promoting sustainable agricultural practices. Additionally, incorporation of these packaged chemicals minimizes the use of pesticides thereby reducing environmental damage and increasing economic returns to farmers. The encapsulation of agrochemicals in HKUST-1 has been developed and described satisfactorily, opening up positive prospects for further applications and evaluations.

1. Field Inspection: The effectiveness of the agrochemicals in HKUST-1 has to be determined through field studies. In these tests, the efficiency of encapsulated agrochemicals with respect to crop yield, quality, and environmental impact should be carefully evaluated.

2. Long-Term Impact Evaluation: Assessing long-term effects of inclusion of HKUST-1-incorporated agrochemicals on crop yield, soil health and general ecological sustainability is essential. The aim of this investigation is to guarantee that the technology remains sustainable over time

3. Global Environmental Improvement: Encouraging encapsulation of organic materials not only helps improve the environment globally but also promotes sustainability. This recommendation sheds light on how embedding technologies could have a valuable global environmental effect.

In addition to contributing towards our understanding on agrochemical encapsulation, these future research attempts will lead to ecologically friendly farming practices that are sustainable in nature.

REFERENCE

Abdelhameed, R. M., Abdelhameed, R. E., & Kamel, H. A. (2019). Iron-based metal-organic-frameworks as fertilizers for hydroponically grown Phaseolus vulgaris. *Materials Letters*, *237*, 72–79. https://doi.org/10.1016/J.MATLET.2018.11.072

Alexandre Meybeck, Jussi Lankoski, Suzanne Redfern, Azzu, N., & Gitz, V. (2012). Building resilience for adaptation to climate change in the agriculture sector. In *Building resilience for adaptation to climate change in the agriculture sector*. The United Nations Organisation For Economic Co-Operation And Development. https://elibrary.fmard.gov.ng/handle/123456789/312

Al-Janabi, N., Hill, P., Torrente-Murciano Laura, Arthur Garforth, Patricia Gorgojo, Flor Siperstein, Xiaolei Fan, (2015). Mapping the Cu-BTC metal–organic framework (HKUST-1) stability envelope in the presence of water vapour for CO2 adsorption from flue gases. *Chemical Engineering Journal, 281(1).pp 669-677.*

Amjad Bashir, M., Raza, Q.-U.-A., Umair Sial, M., Rehim, A., Muhammad Ali Raza, H., Ali Khan, K., Ijaz, M., & Wasif, M. (2022). *Key Aspects of Plant Hormones in Agricultural Sustainability under Climate Change* . https://doi.org/10.5772/intechopen.102601

An, C., Sun, C., Li, N., Huang, B., Jiang, J., Shen, Y., Wang, C., Zhao, X., Cui, B., Wang, C., Li, X., Zhan, S., Gao, F., Zeng, Z., Cui, H., & Wang, Y. (2022). Nanomaterials and nanotechnology for the delivery of agrochemicals: strategies towards sustainable agriculture. *Journal of Nanobiotechnology*, *20*(1). https://doi.org/10.1186/S12951-021-01214-7

Anstoetz, M., Sharma, N., Clark, M., & Yee, L. H. Characterization of an oxalate-phosphate-amine metal-organic framework (OPA-MOF) exhibiting properties suited for innovative applications in agriculture. *Journal of Materials Science*, *51*. https://doi.org/10.1007/s10853-016-0171-6

Anwar, A., Bhat, G., protection, G. S.-A. of plant, & 2002, undefined. (n.d.). Management of sheath blight and blast in rice through seed treatment. *Indianjournals.ComA Anwar, GN Bhat, GS SingharaAnnals of Plant Protection Sciences, 2002 indianjournals.Com*. Retrieved September 17, 2023, from https://www.indianjournals.com/ijor.aspx?target=ijor:apps&volume=10&issue=2&article=025

Bayer, I. S. (2023). Controlled Drug Release from Nanoengineered Polysaccharides. *Pharmaceutics 2023, Vol. 15, Page 1364*, *15*(5), 1364. https://doi.org/10.3390/PHARMACEUTICS15051364

Bennett, T., Coudert, F., James, S., Materials, A. C.-N., & 2021, undefined. (n.d.). The changing state of porous materials. *Nature.ComTD Bennett, FX Coudert, SL James, AI CooperNature Materials, 2021nature.Com*. https://doi.org/10.1038/s41563-021-00957-wï

Bhandari, G. (2014). An Overview of Agrochemicals and Their Effects on Environment in Nepal. *Applied Ecology and Environmental Sciences*, *2*(2), 66–73. https://doi.org/10.12691/aees-2-2-5

Bindra, P., Sharma, S., Sahu, B. K., Bagdwal, H., Shanmugam, V., & Singh, M. (2023). Targeted nutrient application to tomato plant with MOF/Zeolite composite wrapped with stimuli-responsive biopolymer. *Materials Today Communications*, *34*, 105264. https://doi.org/10.1016/J.MTCOMM.2022.105264

Borfecchia, E., Maurelli, S., Gianolio, D., Groppo, E., Chiesa, M., Bonino, F., & Lamberti, C. (2012). Insights into adsorption of NH 3 on HKUST-1 metal-organic framework: A multitechnique approach. *Journal of Physical Chemistry C*, *116*(37), 19839–19850 . https://doi.org/10.1021/JP305756K/SUPPL_FILE/JP305756K_SI_001.PDF

Bourett, T. M., & Howard, R. J. (1990). In vitro development of penetration structures in the rice blast fungus Magnaporthe grisea . *Canadian Journal of Botany*, *68*(2), 329–342. https://doi.org/10.1139/B90-044

Bouson, S., Krittayavathananon, A., Phattharasupakun, N., Siwayaprahm, P., & Sawangphruk, M. (2017). Antifungal activity of water-stable copper-containing metal-organic frameworks. *Royal Society Open Science*, *4*(10). https://doi.org/10.1098/RSOS.170654

Broadley, M. R., White, P. J., Hammond, J. P., Zelko, I., & Lux, A. (2007). Zinc in plants. *New Phytologist*, *173*(4), 677–702. https://doi.org/10.1111/J.1469-8137.2007.01996.X

Chen, Z., Chen, J., Catalysis, Y. L.-C. J. of, & 2017, undefined. (n.d.). Metal–organic-framework-based catalysts for hydrogenation reactions. *Elsevier*. Retrieved September 15, 2023, from https://www.sciencedirect.com/science/article/pii/S1872206717628523

Chiericatti, C., Carlos Basilico, J., Zapata Basilico, M. L., & Zamaro, J. M. (n.d.). *Novel application of HKUST-1 metal-organic framework as antifungal: Biological tests and physicochemical characterizations* . https://doi.org/10.1016/j.micromeso.2012.06.012

Christou, P., reviews, R. T.-N. research, & 2004, undefined. (2003). The potential of genetically enhanced plants to address food insecurity. *Cambridge.OrgP Christou, RM TwymanNutrition Research Reviews, 2004•cambridge.Org*, *17*, 23–42. https://doi.org/10.1079/NRR200373

Chui, S. S. Y., Lo, S. M. F., Charmant, J. P. H., Orpen, A. G., & Williams, I. D. (1999). A chemically functionalizable nanoporous material [Cu3(TMA)2 (H2O)3](n). *Science*, *283*(5405), 1148–1150 . https://doi.org/10.1126/SCIENCE.283.5405.1148/SUPPL_FILE/986116S4_THUMB.GIF

Couch, B. C., Fudal, I., Lebrun, M. H., Tharreau, D., Valent, B., Van Kim, P., Nottéghem, J. L., & Kohn, L. M. (2005). Origins of Host-Specific Populations of the Blast Pathogen Magnaporthe oryzae in Crop Domestication With Subsequent Expansion of Pandemic Clones on Rice and Weeds of Rice. *Genetics*, *170*(2), 613–630. https://doi.org/10.1534/GENETICS.105.041780

Cruz, F. J. R., Ferreira, R. L. da C., Conceição, S. S., Lima, E. U., Neto, C. F. de O., Galvão, J. R., Lopes, S. da C., Viegas, I. de J. M., Cruz, F. J. R., Ferreira, R. L. da C., Conceição, S. S., Lima, E. U., Neto, C. F. de O., Galvão, J. R., Lopes, S. da C., & Viegas, I. de J. M. (2022). Copper Toxicity in Plants: Nutritional, Physiological, and Biochemical Aspects. *Advances in Plant Defense Mechanisms*. https://doi.org/10.5772/INTECHOPEN.105212

Dable-Tupas, G., Talampas-Abundo, M. D., Abundo, I. C. S., & Derecho, C. M. P. (2023). Nutrigenomics in the management and prevention of malnutrition, stunting, and other nutritional disorders. *Role of Nutrigenomics in Modern-Day Healthcare and Drug Discovery*, 147–175 . https://doi.org/10.1016/B978-0-12-824412-8.00005-9

Dagdas, Y. F., Yoshino, K., Dagdas, G., Ryder, L. S., Bielska, E., Steinberg, G., & Talbot, N. J. (2012). Septin-mediated plant cell invasion by the rice blast fungus, Magnaporthe oryzae. *Science*, *336*(6088), 1590–1595. https://doi.org/10.1126/SCIENCE.1222934

De Araújo, L. G., Prabhu, A. S., & De Barros Freire, A. (2000). Development of blast resistant somaclones of the upland rice cultivar araguaia. *Pesquisa Agropecuária Brasileira*, *35*(2), 357–367. https://doi.org/10.1590/S0100-204X2000000200015

Dean, R. A., Talbot, N. J., Ebbole, D. J., Farman, M. L., Mitchell, T. K., Orbach, M. J., Thon, M., Kulkarni, R., Xu, J. R., Pan, H., Read, N. D., Lee, Y. I., Carbone, I., Brown, D., Yeon, Y. O., Donofrio, N., Jun, S. J., Soanes, D. M., Djonovic, S., Dirren, B. W. (2005). The genome sequence of the rice blast fungus Magnaporthe grisea. *Nature 2005 434:7036*, *434*(7036), 980–986. https://doi.org/10.1038/nature03449

Dean, R., Van Kan, J. A. L., Pretorius, Z. A., Hammond-Kosack, K. E., Di Pietro, A., Spanu, P. D., Rudd, J. J., Dickman, M., Kahmann, R., Ellis, J., & Foster, G. D. (2012). The Top 10 fungal pathogens in molecular plant pathology. *Molecular Plant Pathology*, *13*(4), 414–430. https://doi.org/10.1111/J.1364-3703.2011.00783.X

Derosa, M. C., Monreal, C., Schnitzer, M., Walsh, R., & Sultan, Y. (2010). Nanotechnology in fertilizers. *Nature Nanotechnology 2010 5:2*, *5*(2), 91–91. https://doi.org/10.1038/nnano.2010.2

Devreese, B., Gosti, F., Lee, L.-H., Goh, B.-H., Woan-Fei Law, J., Ser, H.-L., Khan, T. M., Chuah, L.-H., Pusparajah, P., & Chan, K.-G. (2017). *The Potential of Streptomyces as Biocontrol Agents against the Rice Blast Fungus, Magnaporthe oryzae (Pyricularia oryzae)* . https://doi.org/10.3389/fmicb.2017.00003

Dong, J., Chen, W., Feng, J., Liu, X., Xu, Y., Wang, C., Yang, W., & Du, X. (2021). Facile, Smart, and Degradable Metal-Organic Framework Nanopesticides Gated with FeIII-Tannic Acid Networks in Response to Seven Biological and Environmental Stimuli. *ACS Applied Materials and Interfaces*, *13*(16), 19507–19520. https://doi.org/10.1021/ACSAMI.1C04118/SUPPL_FILE/AM1C04118_SI_001.PDF

Ebbole, D. J. (2008). Magnaporthe as a model for understanding host-pathogen interactions. *Annual Review of Phytopathology*, *45*, 437–456 . https://doi.org/10.1146/ANNUREV.PHYTO.45.062806.094346

Fang, M., Yan, L., Wang, Z., Zhang, D., & Ma, Z. (2009). Sensitivity of Magnaporthe grisea to the Sterol Demethylation Inhibitor Fungicide Propiconazole. *Journal of Phytopathology*, *157*(9), 568–572. https://doi.org/10.1111/J.1439-0434.2009.01576.X

Fu, Q., Jia, X., Zhang, S., Zhang, J., Sun-Waterhouse, D., Wang, C., Waterhouse, G. I. N., & Wu, P. (2023). Highly defective copper-based metal-organic frameworks for the efficient adsorption and detection of organophosphorus pesticides: An experimental and computational investigation. *Food Chemistry*, *423*, 136319 . https://doi.org/10.1016/J.FOODCHEM.2023.136319

Furukawa, H., Ko, N., Go, Y. B., Aratani, N., Choi, S. B., Choi, E., Yazaydin, A. Ö., Snurr, R. Q., O'Keeffe, M., Kim, J., & Yaghi, O. M. (2010). Ultrahigh porosity in metal-organic frameworks. *Science*, *329*(5990), 424–428. https://doi.org/10.1126/SCIENCE.1192160

Ghatak, A., Willocquet, L., Savary, S., & Kumar, J. (2013). Variability in Aggressiveness of Rice Blast (Magnaporthe oryzae) Isolates Originating from Rice Leaves and Necks: A Case of Pathogen Specialization? *PLoS ONE*, *8*(6). https://doi.org/10.1371/JOURNAL.PONE.0066180

Giraldo, M. C., Dagdas, Y. F., Gupta, Y. K., Mentlak, T. A., Yi, M., Martinez-Rocha, A. L., Saitoh, H., Terauchi, R., Talbot, N. J., & Valent, B. (2013). Two distinct secretion systems facilitate tissue invasion by the rice blast fungus Magnaporthe oryzae. *Nature Communications*, . https://doi.org/10.1038/NCOMMS2996

Gnanamanickam, S. S. (2009). Rice and Its Importance to Human Life. *Biological Control of Rice Diseases*, 1–11. https://doi.org/10.1007/978-90-481-2465-7_1

Gohel, N., H. C.-J. of P. D., & 2008, undefined. (n.d.). Bio-efficacy of fungicides against Pyricularia oryzae the incitant of fice blast. *Indianjournals.ComNM Gohel, HL Chauhan, AN MehtaJournal of Plant Disease Sciences, 2008 indianjournals.Com*. Retrieved September 17, 2023, from https://www.indianjournals.com/ijor.aspx?target=ijor:jpds&volume=3&issue=2&article=012

Granito, M., Paolini, M., & Pérez, S. (2008). Polyphenols and antioxidant capacity of Phaseolus vulgaris stored under extreme conditions and processed. *LWT - Food Science and Technology*, *41*(6), 994–999 . https://doi.org/10.1016/J.LWT.2007.07.014

Greer, C. A., & Webster, R. K. (2001). Occurrence, Distribution, Epidemiology, Cultivar Reaction, and Management of Rice Blast Disease in California. *Plant Disease*, *85*(10), 1096.

Guan, X., Li, Q., Maimaiti, T., Lan, S., Ouyang, P., Ouyang, B., Wu, X., & Yang, S.-T. (2021). Toxicity and photosynthetic inhibition of metal-organic framework MOF-199 to pea seedlings. *Journal of Hazardous Materials*, *409*, 124521. https://doi.org/10.1016/j.jhazmat.2020.124521

Guerber, C., disease, D. T.-P., & 2006, undefined. (2006). Infection of Rice Seed Grown in Arkansas by Pyricularia grisea and Transmission to Seedlings in the Field. *Am Phytopath SocietyC Guerber, DO TeBeestPlant Disease, 2006•Am Phytopath Society*, *90*(2), 170–176. https://doi.org/10.1094/PD-90-0170

Hajano, J.-U.-D., Lodhi, A. M., Pathan, M. A., Ali, M., & Serwar Shah, G. (2012). In-Vitro Evaluation Of Fungicides, Plant Extracts And Bio-Controlagents Against Rice Blast Pathogen Magnaporthe Oryzae Couch. *Pak. J. Bot*, *44*(5), 1775–1778.

Henke, S., Li, W., & Cheetham, A. K. (2014). Guest-dependent mechanical anisotropy in pillared-layered soft porous crystals – a nanoindentation study. *Chemical Science*, *5*(6), 2392–2397. https://doi.org/10.1039/C4SC00497C

Hirooka, T., & Ishii, H. (2013). Chemical control of plant diseases. *Journal of General Plant Pathology*, *79*(6), 390–401. https://doi.org/10.1007/S10327-013-0470-6/TABLES/2

Hou, H., Shao, G., Yang, W., Science, W. W.-P. in M., & 2020, undefined. (n.d.). One-dimensional mesoporous inorganic nanostructures and their applications in energy, sensor, catalysis and adsorption. *Elsevier*. Retrieved August 30, 2023, from https://www.sciencedirect.com/science/article/pii/S0079642520300359

Houbraken, M., Senaeve, D., Fevery, D., & Spanoghe, P. (2015). Influence of adjuvants on the dissipation of fenpropimorph, pyrimethanil, chlorpyrifos and lindane on the solid/gas interface. *Chemosphere*, *138*, 357–363 . https://doi.org/10.1016/J.Chemosphere.2015.06.040

Iavicoli, I., Leso, V., Beezhold, D. H., & Shvedova, A. A. (2017). Nanotechnology in agriculture: Opportunities, toxicological implications, and occupational risks. *Toxicology and Applied Pharmacology*, *329*, 96–111 . https://doi.org/10.1016/J.TAAP.2017.05.025

Ibarra-Laclette, E., Blaz, J., Pérez-Torres, C. A., Villafán, E., Lamelas, A., Rosas-Saito, G., Ibarra-Juárez, L. A., García-ávila, C. de J., Martínez-Enriquez, A. I., & Pariona, N. (2022). Antifungal Effect of Copper Nanoparticles against Fusarium kuroshium, an Obligate Symbiont of Euwallacea kuroshio Ambrosia Beetle. *Journal of Fungi*, *8*(4), 347 . https://doi.org/10.3390/JOF8040347/S1

Islamoglu, T., Goswami, S., Li, Z., Howarth, A. J., Farha, O. K., & Hupp, J. T. (2017). Postsynthetic Tuning of Metal-Organic Frameworks for Targeted Applications. *Accounts of Chemical Research*, *50*(4), 805–813. https://doi.org/10.1021/ACS.Accounts.6b00577/Asset/Images/Medium/Ar-2016-00577a_0011.Gif

Jain, R., Srivastava, S., Solomon, S., Shrivastava, A. K., & Chandra, A. (2010). Impact of excess zinc on growth parameters, cell division, nutrient accumulation, photosynthetic pigments and oxidative stress of sugarcane (saccharum spp.). *Acta Physiologiae Plantarum*, *32*(5), 979–986 . https://doi.org/10.1007/S11738-010-0487-9

John Christopher, D., Suthin Raj, T., Usha Rani, S., & Udhayakumar, R. (2010). Role of defense enzymes activity in tomato as induced by Trichoderma virens against Fusarium wilt caused by Fusarium oxysporum f sp. lycopersici Trichoderma virens against Fusarium wilt caused by Fusarium oxysporum f sp. lycopersici. *Article in Journal of Biopesticides*, *3*(1), 158–162. https://www.researchgate.net/publication/324594421

Kangra, B., Jatrana, A., Maan, S., Chauhan, S., & Kumar, V. (n.d.). *Effective adsorption of chlorpyrifos pesticides by HKUST-1 metal-organic framework.* https://doi.org/10.1007/s12039-022

Kankanala, P., Czymmek, K., Cell, B. V.-T. P., & 2007, undefined. (2007). Roles for rice membrane dynamics and plasmodesmata during biotrophic invasion by the blast fungus. *Academic.Oup.ComP Kankanala, K Czymmek, B ValentThe Plant Cell, 2007 academic.Oup.Com*, *19*(2), 706–724 . https://doi.org/10.1105/tpc.106.046300

Katagiri, M., & Uesugi, Y. (1977). *Disease Control and Pest Management Similarities Between the Fungicidal Action of Isoprothiolane and Organophosphorus Thiolate Fungicides*.

Kato, H. (2001). *RICE BLAST DISEASE RICE BLAST CONTROL Figure 1. Macroconidia Figure 2. Appressoria*. http://www.jcpa

Katz, M. J., Howarth, A. J., Moghadam, P. Z., DeCoste, J. B., Snurr, R. Q., Hupp, J. T., & Farha, O. K. (2016). High volumetric uptake of ammonia using Cu-MOF-74/Cu-CPO-27. *Dalton Transactions*, *45*(10), 4150–4153. https://doi.org/10.1039/C5DT03436A

Kaur, H., & Garg, N. (123 C.E.). Zinc toxicity in plants: a review. *Planta*, *1*, 129. https://doi.org/10.1007/s00425-021-03642-z

Kaur, H., Walia, S., Karmakar, A., Krishnan, V., & Koner, R. R. (2022). Water-stable Zn-based metal-organic framework with hydrophilic-hydrophobic surface for selective adsorption and sensitive detection of oxo-anions and pesticides in aqueous medium. *Journal of Environmental Chemical Engineering*, *10*, 2213–3437. https://doi.org/10.1016/j.jece.2021.106667

Khudsar, T., Mahmooduzzafar, Iqbal, M., & Sairam, R. K. (2004). Zinc-induced changes in morpho-physiological and biochemical parameters in Artemisia annua. *Biologia Plantarum*, *48*(2), 255–260 . https://doi.org/10.1023/B:BIOP.0000033453.24705.F5/Metrics

Kingsolver, C., T. B.-B. of the, & 1984, undefined. (n.d.). Rice blast epidemiology. *Cabdirect.OrgCH Kingsolver, TH Barkside, MA MarchettiBulletin of the Pennsylvania Agricultural Experiment Station, 1984•cabdirect.Org*. Retrieved September 17, 2023, from https://www.cabdirect.org/cabdirect/abstract/19851309761

Kirtphaiboon, S., Humphries, U., Khan, A., & Yusuf, A. (2021). Model of rice blast disease under tropical climate conditions. *Chaos, Solitons & Fractals*, *143*, 110530. https://doi.org/10.1016/J.CHAOS.2020.110530

Knight, S. C., Anthony, V. M., Brady, A. M., Greenland, A. J., Heaney, S. P., Murray, D. C., Powell, K. A., Schulz, M. A., Spinks, C. A., Worthington, P. A., & Youle, D. (2003). Rationale And Perspectives On The Development Of Fungicides. *Https://Doi.Org/10.1146/Annurev.Phyto.35.1.349*, *35*, 349–372. https://doi.org/10.1146/ANNUREV.PHYTO.35.1.349

Kongcharoen, N., Kaewsalong, N., & Dethoup, T. (123 C.E.). Efficacy of fungicides in controlling rice blast and dirty panicle diseases in Thailand. *Scientific RepoRtS |*, *10*, 16233. https://doi.org/10.1038/s41598-020-73222-w

Kumar, P., Pournara, A., Kim, K. H., Bansal, V., Rapti, S., & Manos, M. J. (2017). Metal-organic frameworks: Challenges and opportunities for ion-exchange/sorption applications. *Progress in Materials Science*, *86*, 25–74. https://doi.org/10.1016/J.PMATSCI.2017.01.002

Kumar, S., Kumar, D., & Dilbaghi, N. (2017). Preparation, characterization, and bio-efficacy evaluation of controlled release carbendazim-loaded polymeric nanoparticles. *Environmental Science and Pollution Research*, *24*(1), 926–937. https://doi.org/10.1007/S11356-016-7774-Y/METRICS

Kumar, V., Pandita, S., Singh Sidhu, G. P., Sharma, A., Khanna, K., Kaur, P., Bali, A. S., & Setia, R. (2021). Copper bioavailability, uptake, toxicity and tolerance in plants: A comprehensive review. *Chemosphere*, *262* . https://doi.org/10.1016/J.Chemosphere.2020.127810

Laha, G. S., Singh, R., Ladhalakshmi, D., Sunder, S., Prasad, M. S., Dagar, C. S., & Babu, V. R. (2017). Importance and management of rice diseases: A global perspective. *Rice Production Worldwide*, 303–360 . https://doi.org/10.1007/978-3-319-47516-5_13/FIGURES/14

Lahlali, R., Ezrari, S., Radouane, N., Kenfaoui, J., Esmaeel, Q., El Hamss, H., Belabess, Z., & Barka, E. A. (2022). Biological Control of Plant Pathogens: A Global Perspective. *Microorganisms 2022, Vol. 10, Page 596*, *10*(3), 596. https://doi.org/10.3390/MICROORGANISMS10030596

Laohaudomchok, W., Nankongnab, N., Siriruttanapruk, S., Klaimala, P., Lianchamroon, W., Ousap, P., Jatiket, M., Kajitvichyanukul, P., Kitana, N., Siriwong, W., Hemachudhah, T., Satayavivad, J., Robson, M., Jaacks, L., Barr, D. B., Kongtip, P., & Woskie, S. (2020). Pesticide use in Thailand: Current situation, health risks, and gaps in research and policy. *Https://Doi.Org/10.1080/10807039.2020.1808777*, *27*(5), 1147–1169. https://doi.org/10.1080/10807039.2020.1808777

Liédana, N., Galve, A., Rubio, C., Téllez, C., & Coronas, J. (2012). CAF@ZIF-8: One-step encapsulation of caffeine in MOF. *ACS Applied Materials and Interfaces*, *4*(9), 5016–5021. https://doi.org/10.1021/AM301365H

Lin, L., Peng, Z., Yang, C. L., Wang, M. Y., Zha, Y. B., Liu, L. L., & Zeng, S. D. (2013). Determination of imidacloprid,carbendazim and thiabendazole residues in vegetables and fruits by HPLC. *Advanced Materials Research*, *781–784*, 1392–1396 . https://doi.org/10.4028/WWW.SCIENTIFIC.NET/AMR.781-784.1392

Linxin, D., He, J., Borui, L., Nana, W., & Song, L. (2020). Study of a new 3D MOF and its adsorption, slow release and biological activity in water-soluble and oil-soluble pesticides. *Polyhedron*, *190*, 114752 . https://doi.org/10.1016/J.POLY.2020.114752

Liu, G., Huang, X., Lu, M., Li, L., Li, T., & Xu, D. (2019). Facile synthesis of magnetic zinc metal-organic framework for extraction of nitrogen-containing heterocyclic fungicides from lettuce vegetable samples. *Journal of Separation Science*, *42*(7), 1451–1458. https://doi.org/10.1002/JSSC.201801169

Liu, L., Zhang, X., Xu, W., Liu, X., Li, Y., Wei, J., Gao, M., Bi, J., Lu, X., Wang, Z., & Wu, X. (2020). Challenges for Global Sustainable Nitrogen Management in Agricultural Systems. *Journal of Agricultural and Food Chemistry*, *68*(11), 3354–3361. https://doi.org/10.1021/ACS.JAFC.0C00273/ASSET/IMAGES/MEDIUM/JF0C00273_0005.GIF

Liu, X., Liang, T., Zhang, R., Ding, Q., Wu, S., Li, C., Lin, Y., Ye, Y., Zhong, Z., & Zhou, M. (2021). Iron-Based Metal-Organic Frameworks in Drug Delivery and Biomedicine. *ACS Applied Materials and Interfaces*, *13*(8), 9643–9655. https://doi.org/10.1021/ACSAMI.0C21486/ASSET/IMAGES/MEDIUM/AM0C21486_0012.GIF

Loera-Serna, S., Zarate-Rubio, J., Medina-Velazquez, D. Y., Zhang, L., & Ortiz, E. (2016). Encapsulation of urea and caffeine in $Cu_3(BTC)_2$ metal–organic framework. *Https://Doi.Org/10.1680/Jsuin.15.00017*, *4*(2), 76–87. https://doi.org/10.1680/JSUIN.15.00017

Lu, W., Wei, Z., Gu, Z. Y., Liu, T. F., Park, J., Park, J., Tian, J., Zhang, M., Zhang, Q., Gentle, T., Bosch, M., & Zhou, H. C. (2014). Tuning the structure and function of metal–organic frameworks via linker design. *Chemical Society Reviews*, *43*(16), 5561–5593. https://doi.org/10.1039/C4CS00003J

Lukose, B., Wahiduzzaman, M., Kuc, A., & Heine, T. (2012). Mechanical, electronic, and adsorption properties of porous aromatic frameworks. *Journal of Physical Chemistry C*, *116*(43), 22878–22884 . https://doi.org/10.1021/JP3067102/ASSET/IMAGES/MEDIUM/JP-2012-067102_0009.GIF

Ma, Q., Zhang, Q., Maimaiti, T., Lan, S., Liu, X., Wang, Y., Li, Q., Luo, H., Yu, B., & Yang, S. T. (2021). Carbonization reduces the toxicity of metal-organic framework MOF-199 to white-rot fungus Phanerochaete chrysosporium. *Journal of Environmental Chemical Engineering*, *9*(6), 106705. https://doi.org/10.1016/J.JECE.2021.106705

Ma, S., Yang, X., Wang, Y., Yang, X., Li, Y., & Lü, S. (2023). A core-satellite MOF-on-MOF hybrid for intelligent delivery of multi-agrochemicals for sustainable agriculture. *Applied Surface Science*, *624*, 157129 . https://doi.org/10.1016/J.APSUSC.2023.157129

Magar, P.B., Acharya, B., Pandey, B., 2015. Use of... - Google Scholar. (n.d.). Retrieved September 17, 2023, from https://scholar.google.com/scholarApplied+Science+and+Biotechnology%2C+3+%283%29%2C+474-478.&btnG=

Mahmoud, L. A. M., Dos Reis, R. A., Chen, X., Ting, V. P., & Nayak, S. (2022). Metal-Organic Frameworks as Potential Agents for Extraction and Delivery of Pesticides and Agrochemicals. *ACS Omega*, *7*(50), 45910–45934. https://doi.org/10.1021/ACSOMEGA.2C05978/ASSET/IMAGES/LARGE/AO2C05978_0017.JPEG

Mahmoud, N. E., & Abdelhameed, R. M. (2022). Postsynthetic Modification of Ti-Based Metal-Organic Frameworks with Polyamines and Its Behavior on Biochemical Constituents of Sesamum indicum L. under Heat Stress Conditions. *ACS Agricultural Science and Technology*, *2*(5), 1023–1041. https://doi.org/10.1021/ACSAGSCITECH.2C00169/SUPPL_FILE/AS2C00169_SI_001.PDF

Mandal, A., Sarkar, B., Mandal, S., Vithanage, M., Patra, A. K., & Manna, M. C. (2020). Impact of agrochemicals on soil health. *Agrochemicals Detection, Treatment and Remediation: Pesticides and Chemical Fertilizers*, 161–187. https://doi.org/10.1016/B978-0-08-103017-2.00007-6

Marsh, H., & Rodríguez-Reinoso, F. (2006). Production and Reference Material. *Activated Carbon*, 454–508. https://doi.org/10.1016/B978-008044463-5/50023-6

McGuire, C. V., & Forgan, R. S. (2015). The surface chemistry of metal–organic frameworks. *Chemical Communications*, *51*(25), 5199–5217 . https://doi.org/10.1039/C4CC04458D

Mejías, F. J. R., Trasobares, S., Varela, R. M., Molinillo, J. M. G., Calvino, J. J., & Macías, F. A. (2021). One-step encapsulation of ortho-disulfides in functionalized zinc MOF. Enabling metal−organic frameworks in agriculture. *ACS Applied Materials and Interfaces*, *13*(7), 7997–8005. https://doi.org/10.1021/ACSAMI.0C21488/ASSET/IMAGES/LARGE/AM0C21488_0014.JPEG

Merhej, J., Richard-Forget, F., & Barreau, C. (2011). The pH regulatory factor Pac1 regulates Tri gene expression and trichothecene production in Fusarium graminearum. *Fungal Genetics and Biology*, *48*(3), 275–284. https://doi.org/10.1016/J.FGB.2010.11.008

Miah, G., Rafii, M. Y., Ismail, M. R., Puteh, A. B., Rahim, H. A., Asfaliza, R., & Latif, M. A. (2012). Blast resistance in rice: a review of conventional breeding to molecular approaches. *Molecular Biology Reports 2012 40:3*, *40*(3), 2369–2388. https://doi.org/10.1007/S11033-012-2318-0

Miah, G., Rafii, M. Y., Ismail, M. R., Sahebi, M., Hashemi, F. S. G., Yusuff, O., & Usman, M. G. (n.d.). Blast Disease Intimidation Towards Rice Cultivation: A Review Of Pathogen And Strategies To Control. *The J. Anim. Plant Sci*, *27*(4), 2017.

Misra, A., Phytopathology, D. V.-I., & 1990, undefined. (1990). Efficacy Of Fungicides-Xlvi: Effect Of Fungicidal Seed Treatment Against Heavy Inoculum Pressureof Certain Fungi Causing. *Researchgate.NetAK Misra, D VirIndian Phytopathology, 1990•researchgate.Net*, *43*(2), 175–178 . f

Murinzi, T. W., Clement, T. A., Chitsa, V., & Mehlana, G. (2018). *Copper oxide nanoparticles encapsulated in HKUST-1 metal-organic framework for electrocatalytic oxidation of citric acid* . https://doi.org/10.1016/j.jssc.2018.09.003

Muthayya, S., Sugimoto, J. D., Montgomery, S., & Maberly, G. F. (2014). An overview of global rice production, supply, trade, and consumption. *Annals of the New York Academy of Sciences*, *1324*(1), 7–14 . https://doi.org/10.1111/NYAS.12540

Nagarajan, S. (*EPIDEMIOLOGY AND LOSS OF RICE, WHEAT AND PEARL MILLET CROPS DUE TO DISEASES IN INDIA 21*.

Nemeskéri, E., Molnár, K., & Helyes, L. (2018). Relationships of spectral traits with yield and nutritional quality of snap beans (Phaseolus vulgaris L.) in dry seasons. *Archives of Agronomy and Soil Science*, *64*(9), 1222–1239. https://doi.org/10.1080/03650340.2017.1420903

Nganga, E. M., Kyallo, M., Orwa, P., Rotich, F., Gichuhi, E., Kimani, J. M., Mwongera, D., Waweru, B., Sikuku, P., Musyimi, D. M., Mutiga, S. K., Ziyomo, C., Murori, R., Wasilwa, L., Correll, J. C., & Talbot, N. J. (2022). Foliar Diseases and the Associated Fungi in Rice Cultivated in Kenya. *Plants*, *11*(9), 1264. https://doi.org/10.3390/PLANTS11091264/S1

Nutsugah, S. K., Twumasi, J. K., Chipili, J., Séré, Y., & Sreenivasaprasad, S. (2008). Diversity of the rice blast pathogen populations in Ghana and strategies for resistance management. *Plant Pathology Journal*, *7*(1), 109–113. https://doi.org/10.3923/PPJ.2008.109.113

Oh, Y. (2008). *Genome Wide Transcription Studies on Infection Structure Formation and Function in Magnaporthe grisea*. https://repository.lib.ncsu.edu/handle/1840.16/3602

Oliveira, S. C. C., Kleber, Z., Andrade, C., Varela, R. M., Molinillo, J. M. G., & Macías, F. A. (2019). Phytotoxicity Study of Ortho-Disubstituted Disulfides and Their Acyl Derivatives. *ACS Omega*, *4*(1), 2362–2368 . https://doi.org/10.1021/ACSOMEGA.8B03219

Ou, S. (1985). *Rice diseases*. https://books.google.com/books?hl=en&lr=&id=-k3mewv9nMoC&oi=fnd&pg=PR1&ots=ZmqWryAbbl&sig=PHqPv5q9ov1wQcHE_JjUS_6rlio

Padmanabhan, S. Y. (1965). Studies on forecasting outbreaks of blast disease of rice - I. Influence of meteorological factors on blast incidence at cuttack. *Proceedings of the Indian Academy of Sciences - Section B*, *62*(3), 117–129. https://doi.org/10.1007/BF03051084

Pame, A. R. P., Vithoonjit, D., Meesang, N., Balingbing, C., Gummert, M., Van Hung, N., Singleton, G. R., & Stuart, A. M. (2023). Improving the Sustainability of Rice Cultivation in Central Thailand with Biofertilizers and Laser Land Leveling. *Agronomy 2023, Vol. 13, Page 587*, *13*(2), 587 . https://doi.org/10.3390/AGRONOMY13020587

Panella, B., Hirscher, M., Pütter, H., & Müller, U. (2006). Hydrogen adsorption in metal-organic frameworks: Cu-MOFs and Zn-MOFs compared. *Advanced Functional Materials*, *16*(4), 520–524 . https://doi.org/10.1002/ADFM.200500561

Parida, T., Nayak, M., & Sridhar, R. (1990). Fate of carbendazim in rice tissues after seed or foliage treatments. *Pesticide Science*, *30*(3), 303–308 . https://doi.org/10.1002/PS.2780300307

Pathak, R. K., Baunthiyal, M., Pandey, D., & Kumar, A. (2018). Augmentation of crop productivity through interventions of omics technologies in India: challenges and opportunities. *3 Biotech*, *8*(11), 1–28. https://doi.org/10.1007/S13205-018-1473-Y/TABLES/2

Peng, H., Wang, K., Chen, Z., Cao, Y., Gao, Q., Li, Y., Li, X., Lu, H., Du, H., Lu, M., Yang, X., & Liang, C. (2020). MBKbase for rice: an integrated omics knowledgebase for molecular breeding in rice. *Nucleic Acids Research*, *48*(D1), D1085–D1092. https://doi.org/10.1093/NAR/GKZ921

Phansawan, B., & Prapamontol, T. (2015). A Sensitive Method for Determination of Carbendazim Residue in Vegetable Samples Using HPLC-UV and Its Application in Health Risk Assessment. *Chiang Mai J. Sci*, *42*(3), 681–690. http://epg.science.cmu.ac.th/ejournal/

Prajapati, K., Patel, R., Journal, A. P.-P. R., & 2004, undefined. (n.d.). Field evaluation of new fungicides against blast of rice. *Indianjournals.ComKS Prajapati, RC Patel, AR PathakPesticide Research Journal, 2004•indianjournals.Com*. Retrieved September 17, 2023, from https://www.indianjournals.com/ijor.aspx?target=ijor:prj&volume=16&issue=2&article=007

Prestipino, C., Regli, L., Vitillo, J. G., Bonino, F., Damin, A., Lamberti, C., Zecchina, A., Solari, P. L., Kongshaug, K. O., & Bordiga, S. (2006). Local structure of framework Cu(II) in HKUST-1 metallorganic framework: Spectroscopic characterization upon activation and interaction with adsorbates. *Chemistry of Materials*, *18*(5), 1337–1346 . https://doi.org/10.1021/CM052191G/ASSET/IMAGES/MEDIUM/CM052191GN00001.GIF

Rai, M., & Ingle, A. (2012). Role of nanotechnology in agriculture with special reference to management of insect pests. *Applied Microbiology and Biotechnology*, *94*(2), 287–293. https://doi.org/10.1007/S00253-012-3969-4/FIGURES/1

Raquel Ghini, R. B. (2014). Rice Blast Disease in Climate Change Times. *Rice Research: Open Access*, *03*(01). https://doi.org/10.4172/2375 4338.1000E111

Rasool, A., Akbar, F., Rehman, A., & Jabeen, H. (2020). Genetic Engineering of Rice for Resistance to Insect Pests. *Rice Research for Quality Improvement: Genomics and Genetic Engineering*, 129–148. https://doi.org/10.1007/978-981-15-5337-0_7

Raveloson, H., Ratsimiala Ramonta, I., Tharreau, D., & Sester, M. (2018). Long-term survival of blast pathogen in infected rice residues as major source of primary inoculum in high altitude upland ecology. *Wiley Online LibraryH Raveloson, I Ratsimiala Ramonta, D Tharreau, M SesterPlant Pathology, 2018•Wiley Online Library*, *67*(3), 610–618. https://doi.org/10.1111/ppa.12790

Ren, L., Chong, J., Loya, A., Kang, Q., Stair, J. L., Nan, L., & Ren, G. (2015). Determination of Cu2+ ions release rate from antimicrobial copper bearing stainless steel by joint analysis using ICP-OES and XPS. *Materials Technology*, *30*(B2), B86–B89 . https://doi.org/10.1179/1753555714Y.0000000264

Ribot, C., Hirsch, J., Balzergue, S., Tharreau, D., Nottéghem, J.-L., Lebrun, M.-H., & Morel, J.-B. (2008). Susceptibility of rice to the blast fungus, Magnaporthe grisea. *Journal of Plant Physiology*, *165*, 114–124 . https://doi.org/10.1016/j.jplph.2007.06.013

Riccò, R., Linder-Patton, O., Sumida, K., Styles, M. J., Liang, K., Amenitsch, H., Doonan, C. J., & Falcaro, P. (2018). Conversion of Copper Carbonate into a Metal-Organic Framework. *Chemistry of Materials*, *30*(16), 5630–5638. https://doi.org/10.1021/ACS.

Ricco, R., Malfatti, L., Takahashi, M., Hill, A. J., & Falcaro, P. (2013). Applications of magnetic metal–organic framework composites. *Journal of Materials Chemistry A*, *1*(42), 13033–13045. https://doi.org/10.1039/C3TA13140H

Ricco, R., Pfeiffer, C., Sumida, K., Sumby, C. J., Falcaro, P., Furukawa, S., Champness, N. R., & Doonan, C. J. (2016). Emerging applications of metal–organic frameworks. *CrystEngComm*, *18*(35), 6532–6542 . https://doi.org/10.1039/C6CE01030J

Rojas, S., Rodríguez-Diéguez, A., & Horcajada, P. (2022). Metal−Organic Frameworks in Agriculture. *Cite This: ACS Appl. Mater. Interfaces*, *14*, 16983–17007. https://doi.org/10.1021/acsami.2c00615

Sajid, M. (2016). Toxicity of nanoscale metal organic frameworks: a perspective. *Environmental Science and Pollution Research*, *23*(15), 14805–14807. https://doi.org/10.1007/S11356-016-7053-Y/METRICS

Savary, S., Teng, P., … L. W.-Annu. R., & 2006, undefined. (2006). Quantification and modeling of crop losses: a review of purposes. *Annualreviews.OrgS Savary, PS Teng, L Willocquet, FW Nutter JrAnnu. Rev. Phytopathol., 2006 annualreviews.Org*, *44*, 89–112 . https://doi.org/10.1146/annurev.phyto.44.070505.143342

Schneider, E. F., & Dickert, K. J. (2010). Health Costs and Benefits of Fungicide Use in Agricultur: *Http://Dx.Doi.Org/10.1300/J096v01n01_03*, *1*(1), 19–37. https://doi.org/10.1300/J096V01N01_03

Seebold, K. W., Datnoff, L. E., Correa-Victoria, F. J., Kucharek, T. A., & Snyder, G. H. (2007). Effects of Silicon and Fungicides on the Control of Leaf and Neck Blast in Upland Rice. *Https://Doi.Org/10.1094/PDIS.2004.88.3.253*, *88*(3), 253–258. https://doi.org/10.1094/PDIS.2004.88.3.253

Shalaby, T. A., El-Bialy, S. M., El-Mahrouk, M. E., Omara, A. E. D., El-Beltagi, H. S., & El-Ramady, H. (2022). Acclimatization of In Vitro Banana Seedlings Using Root-Applied Bio-Nanofertilizer of Copper and Selenium. *Agronomy 2022, Vol. 12, Page 539*, *12*(2), 539 . https://doi.org/10.3390/AGRONOMY12020539

Shan, Y., Cao, L., Muhammad, B., Xu, B., Zhao, P., Cao, C., & Huang, Q. (2020). Iron-based porous metal–organic frameworks with crop nutritional function as carriers for controlled fungicide release. *Journal of Colloid and Interface Science*, *566*, 383–393. https://doi.org/10.1016/J.JCIS.2020.01.112

Shan, Y., Xu, C., Zhang, H., Chen, H., Bilal, M., Niu, S., Cao, L., & Huang, Q. (2020). Polydopamine-Modified Metal–Organic Frameworks, NH2-Fe-MIL-101, as pH-Sensitive Nanocarriers for Controlled Pesticide Release. *Nanomaterials 2020, Vol. 10, Page 2000*, *10*(10), 2000 . https://doi.org/10.3390/NANO10102000

Sierra-Serrano, B., García-García, A., Hidalgo, T., Ruiz-Camino, D., Rodríguez-Diéguez, A., Amariei, G., Rosal, R., Horcajada, P., & Rojas, S. (2022). Copper Glufosinate-Based Metal-Organic Framework as a Novel Multifunctional Agrochemical. *ACS Applied Materials and Interfaces*, *14*(30), 34955–34962 . https://doi.org/10.1021/ACSAMI.2C07113/ASSET/IMAGES/LARGE/AM2C07113_0006.JPEG

Singh, J., Jain, J., Jain, S., Lore, J., Genetics, S. U.-I. J. of, & 2018, undefined. (2018). Quantification of resistance among basmati rice genotypes to neck blast, Pyricularia oryzae Cavara. *Isgpb.Org*, *78*(4), 519–522 . https://doi.org/10.31742/IJGPB.78.4.15

Skamnioti, P., & Gurr, S. J. (2009). Against the grain: safeguarding rice from rice blast disease. *Trends in Biotechnology*, *27*(3), 141–150 . https://doi.org/10.1016/J.TIBTECH.2008.12.002

Slater, A. G., & Cooper, A. I. (2015). Function-led design of new porous materials. *Science*, *348*(6238), aaa8075 . https://doi.org/10.1126/SCIENCE.AAA8075/ASSET/0685EADE-31AD-4C29-A5EA-885CB45D1D83/ASSETS/GRAPHIC/348_AAA8075_F6.JPEG

Slater, A., Taylor, S. A., Burling, D., Gartner, L., Scarth, J., & Halligan, S. (2006). Colonic polyps: Effect of attenuation of tagged fluid and viewing window on conspicuity and measurement - In vitro experiment with porcine colonic specimen. *Radiology*, *240*(1), 101–109 . https://doi.org/10.1148/RADIOL.2401050984

Song, J., Han, C., Zhang, S., Wang, Y., Liang, Y., Dai, Q., Huo, Z., & Xu, K. (2022). Hormetic Effects of Carbendazim on Mycelial Growth and Aggressiveness of Magnaporthe oryzae. *Journal of Fungi 2022, Vol. 8, Page 1008*, *8*(10), 1008. https://doi.org/10.3390/JOF8101008

Strange, R. N., & Scott, P. R. (2005). Plant Disease: A Threat to Global Food Security. *Https://Doi.Org/10.1146/Annurev.Phyto.43.113004.133839*, *43*, 83–116. https://doi.org/10.1146/ANNUREV.PHYTO.43.113004.133839

Su, B. L., Sanchez, C., & Yang, X. Y. (2011). Hierarchically Structured Porous Materials: From Nanoscience to Catalysis, Separation, Optics, Energy, and Life Science. *Hierarchically Structured Porous Materials: From Nanoscience to Catalysis, Separation, Optics, Energy, and Life Science*. https://doi.org/10.1002/9783527639588

Sun, M., Huang, S., Chen, L., Li, Y., … X. Y.-C. society, & 2016,. Applications of hierarchically structured porous materials from energy storage and conversion, catalysis, photocatalysis, adsorption, separation, and sensing to. *Pubs.Rsc. Chemical Society Reviews*, 23(3). pp::122-155.

Tan, J. C., & Cheetham, A. K. (2011). Mechanical properties of hybrid inorganic–organic framework materials: establishing fundamental structure–property relationships. *Chemical Society Reviews*, *40*(2), 1059–1080. https://doi.org/10.1039/C0CS00163E

Tang, R., Tang, T., Tang, G., Liang, Y., Wang, W., Yang, J., Niu, J., Tang, J., Zhou, Z., & Cao, Y. (2019). Pyrimethanil Ionic Liquids Paired with Various Natural Organic Acid Anions for Reducing Its Adverse Impacts on the Environment. *Journal of Agricultural and Food Chemistry*, *67*(40), 11018–11024. https://doi.org/10.1021/ACS.JAFC.9B03643

Toan, N. P., Thu Ha, P. T., & Xuan, T. D. (2017). Effects of rice blast fungus (Pyricularia grisea) on phenolics, flavonoids, antioxidant capacity in rice (Oryza sativa L.). *International Letters of Natural Sciences*, *61*, 1–7. https://doi.org/10.18052/WWW.SCIPRESS.COM/ILNS.61.1

Usman Ghazanfar, M., Wakil, W., & Sahi, S. (2009). *Influence of various fungicides on the management of rice blast disease*. *7*(1), 29–34.

Vaillant, N., Monnet, F., Hitmi, A., Sallanon, H., & Coudret, A. (2005). Comparative study of responses in four Datura species to a zinc stress. *Chemosphere*, *59*(7), 1005–1013. https://doi.org/10.1016/J.CHEMOSPHERE.2004.11.030

Vaneault-Fourrey, C., Barooah, M., Egan, M., Wakley, G., & Talbot, N. J. (2006). Autophagic fungal cell death is necessary for infection by the rice blast fungus. *Science*, *312*(5773), 580–583 . https://doi.org/10.1126/SCIENCE.1124550

Varma, C. K. Y., & Santhakumari, P. (2012). Management of rice blast through new fungicidal formulations. *Indian Phytopathology*, *65*(1), 87–88.

Vasseghian, Y., Arunkumar, P., Joo, S.-W., Gnanasekaran, L., Kamyab, H., Rajendran, S., Balakrishnan, D., Chelliapan, S., & Klemeš, J. J. (2022). Metal-organic framework-enabled pesticides are an emerging tool for sustainable cleaner production and environmental hazard reduction. *Journal of Cleaner Production*, *373*, 133966. https://doi.org/10.1016/j.jclepro.2022.133966

Wang, C. Y., Qin, J. C., & Yang, Y. W. (2023). Multifunctional Metal-Organic Framework (MOF)-Based Nanoplatforms for Crop Protection and Growth Promotion. *Journal of Agricultural and Food Chemistry* . https://doi.org/10.1021/ACS.JAFC.3C01094/ASSET/IMAGES/MEDIUM/JF3C01094_0012.GIF

Wang, C.-Y., Liu, Y.-Q., Jia, C., Zhang, M.-Z., Song, C.-L., Xu, C., Hao, R., Qin, J.-C., & Yang, Y.-W. (2023). An integrated supramolecular fungicide nanoplatform based on pH-sensitive metal–organic frameworks. *Chinese Chemical Letters*, 108400. https://doi.org/10.1016/J.CCLET.2023.108400

Weisenburger, D. D. (1993). Human health effects of agrichemical use. *Human Pathology*, *24*(6), 571–576. https://doi.org/10.1016/0046-8177(93)90234-8

Wilson, R. A., & Talbot, N. J. (2009). Under pressure: investigating the biology of plant infection by Magnaporthe oryzae. *Nature Reviews Microbiology 2009 7:3*, *7*(3), 185–195. https://doi.org/10.1038/nrmicro2032

Woloshuk, C. P., Sisler, H. D., Tokousbalides, M. C., & Dutky, S. R. (1980). Melanin biosynthesis in Pyricularia oryzae: Site of tricyclazole inhibition and pathogenicity of melanin-deficient mutants. *Pesticide Biochemistry and Physiology*, *14*(3), 256–264. https://doi.org/10.1016/0048-3575(80)90032-2

Wu, K., Du, C., Ma, F., Shen, Y., Liang, D., & Zhou, J. (2019). Degradation of Metal-Organic Framework Materials as Controlled-Release Fertilizers in Crop Fields. *Polymers 2019, Vol. 11, Page 947*, *11*(6), 947 . https://doi.org/10.3390/POLYM11060947

Wu, K., Xu, X., Ma, F., & Du, C. (2022). *Fe-Based Metal−Organic Frameworks for the Controlled Release of Fertilizer Nutrients*. *7*, 35980 . https://doi.org/10.1021/acsomega.2c05093

Wu, Y., Luo, Y., Zhou, B., Mei, L., Wang, Q., & Zhang, B. (2019). Porous metal-organic framework (MOF) Carrier for incorporation of volatile antimicrobial essential oil. *Food Control*, *98*, 174–178 . https://doi.org/10.1016/J.FOODCONT.2018.11.011

Xiong, Z. T., & Wang, H. (2005). Copper toxicity and bioaccumulation in Chinese cabbage (Brassica pekinensis Rupr.). *Environmental Toxicology*, *20*(2), 188–194. https://doi.org/10.1002/TOX.20094

Xu, C., Cao, L., Liu, T., Chen, H., & Li, Y. (2023). pH-responsive copper-doped ZIF-8 MOF nanoparticles for enhancing the delivery and translocation of pesticides in wheat plants. *Environmental Science: Nano*, *10*(9), 2578–2590. https://doi.org/10.1039/D3EN00300K

Xu, G.-R., An, Z.-H., Xu, K., Liu, Q., Das, R., & Zhao, H.-L. (2020). *Metal organic framework (MOF)-based micro/nanoscaled materials for heavy metal ions removal: The cutting-edge study on designs, synthesis, and applications*. https://doi.org/10.1016/j.ccr.2020.213554

Yruela, I. (2009). Copper in plants: Acquisition, transport and interactions. *Functional Plant Biology*, *36*(5), 409–430. https://doi.org/10.1071/FP08288

Yu Tsivadze, A., Aksyutin, O. E., Ishkov, A. G., -, al, V, V. M., Nageswaran -, G., Wahyu Lestari, W., Adreane, M., Purnawan, C., Fansuri, H., Widiastuti, N., & Budi Rahardjo, S. (2016). Solvothermal and electrochemical synthetic method of HKUST-1 and its methane storage capacity. *IOP Conference Series: Materials Science and Engineering*, *107*(1), 012030. https://doi.org/10.1088/1757-899X/107/1/012030

Yuan, H., Li, J., Pan, L., Li, X., Yuan, Y., Zhong, Q., Wu, X., Luo, J., & Yang, S. T. (2022). Particulate toxicity of metal-organic framework UiO-66 to white rot fungus Phanerochaete chrysosporium. *Ecotoxicology and Environmental Safety*, *247*, 114275. https://doi.org/10.1016/J.ECOENV.2022.114275

Zacher, D., Schmid, R., Wöll, C., & Fischer, R. A. (2011). Surface Chemistry of Metal–Organic Frameworks at the Liquid–Solid Interface. *Angewandte Chemie International Edition*, *50*(1), 176–199 . https://doi.org/10.1002/ANIE.201002451

Zarei Mohammadabad, M., Moeinaddini, M., Nowrouzi, M., Rafiee, R., & Abbasi, A. (2020). Facile and cost-efficient synthesis of highly efficient CO2 adsorbents: a pathway towards a green environment. *Journal of Porous Materials*, *27*(6), 1659–1668. https://doi.org/10.1007/S10934-020-00945-6/TABLES/4

Zhang, C.-Q., Zhou, M.-G., Zhen-Run, S., & Liang, G.-M. (2004). Detection of Sensitivity and Resistance Variation of Magnaporthe grisea to Kitazin P, Carbendazim and Tricyclazole. *Rice Science*, *11*(6), 317 . http://www.ricescience.org

Zhang, H., Li, G., Li, W., & Song, F. (2009). Transgenic strategies for improving rice disease resistance. *African Journal of Biotechnology*, *8*(9), 1750–1757. https://doi.org/10.4314/AJB.V8I9.60376

Zhang, Y., & Goss, G. G. (2022). Nanotechnology in agriculture: Comparison of the toxicity between conventional and nano-based agrochemicals on non-target aquatic species. *Journal of Hazardous Materials*, *439*, 129559. https://doi.org/10.1016/J.JHAZMAT.2022.129559

Zhao, X., Chen, Y., Li, H., & Lu, | Jinying. (2021). *Influence of seed coating with copper, iron and zinc nanoparticles on growth and yield of tomato*. https://doi.org/10.1049/nbt2.12064

Zhou, H. C. J., & Kitagawa, S. (2014). Metal–Organic Frameworks (MOFs). *Chemical Society Reviews*, *43*(16), 5415–5418. https://doi.org/10.1039/C4CS90059F

Zhou, H. C., Long, J. R., & Yaghi, O. M. (2012). Introduction to metal-organic frameworks. *Chemical Reviews*, *112*(2), 673–674 . https://doi.org/10.1021/CR300014X/ASSET/IMAGES/MEDIUM/CR-2012-00014X_0003.GIF

Zhu, Y. Y., Fang, H., Wang, Y. Y., Jin, X. F., Yang, S. S., Twng, W. M., & Mundt, C. C. (2007). Panicle Blast and Canopy Moisture in Rice Cultivar Mixtures. *Https://Doi.Org/10.1094/PHYTO-95-0433*, *95*(4), 433–438 . https://doi.org/10.1094/PHYTO-95-0433

Zibaee, A., Sendi, J. J., Ghadamyari, M., Alinia, F., & Etebari, K. (2009). Diazinon Resistance in Different Selected Strains of Chilo suppressalis (Lepidoptera: Crambidae) in Northern Iran. *Journal of Economic Entomology*, *102*(3), 1189–1196. https://doi.org/10.1603/029.102.0343